NASA CONTRACTOR REPORT

NASA CR-607

DESIGN AND DEVELOPMENT OF A WATER VAPOR ELECTROLYSIS UNIT

by W. J. Conner, B. M. Greenough, and G. M. Cook

Prepared by
LOCKHEED AIRCRAFT CORPORATION
Palo Alto, Calif.
for Ames Research Center

NATIONAL AERONAUTICS AND SPACE ADMINISTRATION • WASHINGTON, D. C. • SEPTEMBER 1966

NASA CR-607

DESIGN AND DEVELOPMENT OF A WATER VAPOR ELECTROLYSIS UNIT

By W. J. Conner, B. M. Greenough, and G. M. Cook

Prepared under Contract No. NAS 2-2630 by
LOCKHEED AIRCRAFT CORPORATION
Palo Alto, Calif.

for Ames Research Center

NATIONAL AERONAUTICS AND SPACE ADMINISTRATION

For sale by the Clearinghouse for Federal Scientific and Technical Information
Springfield, Virginia 22151 – Price $3.00

LIBRARY CARD ABSTRACT

Development of a water vapor electrolysis cell using sulfuric acid as the electrolyte proved that this system is competitive with other zero-gravity methods of generating breathing oxygen. The properties of sulfuric acid were studied and the results indicate that it is a suitable electrolyte with a high water absorption characteristic. The immobilizing gel matrix materials tested were generally unsuitable for the water vapor electrolysis cell. Experimental gelled matrix cells were operated under adverse operational conditions to determine failure modes. Unique liquid electrolyte-absorbent matrix cells were efficiently operated at high current densities and water absorption rates. A 1-man unit of this design would require 14 cells, 284 W, 2.24 V at 100 mA/cm^2, weigh 19.7 lb, and occupy 0.19 ft^3.

ABSTRACT

A water vapor electrolysis cell utilizing sulfuric acid as the electrolyte has been shown to be capable of operating efficiently on the typical humidity of cabin air. Concentrated sulfuric acid can absorb enough water from a 50% relative humidity air stream at 75°F to permit an electrolysis cell to operate at a current density as high as 150 mA/cm^2. Sulfuric acid was examined for physical properties applicable to its use in the water-vapor electrolysis cell. An evaluation of the factors affecting the water absorption properties indicated that the vapor pressure difference between the inlet air stream and the acid coupled with the air flowrate were controlling factors for water absorption. Experimental tests were conducted to prove the theoretical equations; the results agreed closely with the equation.

Electrode performance in bulk sulfuric acid was evaluated; it was found that the anode overvoltage is the largest contributor to the cell overvoltage. This is especially true in the acid that is sufficiently concentrated to absorb enough water from the air stream. An electrode made from tantalum screen with black platinum held in place with a fluoro-carbon resin was shown to reduce both anodic and cathodic overvoltage compared to a black-platinized platinum electrode.

Secondary cell reactions, principally ozone, were studied and the ozone threshold anodic overvoltage was found to be approximately 2.07 V. Measurements in test cells verified the result.

Immobilizing gel matrix materials were studied including a synthetic zeolite, silicic acid, and a finely divided silica. These materials were characterized. Test cells were built and operated with these materials as the immobilizing matrix. The zeolite slowly reacted with the concentrated sulfuric acid resulting in poorer cell performance.

All the matrices were vibration or compression sensitive and gas cross-leakage occurred resulting in cell failure. Operation under adverse inlet air conditions also caused cell failure. The best gel-type matrix material appears to be silicic acid; a cell built with this matrix had an operational voltage of 2.00 V at 35 mA/cm^2.

Liquid electrolyte-absorbent matrix cells were built, tested, and operated efficiently. In this cell design, bulk liquid electrolyte flows between two absorbent matrices which are contiguous to the operating electrodes. The matrix provides the zero-gravity phase separation. The circulating electrolyte maintains electrolyte equilibrium in the matrix in the cell preventing performance deterioration under adverse operating conditions. The electrolyte also acts as the heat exchange medium for the cell. High electrolysis and absorption rates are possible with this cell. The cell operates at 2.20 V at 75 mA/cm^2 with a water absorption efficiency greater than 50% per pass at an inlet air flow of 27 cm^3/sec (3.05 ft^3/hr) and 48% relative humidity at 75° F.

Scale-up calculations indicate that a water-vapor electrolysis cell using the liquid electrolyte-absorbent matrix design would efficiently operate at 2.24 V at 100 mA/cm^2. A 1-man, 14-cell unit at this 100 mA/cm^2 design point would weight 19.7 lb and occupy 0.19 ft^3. The power requirement would be 284 W.

These estimates indicate that this type of water vapor electrolysis cell is competitive with other life-support systems which generate oxygen by water electrolysis.

CONTENTS

ILLUSTRATIONS

TABLES

Section 1
INTRODUCTION

The water-vapor electrolysis cell operates by absorbing the water that it electrolyzes. Because the operation is with air, an acidic electrolyte is required to prevent an irreversible reaction between the electrolyte and carbon dioxide in the air. Previous research studies (Ref. 1) on the water-vapor electrolysis cell using phosphoric acid indicated that, although the approach was feasible, the power and weight requirement for the cell was extremely high. This was found to be true because concentrated acid was required for the dehumidifying effect necessary to the operation of the cell. The concentrated acid caused a high overvoltage at a low current density.

Projections to a 1-man or larger unit indicated that further work was needed to improve the system. One possibility was the use of a more conductive electrolyte while retaining the dehumidifying effect. Another improvement was in the electrode itself, since the previous work used platinized-platinum screen. Because the electrolyte is held immobilized in a matrix to effect the zero-gravity phase separation, improvements could be made in the matrix to reduce its ohmic resistance and increase its acid retentivity. Good design procedures could be applied to the cell to increase its operational efficiency. At the beginning of this study, cell voltages as high as 4.2 V and as low as 2.45 V had been reported. This last voltage, at a current density of 35 mA/cm^2, represented the best cell performance of a phosphoric acid, immobilized-matrix, water-vapor electrolysis cell (Ref. 2).

When compared with prior studies, the objectives of the present study were to perform research and development to increase the reliability and to reduce the power requirements of a water vapor electrolysis cell. The specific objectives of the program were as follows:

- To investigate the basic nature of sulfuric acid as an electrolyte
- To investigate matrices composed of zeolite gels or other compatible materials

- To select an optimized matrix and electrode combination and to develop these into an operating laboratory model
- To study scale-up parameters and to provide design guidelines for a unit capable of providing oxygen for 1-man for 1 day

The research and development program emphasized six different areas:

- The fundamental properties of sulfuric acid were studied, including the physical and electrochemical properties of the electrolyte.
- Immobilizing matrix materials were evaluated and selected ones were characterized.
- Cell testing was conducted to evaluate the performance of the gelled immobilized matrix cell. Studies include water absorption, cell electrolytic performance, and life testing.
- Cell testing was conducted on a liquid electrolyte-absorbent matrix electrolysis cell. Studies include water absorption, cell electrolytic performance, and life testing.
- Concurrent with these studies, the secondary cell reactions possible in a sulfuric and cell were evaluated. This study included ozone and sulfur dioxide.
- Scale-up calculations were made for the water vapor electrolysis cell.
- Design guidelines were formulated and a feasible design was developed.

The results of this study, together with the work on the phosphoric acid electrolyte-immobilized matrix cell (Ref. 3) further the state-of-the-art of the water-vapor electrolysis cell, making this system competitive with other methods for generating breathing oxygen by water electrolysis.

Section 2
RESULTS AND TECHNICAL DISCUSSION

2.1 FUNDAMENTAL PROPERTIES OF SULFURIC ACID

2.1.1 Introduction

In a water-vapor electrolysis system, the electrolyte performs primary functions in the electrolysis process and in the water absorption process. Current for water electrolysis is carried through the electrolyte by the ionic conduction mechanism. The use of an electrolyte solution rather than pure water reduces the resistance between the electrodes, and, thus, reduces the power required for a given electrolysis rate. The electrolyte must also readily absorb water to replace that which is removed from the system by electrolysis.

Sulfuric acid is considered a candidate electrolyte for use in a water-vapor electrolysis system. Although much is known of its fundamental properties, the information required for construction of an apparatus for the electrolysis of water from a concentrated sulfuric acid electrolyte is limited to a small portion of the total body of information available for these electrolyte solutions. It has been determined that much of the needed information regarding highly concentrated solutions is lacking in the literature. The purpose of this phase of the work was to obtain the necessary data on the fundamental properties from the open literature and from experimental studies. The experimental studies were composed of two parts: physical properties which determine the water absorption characteristics, and electrochemical properties which describe applicability as an electrolyte.

2.1.2 Physical Properties of Sulfuric Acid

Knowledge of the physical properties of sulfuric acid solutions is necessary to describe the performance of a water-vapor electrolysis system which utilizes sulfuric acid as both the water-vapor absorption medium and the electrolyte. The relative humidity of air over sulfuric acid solutions of various concentrations and the conductivity of these solutions must be known to define the useful limits of acid concentration. The rate of transfer of water vapor from a moving humid-air mass to the surface of a sulfuric acid solution and the efficiency of the transfer must be determined as a function of environmental conditions to establish operating limits for the electrolysis cell.

2.1.2.1 Conductance

Conductance curves for sulfuric acid were obtained experimentally by determining values of conductance as a function of temperature and concentration. The resistance of various sulfuric acid solutions at controlled temperatures was determined in a glass conductivity cell having smooth platinum electrodes and a cell constant of 87.5. Resistance measurements were made on an AC impedance bridge* at a frequency of 1000 cps. With these measurements and additional data obtained by other workers (Refs. 4 and 5), the conductance curves shown in Fig. 2-1 were compiled. Values of conductance for temperatures other than those shown can be estimated or obtained from temperature versus conductance curves derived from these data.

2.1.2.2 Ionic Species

Other workers (Ref. 6) have studied the Raman spectra of sulfuric acid solutions to determine the ionic species present. Because the solutions of greatest interest in this study are those of relatively high acid concentration, and because it is in these that the deviations from the ideal are greatest, it is of interest to know the variation of species with concentration. These data are shown in Fig. 2-2 for solutions at 77°F.

*General Radio 1650A, Concord, Mass.

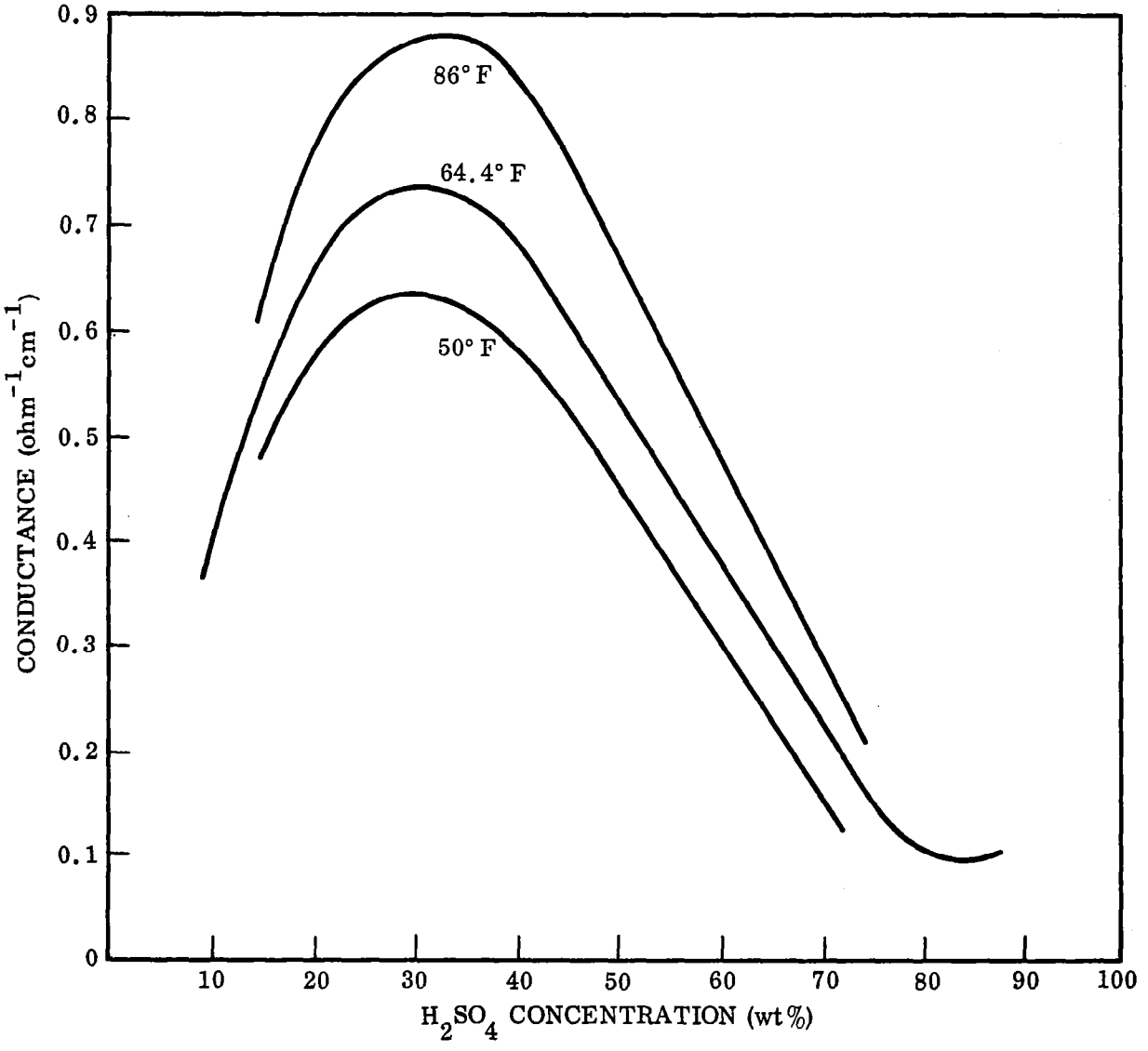

Fig. 2-1 Electrical Conductance Variation With H_2SO_4 Concentration

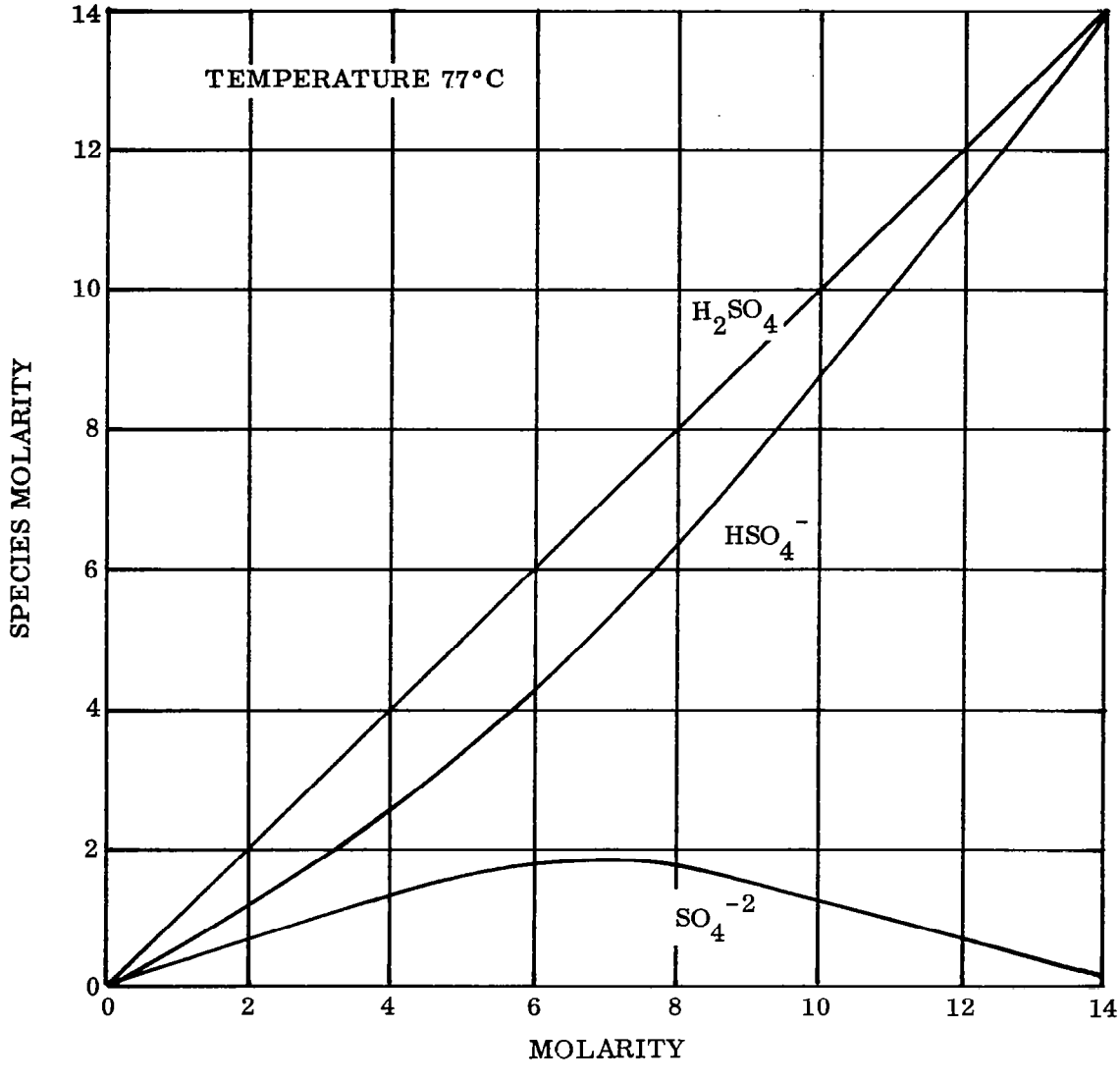

Fig. 2-2 Ionic Specie Concentration Variation With H_2SO_4 Concentration

The figure shows that an increase in the bisulfate ion (or decrease in the sulfate ion) occurs with increasing concentration of the acid, with a simultaneous and corresponding decrease in hydrogen ion.

2.1.2.3 Concentration

In the literature, data for sulfuric acid are usually reported in the concentration units of molarity or as a function of the weight percent acid in the solution. Figure 2-3 is a plot of the weight percent H_2SO_4 as a function of the molarity of the solution (Ref. 7).

2.1.2.4 Water Absorption

The variation in relative humidity over suflfuric acid as a function of acid concentration at a temperature of 77°F under non-flow conditions is shown in Fig. 2-4. In an electrolysis system where water is introduced into the electrolyte by flowing humid air over an electrode in contact with the electrolyte, environmental conditions and electrolysis cell characteristics will influence the water-transfer process. The driving force for water absoprtion consists of the difference between the vapor pressure of the incoming air and the vapor pressure of the acid in the cell. The velocity of the air flowing over the electrode determines the rate at which water vapor is made available for absorption. Water-transfer efficiency is a function of the flow pattern of air over the electrode surface and, therefore, is related to the geometry of the gas flow channel, the physical surface of the electrode, and the gas flow rate.

Analytical analysis. A mathematical analogy to the real water-transfer process can be made using appropriate modifications of Fick's law for diffusion. In a nonflow system, Fick's law has the mathematical form

$$\frac{dw}{dt} = AD\frac{\Delta p}{\delta} \qquad (1)$$

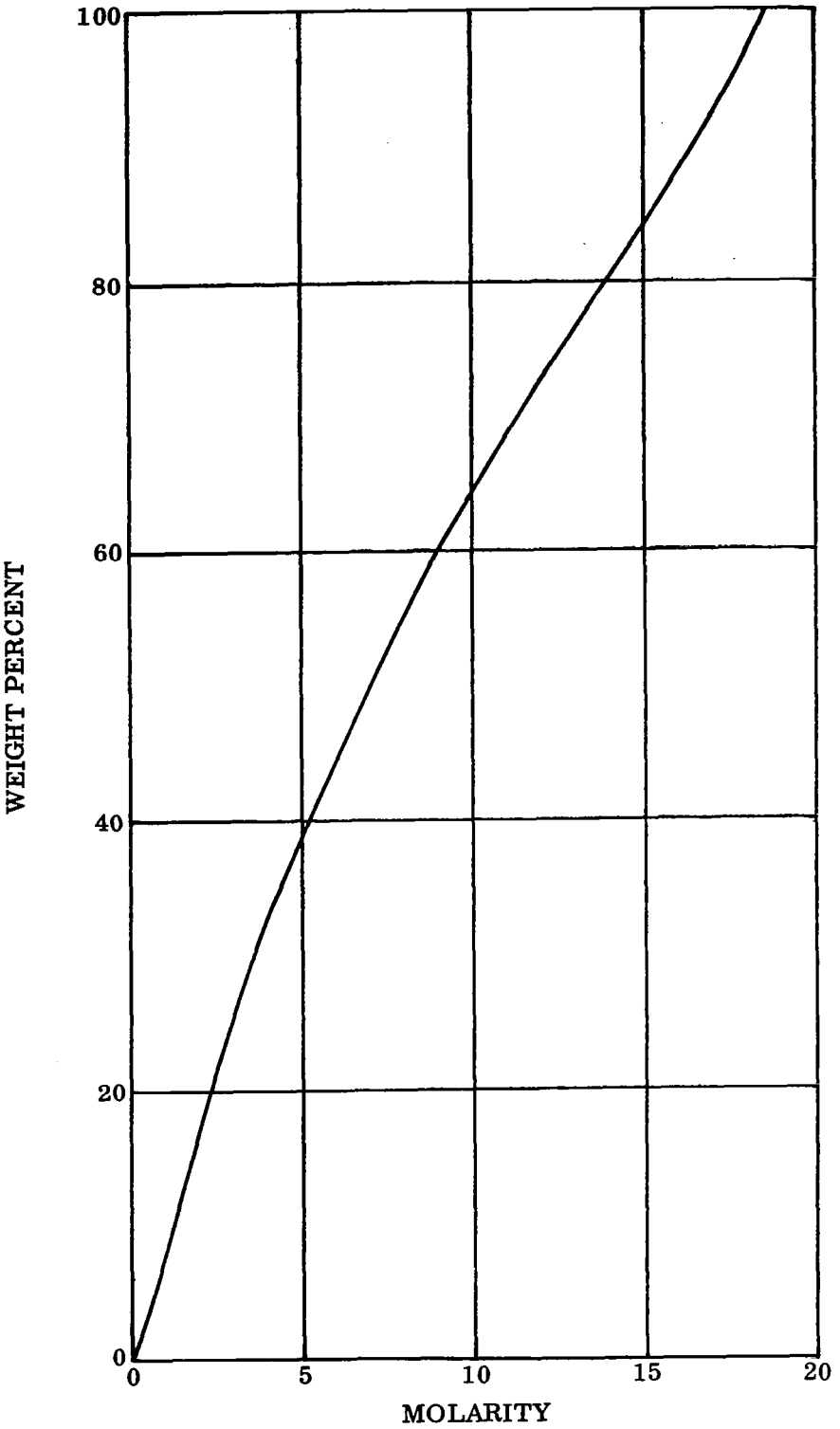

Fig. 2-3 Conversion Graph – H_2SO_4 Molarity to Weight Percent

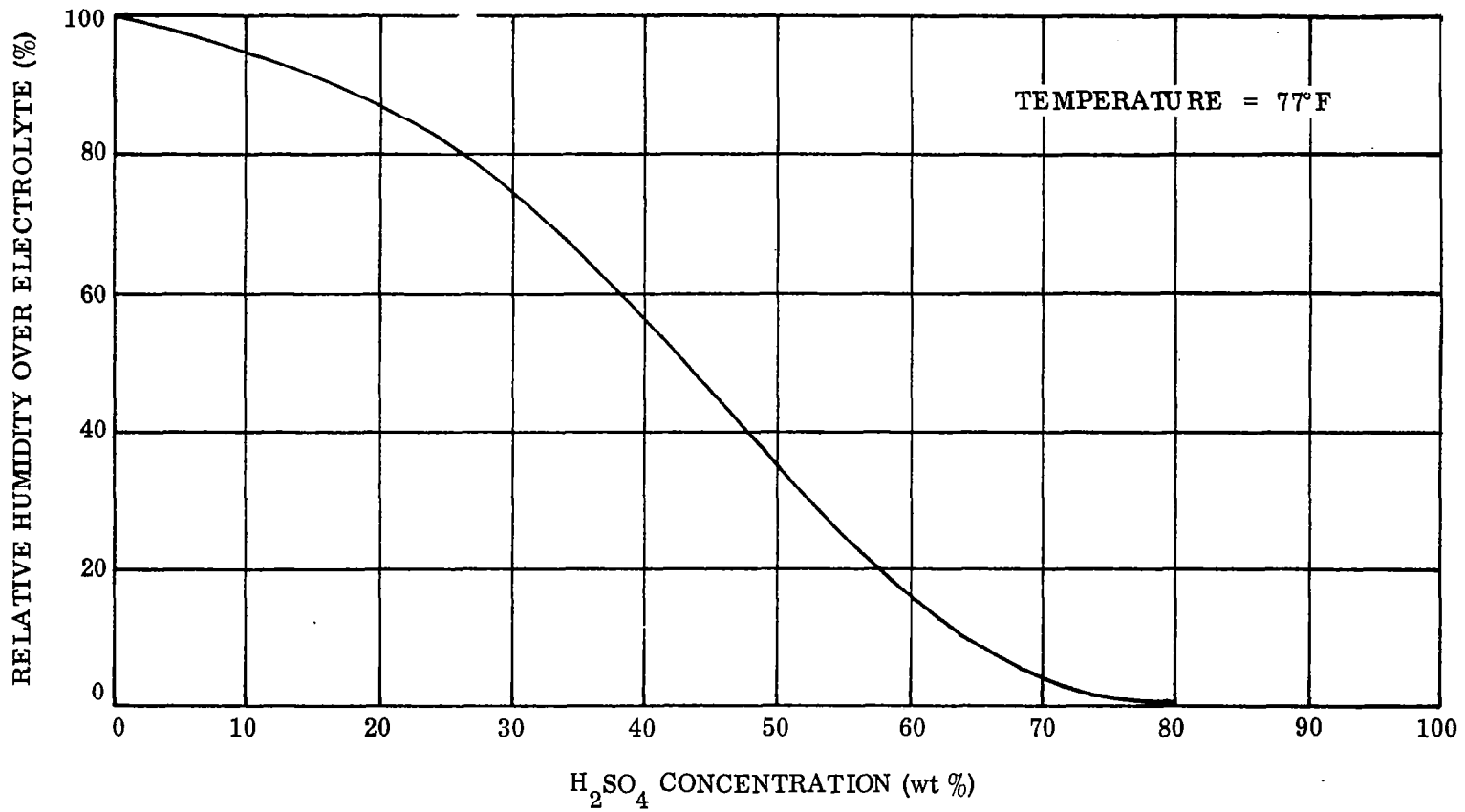

Fig. 2-4 Relative Humidity Variation With H_2SO_4 Concentration

where

dw/dt = weight H_2O transferred per unit time (gm/hr)
A = area (cm^2)
D = diffusion constant (cm^2/hr)
δ = diffusion layer thickness (cm)
Δp = water vapor pressure driving force (gm/cm^3)

In a flowing system, new material is continuously being brought to the surface, and the diffusion layer thickness δ must now contain a flow velocity factor. For the simple case in which the sample is a wide rectangular plate lying in the path of laminar flow, it is possible to write the diffusion layer thickness as (Ref. 8)

$$\delta = \frac{1}{c}\left(\frac{\nu x}{v}\right)^{1/2} \tag{2}$$

where

c = constant
v = the flow velocity in the bulk (cm/sec)
ν = the kinematic viscosity (cm^2/sec)
x = a characteristic dimension of the system (cm)

The proper choice of a characteristic dimension x to describe the diffusion layer thickness is not obvious. This critical dimension probably depends at least on the conditions upstream from the absorbing surface, the geometry of the system, and the roughness of the surface. Length in the direction of air flow has been arbitrarily chosen as the characteristic dimension in Eq. (2) because of the similarity of this system to the heat-transfer system where a film coefficient is generally described for flow parallel to a flat plate in terms of plate length.

Substituting the sample dimensions x and y for the area A and combining Eqs. (1) and (2), a modified form of Fick's law is obtained

$$d\left(\frac{dw}{dt}\right) = \frac{Dc\Delta p v^{1/2}}{\nu^{1/2} x^{1/2}}\, dx \tag{3}$$

which is an expression for the water-transfer rate over a differential area, y dx. Thus, it is seen that the rate of transfer depends upon the viscosity of the flowing fluid, the length and width of the sample, the flow velocity, and the pressure gradient of the water vapor from the air to the absorbent. Assuming the viscosity of the air to be constant, this equation can be written

$$d\left(\frac{dw}{dt}\right) = \frac{Ky\Delta pv^{1/2}}{x^{1/2}}\,dx \tag{4}$$

where

$$K = \frac{Dc}{\nu^{1/2}}$$

In a rectangular cell with air flow entering along one edge, the water vapor driving force Δp in Eq. (4) is a function of the distance x. If the acid concentration is assumed constant, this function can be expressed

$$\Delta p = \Delta p_o \exp\left[\frac{-2K}{az}\left(\frac{x}{v}\right)^{1/2}\right] \tag{5}$$

where

Δp_o = initial water vapor pressure difference (gm/cm^3)
a = constant
z = height of the flow chamber (cm)

By using these assumptions and combining Eqs. (4) and (5), the water-transfer rate as a function of cell geometry is obtained

$$d\left(\frac{dw}{dt}\right) = Ky\Delta p_o\left(\frac{v}{w}\right)^{1/2} \exp\left[-\left(\frac{2K}{az}\right)\left(\frac{x}{v}\right)^{1/2}\right] dx \tag{6}$$

In working systems, the integral form of this equation is more useful. The total amount of water transferred per unit time over an absorbent liquid of area $A = (x_2 - x_1)y$, where cell length $L = x_2 - x_1$, is given as

$$\left.\frac{dw}{dt}\right|_L = ayz\Delta p_o v\left[\exp\left(\frac{-2K}{azv^{1/2}}\, x_1^{1/2}\right) - \exp\left(\frac{-2K}{azv^{1/2}}\, x_2^{1/2}\right)\right] \qquad (7)$$

According to this equation, the water-transfer rate dw/dt in a rectangular cell is not directly proportional to the cell length L, i.e., water-transfer rate per unit length is not constant but decreases in the direction of flow.

The mathematical description given in Eq. (7) can be applied to the design of a practical cell. For example, the decrease in absorption rate with distance (in the direction of flow) predicted by this equation for a rectangular cell can be minimized by inserting baffles in the flow chamber to increase the velocity as a function of distance.

It should be noted, however, that a rigorous treatment has not been given to the derivation of Eq. (7). In a practical cell, the diffusion layer thickness δ at the point of initial contact of moist air with the absorbing acid surface $x = x_1$, is not necessarily a boundary or initial diffusion layer thickness. The true boundary condition exists at $x = 0$, which in a practical system is some point upstream from the leading edge of the absorbing surface (defined here as $x = x_1$). To illustrate that x cannot be a true boundary point, we let $x_1 = 0$. Then at $x = x_1 = 0$, the diffusion layer thickness, Eq. (2), is zero and the water transfer rate, Eq. (3), is infinite; a situation which cannot exist in a real cell. Because the derivation includes the assumption of constant acid concentration in the direction of air flow, Eq. (7) is a gross simplification of the real water transfer process. For a rigorous description of the water transfer process in an operating electrolysis cell, an empirical derivation procedure based on actual experimental data is suggested.

Experimental results. Experiments were designed to determine the effects on the water transfer rate in a gas-sulfuric acid system resulting from changes in vapor pressure gradient and gas flow rate.

Nitrogen was used as the gas phase in the experiments. Humidification of the gas took place in a temperature-regulated bubbler system, and the humid gas was then passed through a test cell containing sulfuric acid. The gas flow rate was determined by measuring the amount of water condensed in a test tube (at -108 °F) in a 1-min interval with the assumption that the vapor pressure of the gas was fixed by the humidifier.

Figure 2-5 is a diagram of the test apparatus. The test cell consisted of a glass tube containing a ceramic boat which held the sulfuric acid sample. Water absorption rates were determined by periodically weighing the boat. The data are presented as the average rate of water transfer as a function of the average H_2SO_4 concentration.

Some representative results for these experiments are presented in Fig. 2-6. The initial points at the highest concentration levels are somewhat high because temperature equilibrium had not been reached. As was predicted, an increased flow rate results in an increased water-transfer rate. Figure 2-7 shows how a change in the pressure gradient affects the rate of water transfer. The pressure gradient is obtained by subtracting the vapor pressure of 54 wt% H_2SO_4 from the water vapor pressure saturated by the bubblers. In the concentration region covered by the data presented, dp/dc (slope of the vapor pressure-concentration curve) is a constant. At constant flow, the predicted rate is proportional to the pressure gradient. The experimental data agree with this, since the slope of each of the three curves is the same; i.e., $\frac{dw/dt}{\Delta p}$ = constant.

The correlation between the mathematical model given in Eq. (4) and the experimental results is within the deviation limits to be expected from a comparison of the theoretical model with a non-ideal experimental system. The model is useful as a guideline in optimizing an operational system.

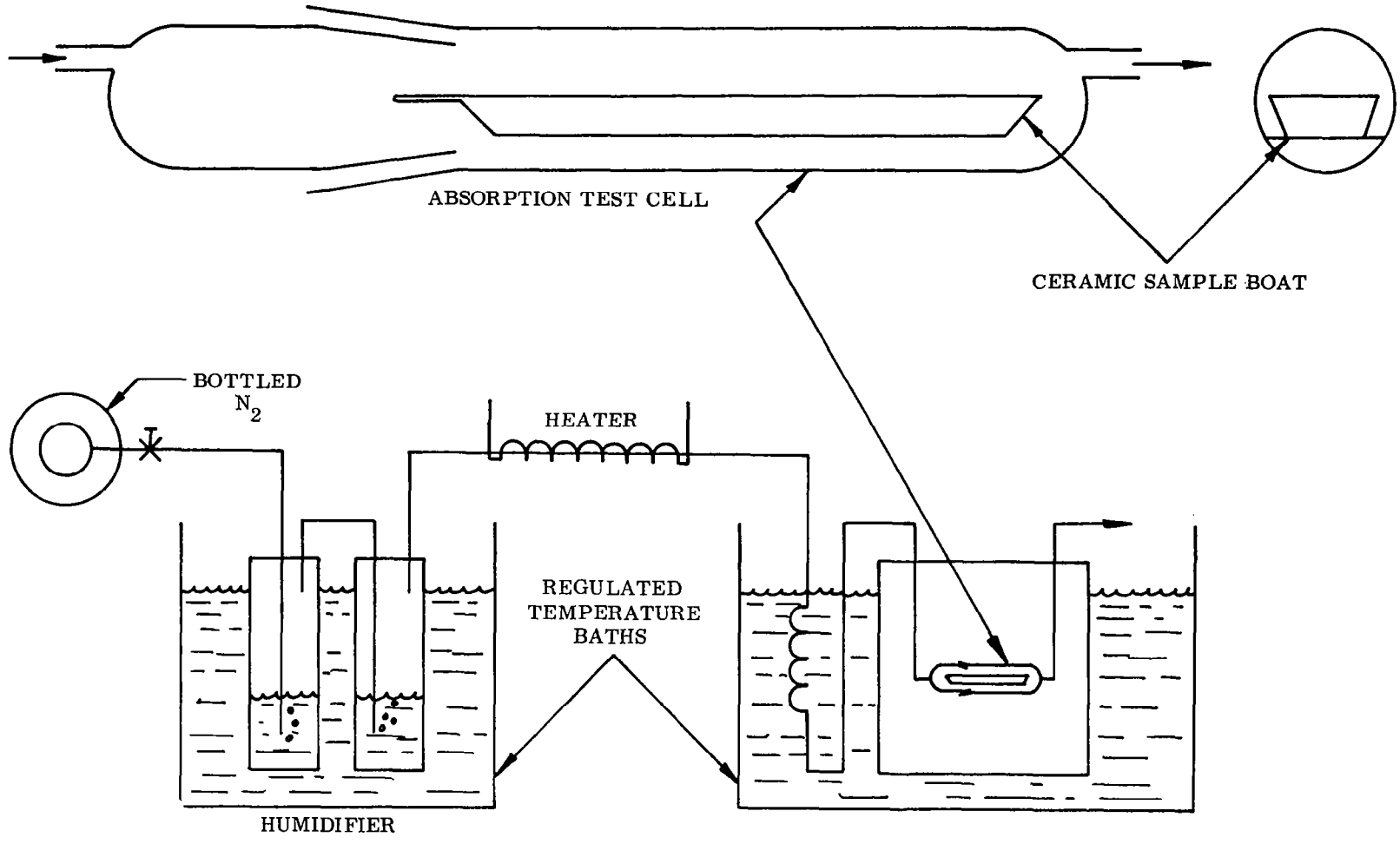

Fig. 2-5 Water Absorption Test Apparatus

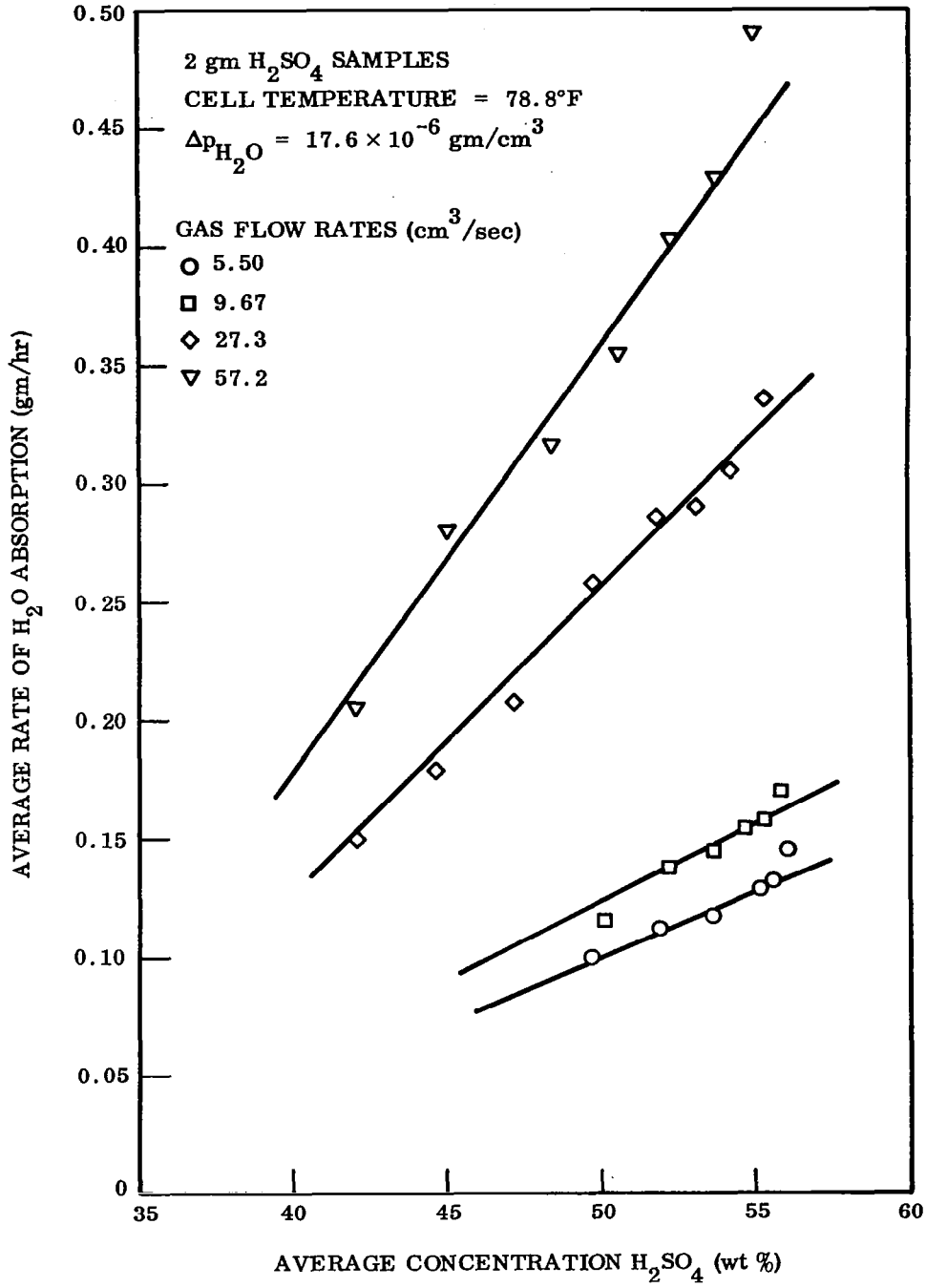

Fig. 2-6 Water Absorption Rate Variation With Various Concentrations of H_2SO_4 at Different Gas Flow Rates

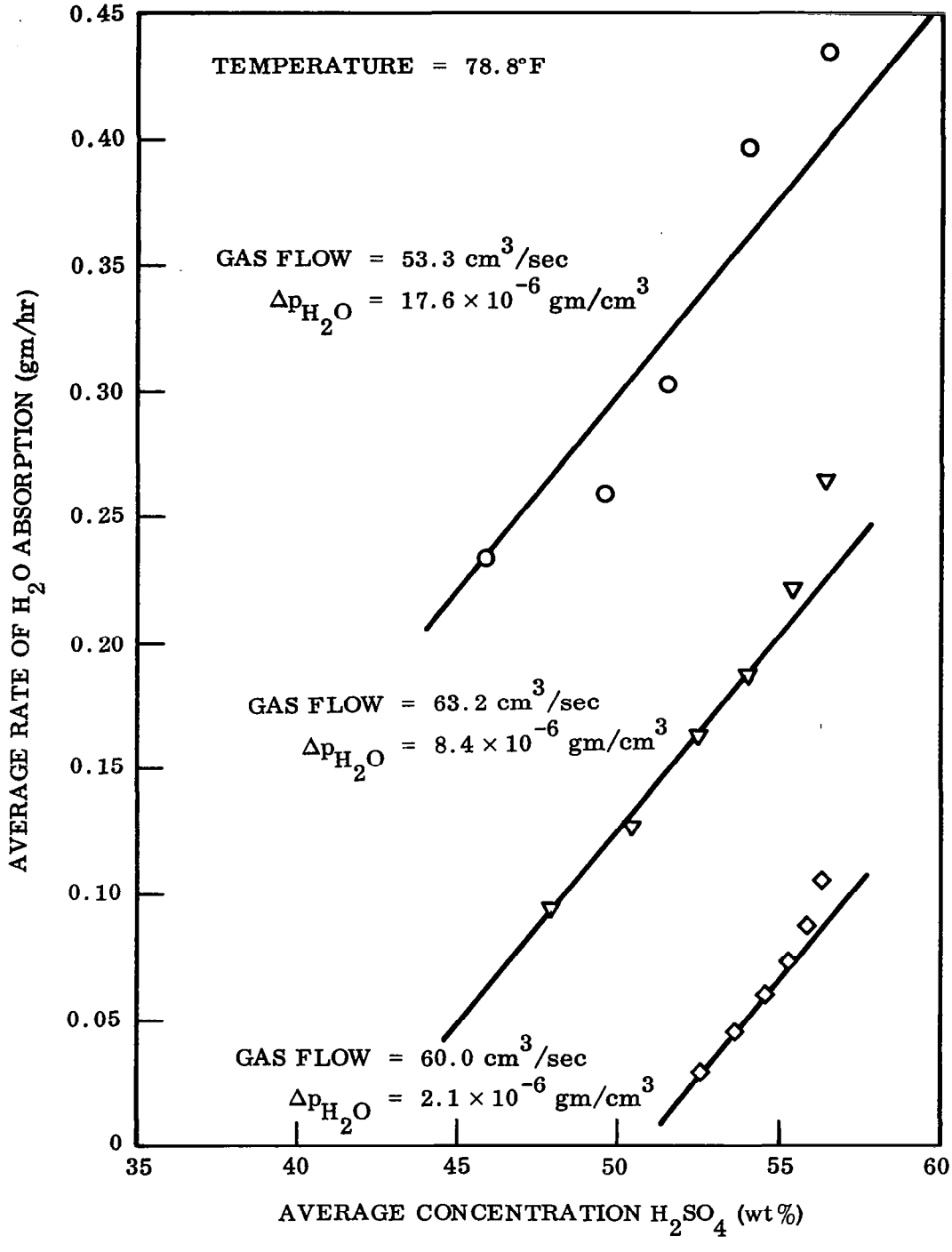

Fig. 2-7 Water Absorption Rate Variation With Various Concentrations of H_2SO_4 at Different Water Vapor Pressures

2.1.3 Electrochemical Properties of Sulfuric Acid

2.1.3.1 Heat Balance

A study of the electrochemical properties of sulfuric acid solutions includes an examination of the thermodynamics (Ref. 9) of the desired electrode reactions to determine the rate of heat production in an operating electrolysis cell.

Half Cell Reactions	Heat of Reaction	
$H^+ + e^- = \frac{1}{2}H_2(g)$	$\Delta H = 0$	(8)
$\frac{1}{2}H_2O(\ell) = H^+ + e^- + \frac{1}{4}O_2(g)$	$\Delta H = +34.16$ Kcal/equivalent	(9)

The heating of the system by these electrode reactions can be predicted theoretically and expressed in terms of cell potential and reaction entropy.

A short derivation of such an expression for the electrode heat effect of an operating electrolysis system is summarized in the following equations.

For a system at constant pressure, with electrical work, the first law of thermodynamics can be written as

$$\Delta H = \Delta Q - \Delta W_e \tag{10}$$

where

- ΔH is the enthalpy change of the system
- ΔQ is the amount of heat added to the system
- ΔW_e is the electrical work done on the environment, which is $n\underline{F}(-V_c)$ where n and $\underline{F}$ are constants and V_c is the applied cell voltage

By combining Eq. (10) with the second law of thermodynamics, $\Delta F = \Delta H - T\Delta S$, the expression can be written

$$\Delta F = \Delta Q - n\underline{F}(-V_c) - T\Delta S \tag{11}$$

where

ΔF is the free energy change of the system

T is the temperature

ΔS is the entropy change of the system

But we also can write:

$$-n\underline{F}V^{o} = \Delta F^{o}_{\text{galvanic}} = -\Delta F^{o}_{\text{electrolysis}} \tag{12}$$

where V^{o} is the open circuit voltage and $\Delta F^{o}_{\text{electrolysis}}$ is the free energy of the system as used in Eq. (11).

By combining Eqs. (11) and (12) above and solving for $-\Delta Q$, the heat added to the environment, we obtain the following expression for the heat production of the operating electrolysis system:

$$\text{heat output} = -\Delta Q = n\underline{F}(V_c - V^{o}) - T\Delta S = n\underline{F}\eta - T\Delta S \tag{13}$$

where η is the overvoltage for the system.

If the net heating is zero, then $Q = 0$, and

$$nF\eta = T\Delta S \tag{14}$$

or

$$\eta = \frac{T\Delta S}{nF} \tag{15}$$

To find the solution to this equation for the acid system used, the following thermodynamic values may be employed. For

$$\tfrac{1}{2}H_2O(\ell) = \tfrac{1}{2}H_2(g) + \tfrac{1}{4}O_2(g)\ (25°C) \qquad \Delta H = 34.16\ \text{Kcal/equiv.},$$

$$\Delta S = 19.5\ \text{cal/deg}\ (25°C) \qquad V^o = 1.23\ V$$

If Eqs. (14) and (15) are used, the no-heat voltage for the cell is 1.48 V, and $\eta = 0.25$ V. At this cell voltage (exclusive of resistance heating due to the electrolyte), there will be no net heating of the cell. Below this voltage, the cell will tend to be cooled by the reaction.

The effect of inefficient electrolysis and the heat of solution are not important in the calculation of the no-heat voltage. These effects are described below.

Effect of inefficient electrolysis. In a system such as that described, a certain amount of water migrates from the water source at the O_2 electrode to the H_2 electrode. When the H_2 is produced, it is saturated with water vapor at a pressure which is determined by the concentration of the acid at the H_2 electrode. This process leads to an inefficiency in the electrolysis process. Heat can arise from such an inefficiency if the acid concentration is different at the point of evaporation than that at the point of absorption. The amount of heating is proportional to the amount of water lost by this process. At an acid concentration of 54 wt%, the vapor pressure of water is 8 mm of Hg. Thus, for a total pressure of one atmosphere (760 mm Hg), the mole ratio of water to hydrogen is just equal to the ratio of the pressures of the two species, which is 0.0106.

The International Critical Tables (Ref. 4) may be used to estimate the amount of heating due to the difference in the heat of solution at the two electrodes. With a concentration difference of 10%, this heating is about 2 Kcal/mole of water transported. With the mole ratio for water-to-hydrogen above, this amounts to only 20 cal/mole of H_2 produced, a very small effect when compared to that of the electrolysis process itself.

Effect of the heat of solution. In an operating system for the continuous absorption and electrolysis of water, a heat effect occurs from the heat of solution of the water being absorbed in the concentrated sulfuric acid. The net heat effect of forming liquid water and drier air from moist air is negligible (Ref. 10) at 25°C. It is less than 2% of the heat of vaporization. There is also a change in the heat effect of the electrolysis, since an acid solution is used rather than pure water. The standard heat of reaction as given is for the reference state of both reactants and products. However, the two heat effects really must be combined. It is useful to employ the following diagram to visualize these effects:

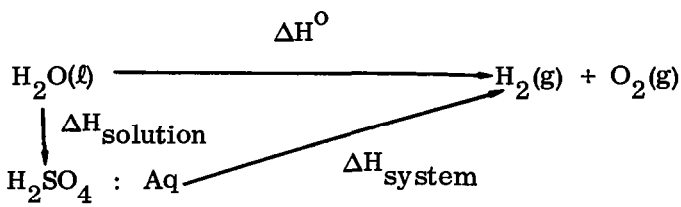

At constant temperature and pressure:

$$\Delta H_{system} = \Delta H^o - \Delta H_{solution} \tag{16}$$

The total heat effect of these two processes, the water going into solution and the subsequent electrolysis of it, is merely

$$\Delta H_{total} = \Delta H_{system} + \Delta H_{solution} = \Delta H^o \tag{17}$$

That is, only the one heat of reaction is necessary to describe the system. Both of the processes occur at the same instantaneous concentration which exists at the electrode-electrolyte interface. Thus, it is not important that part of the water may be transported through the electrolyte, or that the electrolysis reaction is less than 100% efficient.

2.1.3.2 Polarization Studies

Bulk liquid electrolyte tests were performed to obtain baseline polarization data for different electrode configurations. The use of bulk liquid tests eliminate many of the complicating factors inherent with a matrix type cell. These tests are useful in determining the performance characteristics of electrodes operating in various electrolyte concentrations.

The apparatus for this test work is shown schematically in Fig. 2-8. The central portion, or the electrolysis section, consists of two compartments separated by a sintered glass disc with a means of inserting a capillary reference lead into each compartment. Each reference cell consists of a modified H-cell with a capillary electrolyte bridge to connect it with the electrolysis section. In the reference H-cell, there are three black platinized platinum electrodes, one inserted from the bottom of each side of the H-cell and one suspended from above on the side nearest the electrolysis cell. The two lower electrodes are used to electrolyze the reference acid solution to produce hydrogen gas which bubbles over the reference electrode suspended from above. A 6.1 M H_2SO_4 solution was used in the reference electrode compartment. The plotted polarization voltages were corrected to correspond to the values which would be obtained with a hydrogen reference electrode in acid the same concentration as the electrolyte being studied. In all tests a working electrode with a geometric area of 2.4 cm^2 was used. Three different electrodes were used: bright platinum sheet, black-platinized platinum sheet,* and commercially available electrode material.**

The commercial electrode is made from tantalum screen with a mixture of fluorocarbon and black platinum pressed into the openings of the screen.*** In the tests with the commmercially available electrode material, a special electrode-holding fixture was used to allow the gas generated by the electrode to escape without flowing

---

*Exact platinum black content unknown, but probably about 4 mg/cm^2
**American Cyanamid Corp., Type AA-1
***Approximately 9 mg black platinum per square centimeter apparent area

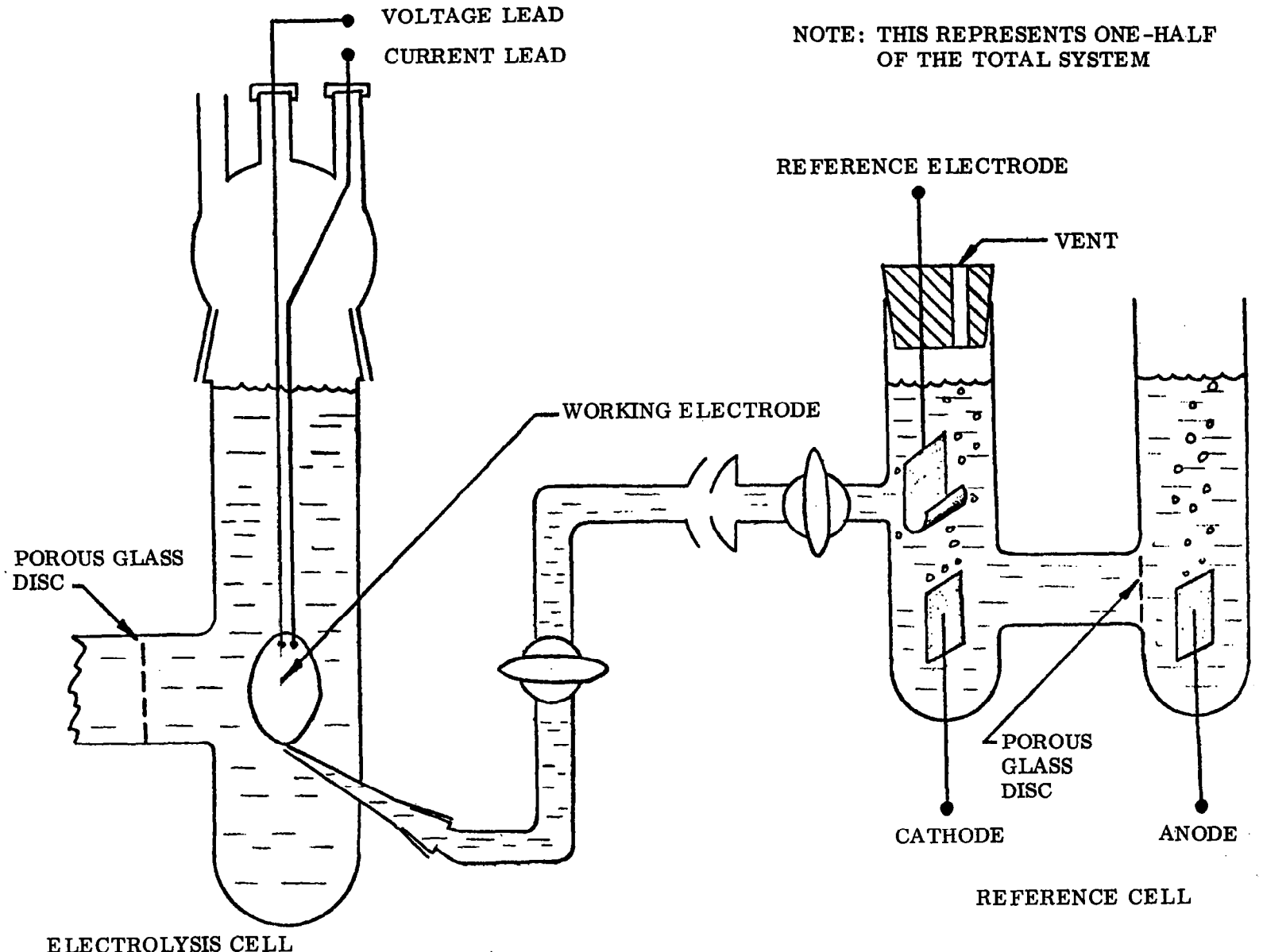

Fig. 2-8 Electrode Polarization Apparatus

over the working face of the electrode. The other electrodes were covered on the back with platers tape to prevent electrolysis on the nonworking face.

Data were obtained from the electrode samples by measuring the reference voltage versus the working electrode for different current densities. For the platinum sheet, both bright and platinized, two different polarization values for the oxygen electrode were found at the same current density. The different states were approximately 40 mV apart and the observance of these two states depended upon the conditions imposed on the electrode. If the current through the cell was reversed or if the system was idle for sometime (overnight), the lower polarization value was observed. However, when the polarization of the oxygen electrode exceeded about 2.07 V, the second polarization state was obtained and the electrode tended to remain in this state. This potential is the thermodynamic potential for the formation of ozone which may account for this phenomena; these two electrode potential states were not observed with the commercially available electrode material.

Results of these experiments are shown in Figs. 2-9 and 2-10. The first figure compares the anode and cathode polarizations for the three different electrodes in approximately the same acid concentration. The superior performance of the commercially available electrode can be seen quite readily. Since more platinum black can be placed on these electrodes, the considerably greater surface area is manifested in a lower polarization voltage at the same apparent current density; the real current density of the screen type electrode is much lower than the apparent, or geometric, current density because of its high surface area. Figure 2-10 illustrates the IR free-cell voltage (the sum of the anodic and cathodic polarizations) for two electrode types at different current densities and H_2SO_4 concentrations. By chossing the operating acid concentration and an operating current density (based on geometrical area), the corresponding cell voltage may be determined. This voltage is an IR free voltage, i.e., one that does not include the voltage loss attributed to the resistance of the cell or to any mass transfer restrictions imposed by the immobilizing matrix.

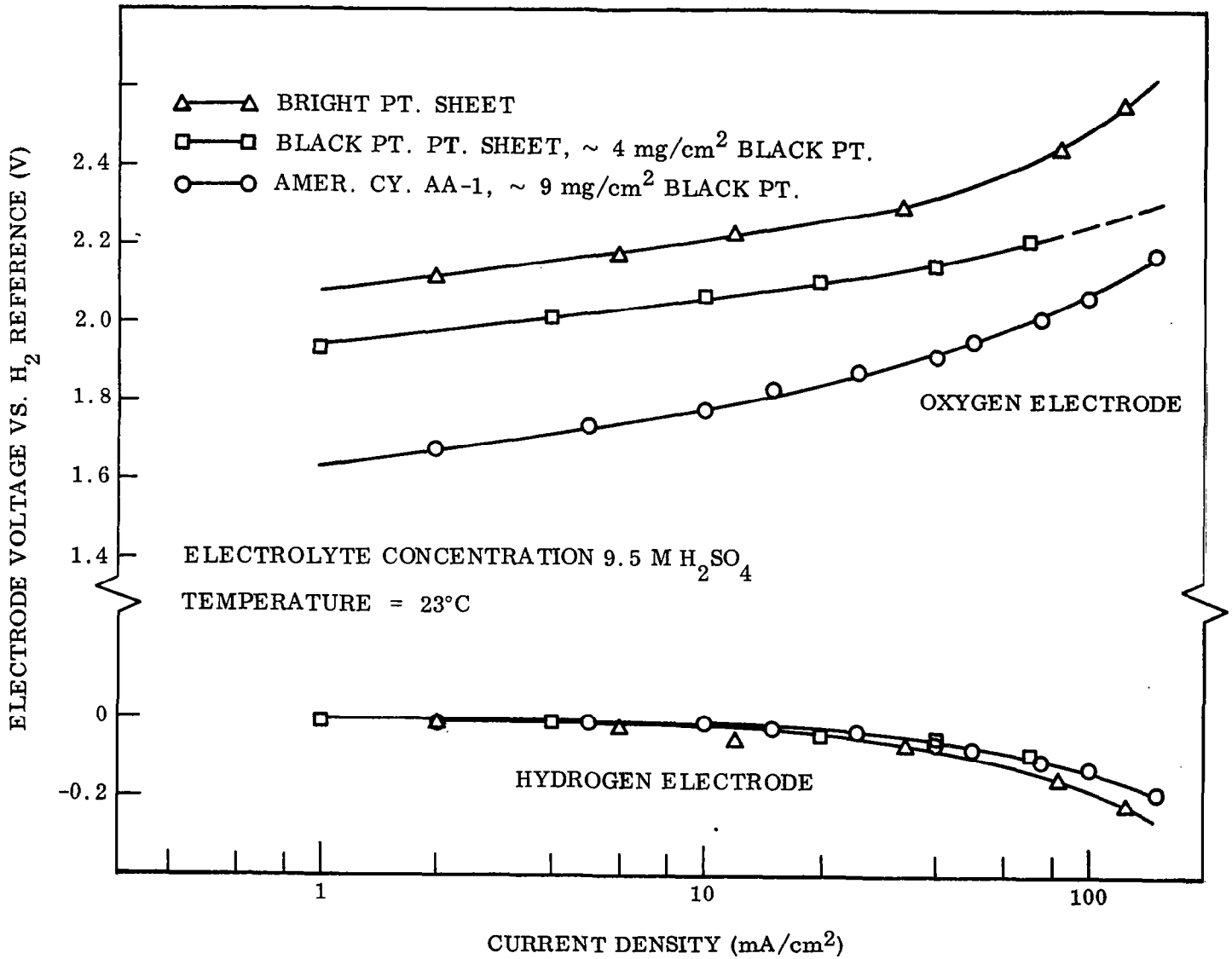

Fig. 2-9 Electrode Polarization Characteristics in 9.5 M H_2SO_4

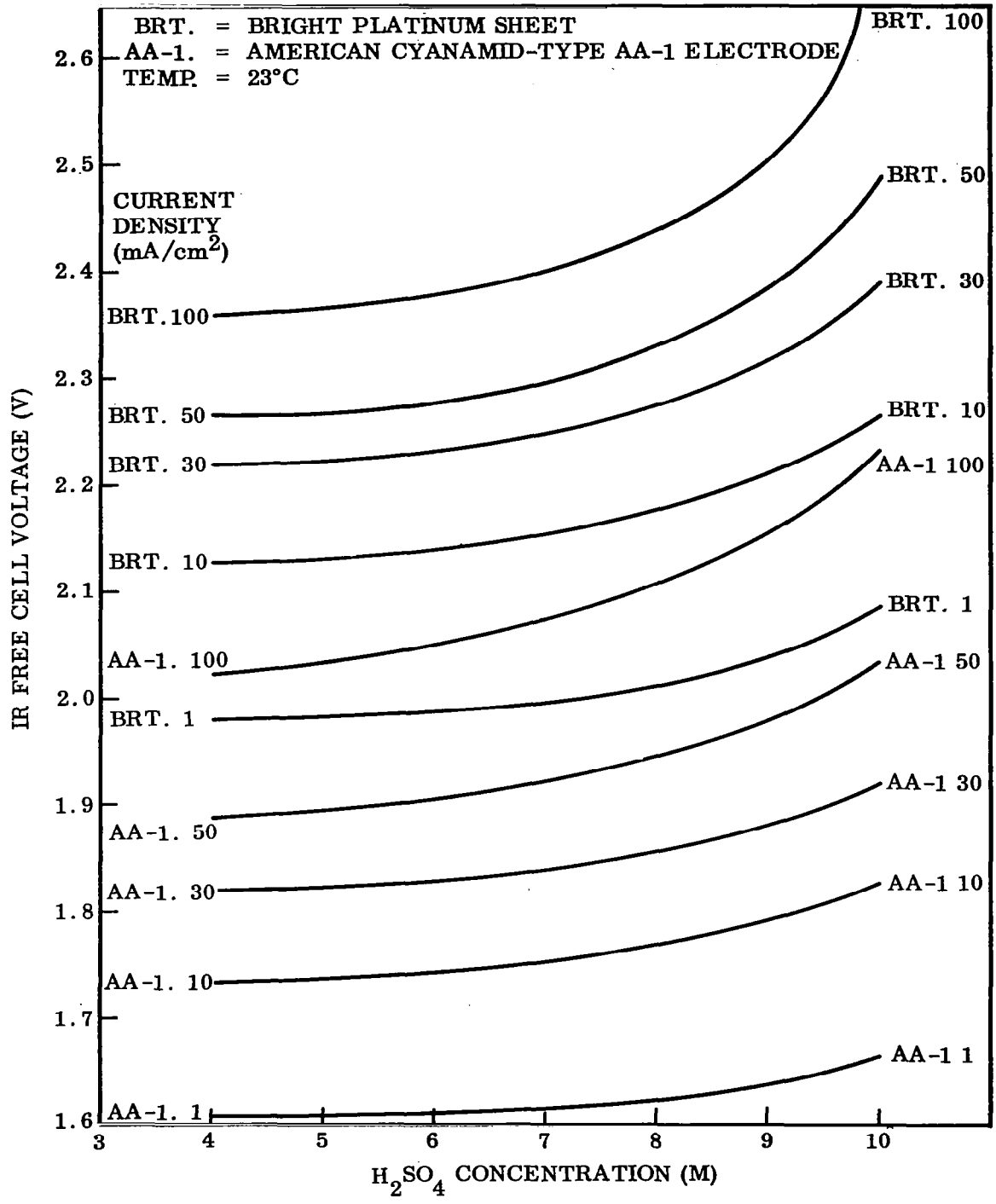

Fig. 2-10 Cell Polarization Variation With H_2SO_4 Concentration at Different Current Densities – Two Electrode Types

2.1.3.3 Secondary Cell Reactions

A factor which can greatly affect the operation of the sulfuric acid electrolysis system is the presence of unwanted side reactions. Some of the major reactions are presented in Table 2-1.

Table 2-1

H_2SO_4 ELECTROLYSIS HALF-CELL REACTIONS

	Reaction	Voltage[(a)]
Cathodic	$SO_4^{-2} + 4H^+ + 2e^- = SO_2 + 2H_2O$	0.17
	$HSO_4^- + 3H^+ + 2e^- = SO_2 + 2H_2O$	0.11
	$2H^+ + 2e^- = H_2$	0.00
Anodic	$2H_2O = O_2 + 4H^+ + 4e^-$	-1.23
	$2H_2O = H_2O_2 + 2H^+ + 2e^-$	-1.77
	$O_2 + H_2O = O_3 + 2H^+ + 2e^-$	-2.07
	$2SO_4^{-2} = S_2O_8^{-2} + 2e^-$	-2.01

(a) Relative to a hydrogen reference electrode.

The nongaseous products formed at the oxygen electrode are not very stable in the electrolyte system, especially when in contact with platinum. In addition, these products can migrate to the cathode and be reduced electrochemically. As long as the steady-state concentration is low and the spontaneous decomposition does not produce appreciable quantities of O_2 in the electrolyte, no particular difficulty is presented.

Ozone production. The most troublesome anodic side reaction is the generation of ozone. If ozone is generated at the oxygen electrode, it must be reduced by some

external device to prevent the cabin atmosphere from being contaminated. Because this requires auxiliary equipment, the logical place to prevent ozone evolution is at the electrode. Furthermore, the presence of ozone at the oxygen electrode may have a deleterious effect on the long-term performance of the electrode. To study the generation of ozone by an electrode in H_2SO_4, an ozone meter* was used to monitor the ozone concentration of the oxygen gas stream. The bulk liquid electrolyte apparatus described in the previous section and shown in Fig. 2-8 was used for the ozone tests. The ozone meter samples the gas at a rate of 140 cm^3/min and since this rate could not be met by the O_2 produced in the electrolysis cell, the room atmosphere was used to sweep through the cell to make up the difference. The true ozone concentration was then calculated by assuming that the O_2 process was 100% efficient, and a correction made for the large volume of air required by the sampling device. The amount of ozone in the effluent gas stream is the ratio of the ozone concentration in the sample air stream (as measured by the ozone meter) to the oxygen produced. For the ozone meter used (where the sampling rate is 140 cm^3/min):

$$\text{ozone concentration (ppm)} = 3.69 \times 10^{-7}\ Z/I \qquad (18)$$

where Z = measured ozone concentration, parts/hundred million; I = electrolytic current (amp). Sample electrode materials were tested at different oxygen electrode overvoltages. The ozone produced was measured, the production rate was calculated, and the results of this series of tests were plotted (Fig. 2-11). Because the black platinum has a catalytic effect tending to decompose the ozone, the black platinum catalyzed electrodes have a higher electrode voltage for a given ozone production. The same amount of ozone is probably produced by the electrode, but some of it is decomposed before it leaves the electrode surface. The open structure of the AA-1 electrode, coupled with the waterproofing incorporated in the electrode, tends to make the produced gases adhere to the surface of the electrode when the electrode is immersed in bulk electrolyte. Compared with the sheet electrodes, relatively large gas bubbles form on the AA-1 electrode. This longer bubble residence time allows

*Model H-100-LC ozone meter and Model R-100 potentiometer recorder, Welsbach Corp., Philadelphia, Pa.

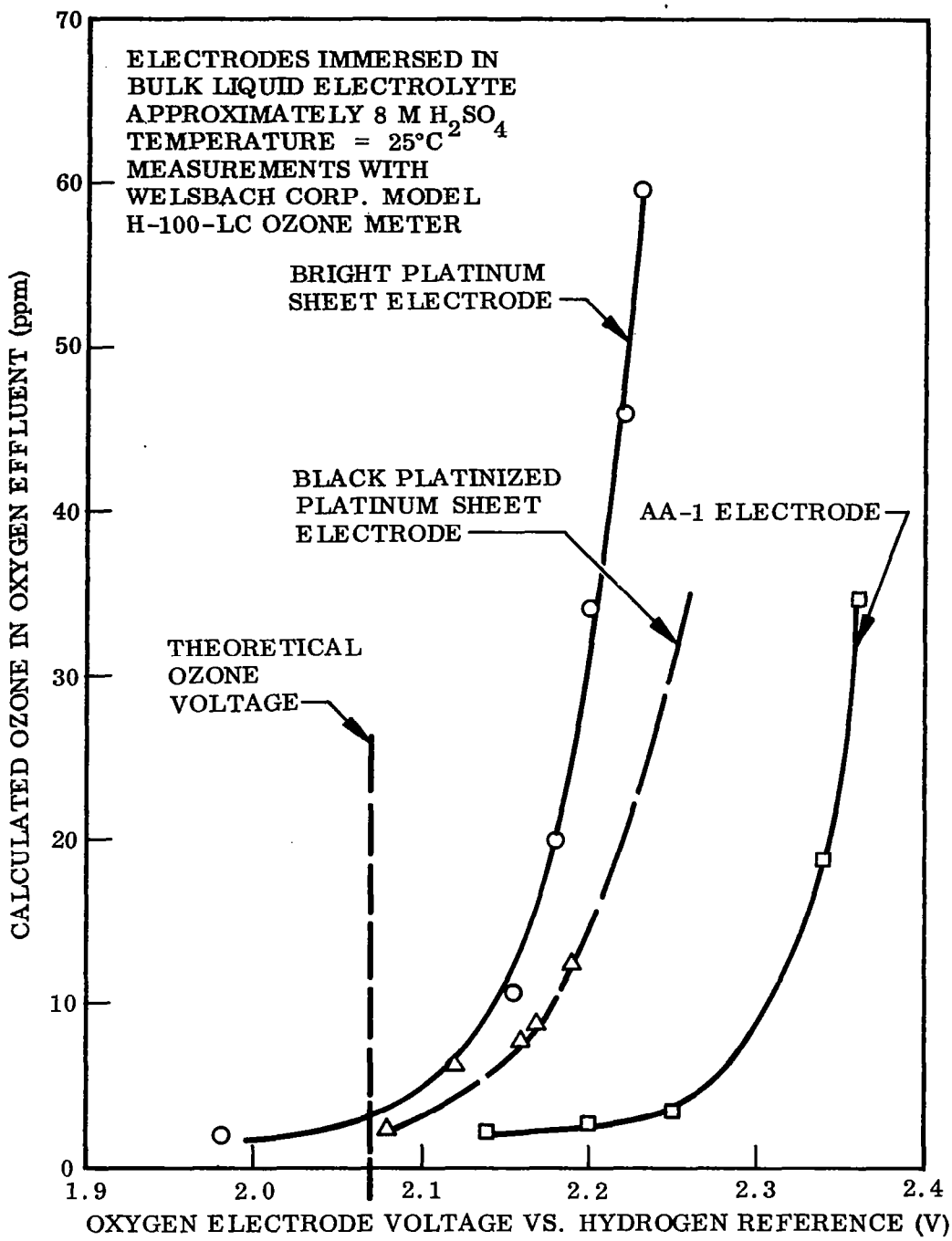

Fig. 2-11 Ozone Production Variation With Oxygen Electrode Voltage – Three Electrode Types

the ozone to become further decomposed with these electrodes; hence, this measured ozone rate is lower at a given overvoltage than the sheet electrodes. In a practical cell, the gas flows away from the electrode surface at a faster rate than in the bulk liquid tests since there is no liquid to limit the rate of bubble removal. Ozone then, in the matrix cells, should be generated at lower electrode voltages than described by this curve, as was found to be true when the effluent from a liquid electrolyte-absorbent matrix cell was measured (see Section 2.4.4).

Although the curve of ozone generation versus overvoltage appears to change gradually with increasing oxygen electrode voltage, the generation of ozone is probably a rather abrupt function of this voltage. For practical purposes, any oxygen electrode (referenced to a hydrogen electrode) voltage over 2.07 V (the theoretical ozone voltage) may be considered to produce large quantities of ozone from a trace contaminant standpoint.

Data obtained from the bulk liquid tests did not clearly indicate the effect of acid concentration on the anodic overvoltage for ozone evolution, although the acid concentration may well effect this voltage. Cell tests discussed later, did not cover a wide range of acid concentrations. However, lacking detailed and conclusive evidence, the anodic overvoltage value of 2.07 V should be used as a limiting guideline for practical cell operation.

Because levels greater than 1 to 2 ppm of ozone are undesirable, it is necessary to keep the oxygen electrode voltage below this level. This is an important factor in the trade-off of acid concentration versus cell performance, since the lower acid concentrations allow the anode to operate at lower overvoltages although the water absorption rate diminishes.

Reduction of H_2SO_4. The reduction of the H_2SO_4 in the electrolyte, even to a small extent, lends to eventual loss of usefulness of the electrolysis cell because of a loss of conductivity and water absorption capability. In the reduction process, the possible products may be SO_2, H_2S, or S. Several workers have observed H_2S in the operation of H_2SO_4 electrolyte fuel cells at elevated temperatures. Because the test cells

now being used are small, the reduction product, if any, will also be small in quantity. Evaluation of methods of detecting small quantities of the product indicated that the detection of these materials is impractical at the present time. The main consideration was the accuracy of detection, although the cost to perform the experiments was found to be prohibitively high. An experiment was conducted, however, to determine the effect of SO_2 on the hydrogen electrode since this product may affect the catalytic behavior of the platinized electrode.

The standard bulk liquid electrolyte polarization electrode apparatus (Fig. 2-8) was altered to admit SO_2 as small bubbles near the working hydrogen electrode. A baseline polarization curve was obtained prior to admitting the gas. The cell was then set to operate at 1 mA/cm^2. When the gas was first admitted, the polarization dropped but then rose slowly with time, as shown in Fig. 2-12. During the run, no visible signs of hydrogen evolution were visible. When the current density was increased to 200 mA/cm^2 and then decreased, a hysteresis curve was traced, as shown in Fig. 2-13. The polarization characteristics of the electrode in the absence of SO_2 are shown by the lower curve; the polarization characteristics with SO_2 are shown in the upper curve. The arrows indicate the direction of current application. A film of sulfur on the electrode may increase the polarization, but gas evolution at high current densities dislodges the film, thereby improving the electrode polarization. After an extended period of operation, a milky cloudiness due to sulfur formation was observed in the electrolyte. An examination of the hydrogen electrode after operation showed the presence of a thin film of sulfur over the electrode surface.

The fact that free sulfur was obtained from the action of SO_2 on the electrode during electrolysis indicates the possibility of detecting H_2SO_4 degradation by monitoring for free sulfur. To observe this phenomenon further, a lead (Pb) electrode was prepared for use as the hydrogen electrode in a solution of 8.1 M H_2SO_4. The electrode was operated at 200 mA/cm^2 for one hour at a hydrogen overpotential of 1.5 V, about 7.5 times the polarization of a smooth platinum electrode. No SO_2 was bubbled into the electrolyte. The electrolyte did not become cloudy, and no sulfur was found on the electrode after the test. Furthermore, the theoretical amount

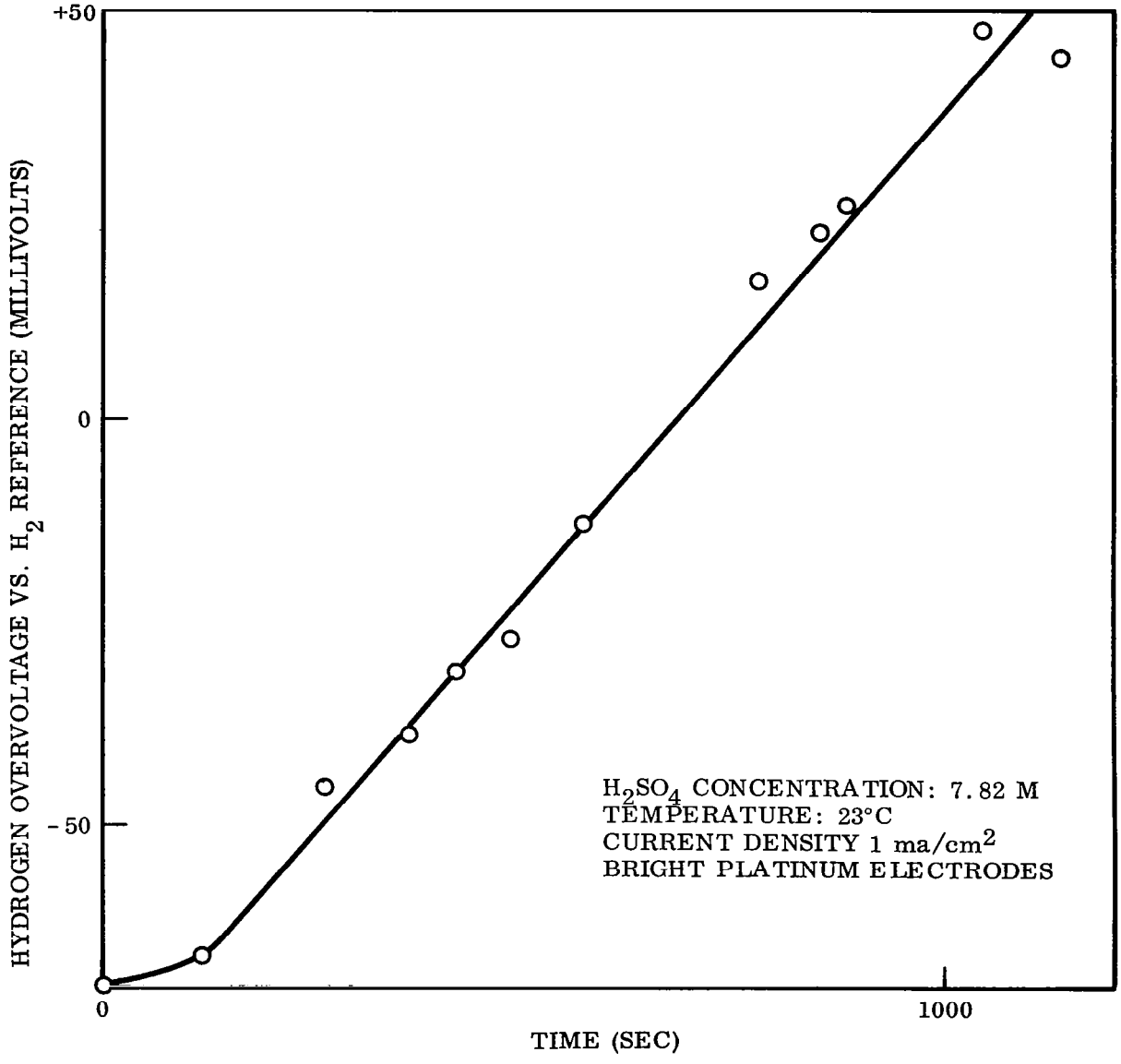

Fig. 2-12 Hydrogen Electrode Polarization Variation With Time With Addition of SO_2 to the Electrolyte

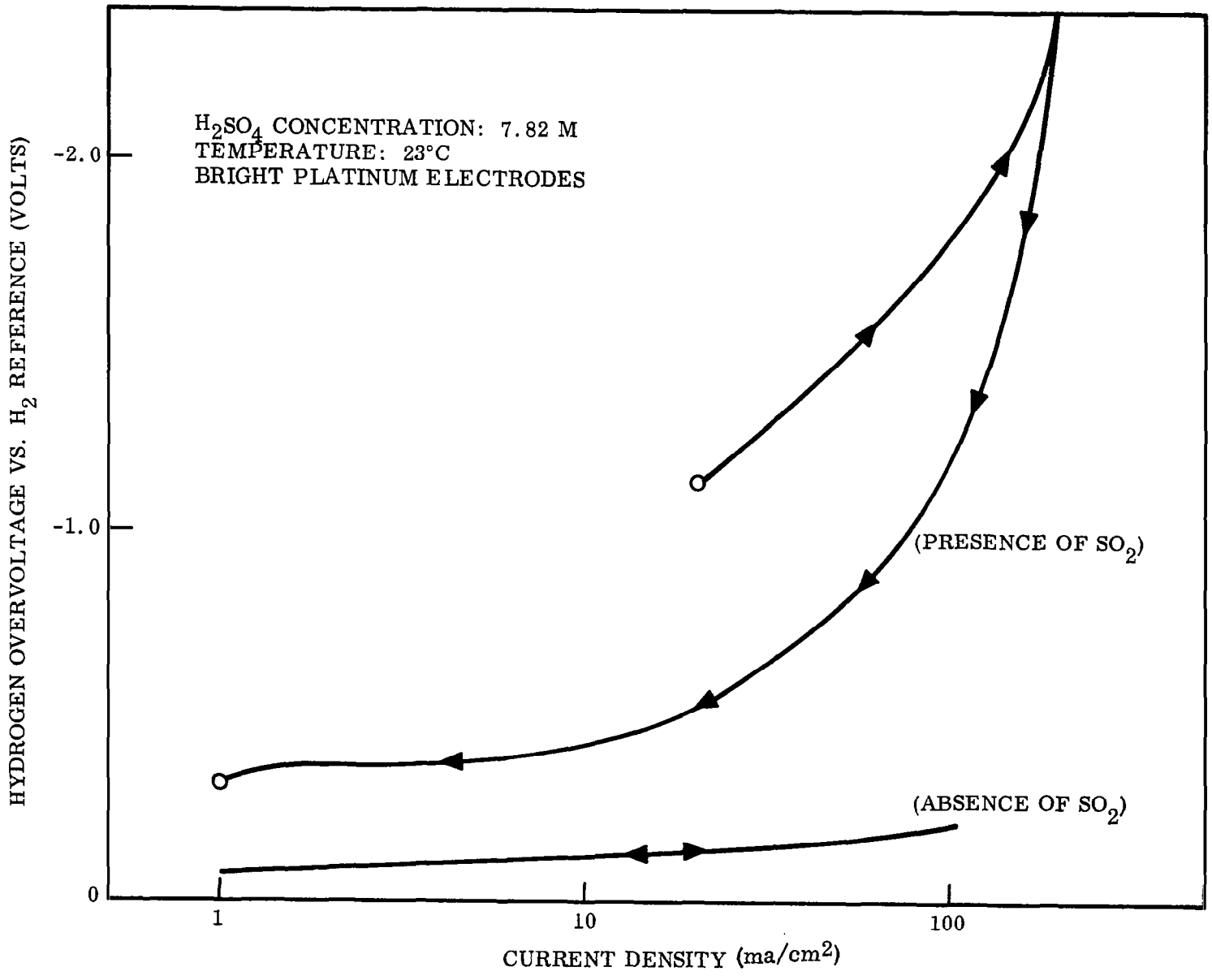

Fig. 2-13 Hydrogen Electrode Polarization Variation With Current Density With Addition of SO_2 to the Electrolyte

of hydrogen was generated within experimental accuracy. This test seems to indicate that a high overvoltage will not generate SO_2, at least not on a lead electrode. This overvoltage is well beyond that which may be expected for a platinum or a platinized electrode.

2.2 IMMOBILIZING MATRIX MATERIALS

2.2.1 Introduction

To facilitate the gas-liquid phase separation that must take place at the electrode of a water electrolysis cell, the electrolyte, if it is a liquid, must be restrained from flooding the electrode. A contrary requirement is that the electrolyte be available at the electrode in sufficient quantities to allow the electrode reaction to occur efficiently. Many schemes have been tried to satisfy these unique requirements, but most systems rely on the capillary force of some absorbent matrix to provide the necessary properties required. The absorbent material or matrix must either be inert or aid in the cell operation.

Because the matrix material generally does not aid in the electrode reaction, it increases the cell resistance and decreases the activity of the absorbed electrolyte at the electrode. A further requirement of the matrix is that it be impermeable to the gases being generated at the two electrodes; i.e., it must not allow the generated gases to diffuse through the matrix. The electrolytes used in the electrolysis reaction are always quite corrosive and active; those matrix materials which meet all of the necessary requirements are few.

The unique requirement of the water vapor cell is that the matrix-electrolyte combination must not deteriorate under adverse operating conditions such as those found when the cell either receives too much or too little water from the air stream to meet the electrolysis requirement. Solid structures such as asbestos and various types of filter paper and cloths are sometimes difficult to assemble into a practical cell structure. Consequently, an objective of this program was to study immobilizing matrix

materials that make gel-like mixtures when mixed with the electrolyte, in this case H_2SO_4. It was found that the gels may vary all the way from a thixotropic mixture to a true gel which does not change its integrity when either compressed or vibrated.

Three solids have been evaluated for producing an immobilized H_2SO_4 electrolyte: a synthetic zeolite, silicic acid, and a very fine silica. Two distinct forms of electrolyte were obtained from these mixtures. The first two materials produced thixotropic electrolytes when mixed with H_2SO_4; the fine silica produced a gel. Each of these immobilized electrolytes has definite advantages and disadvantages. The thixotropic mixtures exhibit these advantages:

- The high-solids content can result in a close approximation to a porous solid matrix which retains its structural integrity when dried.
- The liquidlike nature of these materials under vibration allows the material to be compacted in a cell.

The disadvantages are as follows:

- The high-solids content results in a high electrical resistance.
- The liquidlike nature may allow settling under certain conditions of vibration and acceleration.

The gels, on the other hand, exhibit these advantages:

- The low-solids content results in high electrical conductivity, approaching the conductivity of the liquid electrolyte used.
- They are mechanically more stable than the thixotropic mixtures under vibration.

The disadvantages, however, are as follows:

- Handling is more difficult since bubbles of air can be entrapped during preparation and cannot be readily removed.
- The surfaces of the electrolyte matrix cannot be easily smoothed.

The specific materials evaluated were a synthetic zeolite, Zeolon-H,* a commercially available technical grade silicic acid,** and a finely divided silica, Cab-o-sil.*** Mixtures of Zeolon-H or silicic acid with 8.1 M H_2SO_4 produce thixotropic mixtrues. Cab-o-sil forms a gel in most proportions with H_2SO_4. The liquid capacity, specific resistance, and chemical degradation of these materials were evaluated.

2.2.2 Liquid Capacity of the Matrix

Centrifugal filtration of the three types of matrix-H_2SO_4 mixtures under a nominal 30-g acceleration was used to establish a baseline condition for comparison of the liquid capacity of the matrices.

The procedure for determining the amount of liquid retained by each type of matrix consisted of placing a weighed sample of solids in a coarse-frit Gooch crucible, wetting the matrix with the desired electrolyte, and centrifuging at 30 g for a known period of time. Repetitive measurements of weight percent liquid retained by the sample as a function of time in the centrifuge permitted extrapolation of liquid retention to infinite time, i.e., the limiting amount of liquid held by the matrix under the 30 g baseline condition. The extrapolation results are shown in Table 2-2. Because these values are the result of an extrapolative process, the third significant figure is uncertain.

Table 2-2

LIQUID RETENTIVITY IN THREE MATRIX MATERIALS UNDER A 30-g ACCELERATION[(a)]

Liquid	Solid		
	Zeolon-H	Silicic Acid	Cab-o-sil
H_2O	36.2	47.0	–
8.1 M H_2SO_4	47.7	55.8	90.4
12.0 m H_2SO_4	53.4	60.7	–

(a) Values are weight percent liquid in the mixture.

*Zeolon-H, Norton Chemical Products, Worcester, Mass.
**Silicic acid, Fisher Scientific Co., Fair Lawn, N. J., Lot 794158.
***Cab-o-sil, Cabot Corp., Boston, Mass.

The minimum amount of liquid required to make a mixture of usable consistency was determined by adding 8.1 M H_2SO_4 to a known weight of Zeolon-H until the desired consistency was reached. It was found that this minimum liquid content was 45.2 wt% as compared with the maximum content of 47.7% shown in Table 2-1. Hence, the composition of the matrix is quite critical since there is little difference in weight percent liquid between the too wet and the too dry mixtures. If the mixture is drier than 45.2%, it tends to crumble and lose the necessary mechanical properties required for good cell operation. On the other hand, if the cell becomes too wet, liquid could be withdrawn under adverse operational conditions. From this and from data obtained from the test cells (described later in this report) it appears that the Zeolon-H may not be suitable for the requirements of the water vapor electrolysis cell without some barrier to prevent cross-leaks or some supporting structure to maintain the structural integrity of the electrolyte under adverse operating conditions.

2.2.3 Resistivity of the Matrix – H_2SO_4 Mixtures

The cell shown in Fig. 2-14 was used for the study of immobilized-electrolyte resistance. The 1000 cps impedance bridge* was used for the measurements. The capacitance effects were eliminated by calculating the resistance from the dissipation factor and the system capacitance assuming series capacitance and resistance. The specific resistance values for several H_2SO_4-matrix material systems are presented in Table 2-3.

Samples 4, 7, and 8 can be compared since they are representative of similar preparative techniques on different materials. These mixtures are related to each other by the amount of liquid retained in these immobilizing materials at a 30-g acceleration (Table 2-2). Because a greater solid content is required for the Zeolon-H matrix, its specific resistance is the highest of these three optimized mixtures. Because the Cab-o-sil solid content is low, its conductivity is high although the introduction of only 6.5 vol. % of solid yields a matrix with only 67% conductivity based on the bulk liquid conductivity. If the conductivity of the matrix is related only to the porosity of the matrix in terms of its void volume fraction, the conductivity would vary directly with

*General Radio 1650A

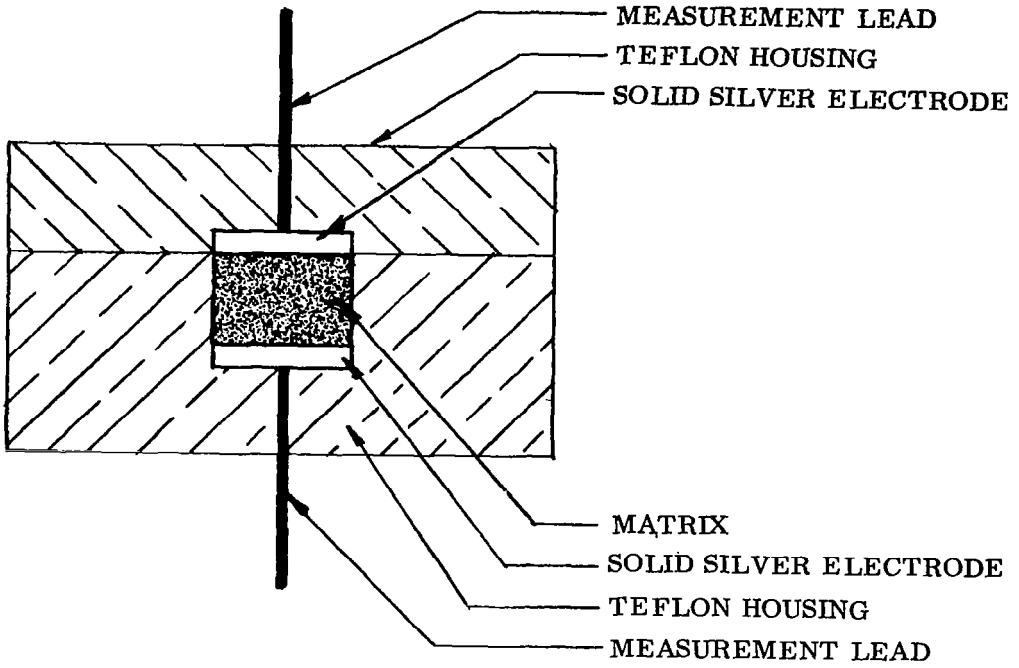

Fig. 2-14 Conductivity Test Cell

Table 2-3

ELECTRICAL CONDUCTIVITY OF VARIOUS IMMOBILIZED H_2SO_4 ELECTROLYTES

Sample	Electrolyte Matrix (Weight percent of liquid)	Specific Resistance (ohm-cm)	Conductivity ($ohm^{-1}cm^{-1}$)	Volume Percent Liquid (%)(a)	Mixture-to-Liquid Conductivity Ratio (%)	Deviation (Volume Percent less Cond. Ratio) (%)
1	100% 4.95 M H_2SO_4	2.56	0.392	100	100	0
2	100% 8.10 M H_2SO_4	2.96	0.338	100	100	0
3	43% 8.10 M H_2SO_4-Zeolon-H	13.35	0.075	57.8	22	35.8
4	46% 8.10 M H_2SO_4-Zeolon-H	8.55	0.117	60.6	34	26.6
5	49% 8.10 M H_2SO_4-Zeolon-H	7.75	0.130	63.4	38	25.4
6	40.6% 4.95 M H_2SO_4-Zeolon-H	8.93	0.112	55.1	29	26.1
7	54.8- 8.10 M H_2SO_4-Silicic Acid	6.88	0.146	66.0	43	23.0
8	90% 8.10 M H_2SO_4-Cab-o-sil	4.41	0.227	93.5	67	26.5

(a)Values for volume percent were derived from the specific gravities of the materials and do not account for water absorbed or the way in which the liquids are taken up by the solids, i.e., the Zeolon-H may actually take the acid into the crystalline structure which may change the volume ratio.

this parameter. Experimentally, it was found that this is not the case; the main reasons for the deviation are entrapment of air bubbles in the matrix during preparation (particularly bad for the Cab-o-sil matrix) and poor contact (as compared to bulk liquid) with the test electrode surface. Interaction of the H_2SO_4 with the solid may also reduce the conductivity. As indicated by the deviations shown in Table 2-3 for these three mixtures (4, 7, and 8), the silicic acid more closely approximates a porous matrix material since its deviation (liquid volume percent less conductivity ratio) is closest to zero.

The Zeolon-H and Cab-o-sil materials exhibit similar deviations. Samples 4 and 6 are similar in that the same volumes of liquid were used for the preparation of the samples. Sample 6 exhibited a drier appearance, as seen also by the liquid volume fraction. Although the conductivities are very close for these two samples, the mixture-to-liquid conductivity ratio is poorer for sample 6 probably because the lower void volume fraction of sample 6 reduced the amount of liquid available for conduction. Furthermore, the driest Zeolon-H mixture (sample 3) yields both the poorest conductivity and the largest percent deviation. Again, this is probably due to the unavailability of liquid in the matrix and at the electrode surface.

From these data, it would appear that the silicic acid matrix (sample 7) with its low-deviation value might be the best immobilizing matrix material; i.e., the sample exhibits the greatest conductivity for the amount of acid retained.

2.2.4 Matrix Degradation

When samples of Zeolon-H (lot number BJ-2) and H_2SO_4 were mixed for the test of the water absorption characteristics, samples with the more concentrated acid tended to dry out. Because the concentrated acid samples should tend to become wetter because of their low vapor pressures, a test was made to determine if the acid concentration had diminished because of reaction with the Zeolon-H. A sample was washed with water to dissolve the soluble species. The wash water was made slightly

basic with ammonium hydroxide, and the white gelatinous precipitate of aluminum hydroxide was formed. It appeared that the sulfuric acid had reacted with the Zeolon-H by dissolving aluminum from the complex as the sulfate. Because this result was contrary to that predicted by the manufacturer, two different batches of Zeolon-H were tested. Weighed samples of Zeolon-H and 8.10 M H_2SO_4 were allowed to stand for some time before titration of the acidity was performed. In this manner it was possible to compare the final acidity with that at the onset of the experiment and thereby evaluate the degradation of the Zeolon-H as a change in acidity. The results are shown in Table 2-4.

Table 2-4

DEGRADATION OF ZEOLON-H IN 8.1 M H_2SO_4

Sample	Zeolon-H Lot No.	Acidity (milli-equivalents)		Stand Time (days)	Estimated Degradation (%)
		Initial	Final		
1	AD-20	8.13	8.02	30	3.0
2	BJ-2	7.81	7.49	30	9.0

In addition to this quantitative information on the comparative extent of reaction, the appearance of the sample from lot number AD-20 remained the same for the duration of the experiment, while the other became filled with bubbles and took on a crystalline appearance. These results indicate that the stability of the Zeolon-H must be determined on a batch-to-batch basis.

The silicic acid and Cab-o-sil matrix materials contain in their chemical compositions no species which are reactive with sulfuric acid. The silicic acid material is a hydrated silicon dioxide compound, and the Cab-o-sil material consists of finely-divided particles of silicon dioxide. Without gross contamination by reactive species, no matrix degradation is possible in mixtures of silicic acid or Cab-o-sil with sulfuric acid.

The silicic acid and Cab-o-sil materials appear to be better candidates for use as an immobilizing matrix because they are inert in contact with sulfuric acid. Another advantage is that these materials do not have a complex structure like that of the synthetic zeolites (such as Zeolon-H), and, for this reason would not be expected to vary in composition from batch to batch.

2.3 IMMOBILIZED MATRIX CELLS

2.3.1 Introduction

The matrix-type electrolysis cell consists of an immobilized liquid electrolyte contained between two active electrodes. The electrolyte matrix may be a mixture of sulfuric acid and finely divided solids which combine to form a gel, or it may be sulfuric acid contained in the pores of an absorbent material such as asbestos or glass paper. The purpose in immobilizing the sulfuric acid is to affect a gas-liquid phase separation which will permit collection of the evolved hydrogen and oxygen in a zero-gravity environment and prevent mixing of the two gases. Feed water is absorbed from the air by the acid; waste heat generated in the electrolysis reaction is removed by conduction and convection.

2.3.2 Test Facility

A facility for testing single cells was designed and built. The system schematic is shown in Fig. 2-15.

The constant temperature baths for the humidifiers and the cell bath are cooled by a cooling coil and heated with electrical resistance heaters. The baths are stirred and temperature control is accomplished with thermostats for the heaters.

The three test cell compartments are made with formed stainless steel pieces glued to the acrylic box. These compartments assume the temperature of the water in the bath surrounding them and maintain a constant temperature environment for the test cell.

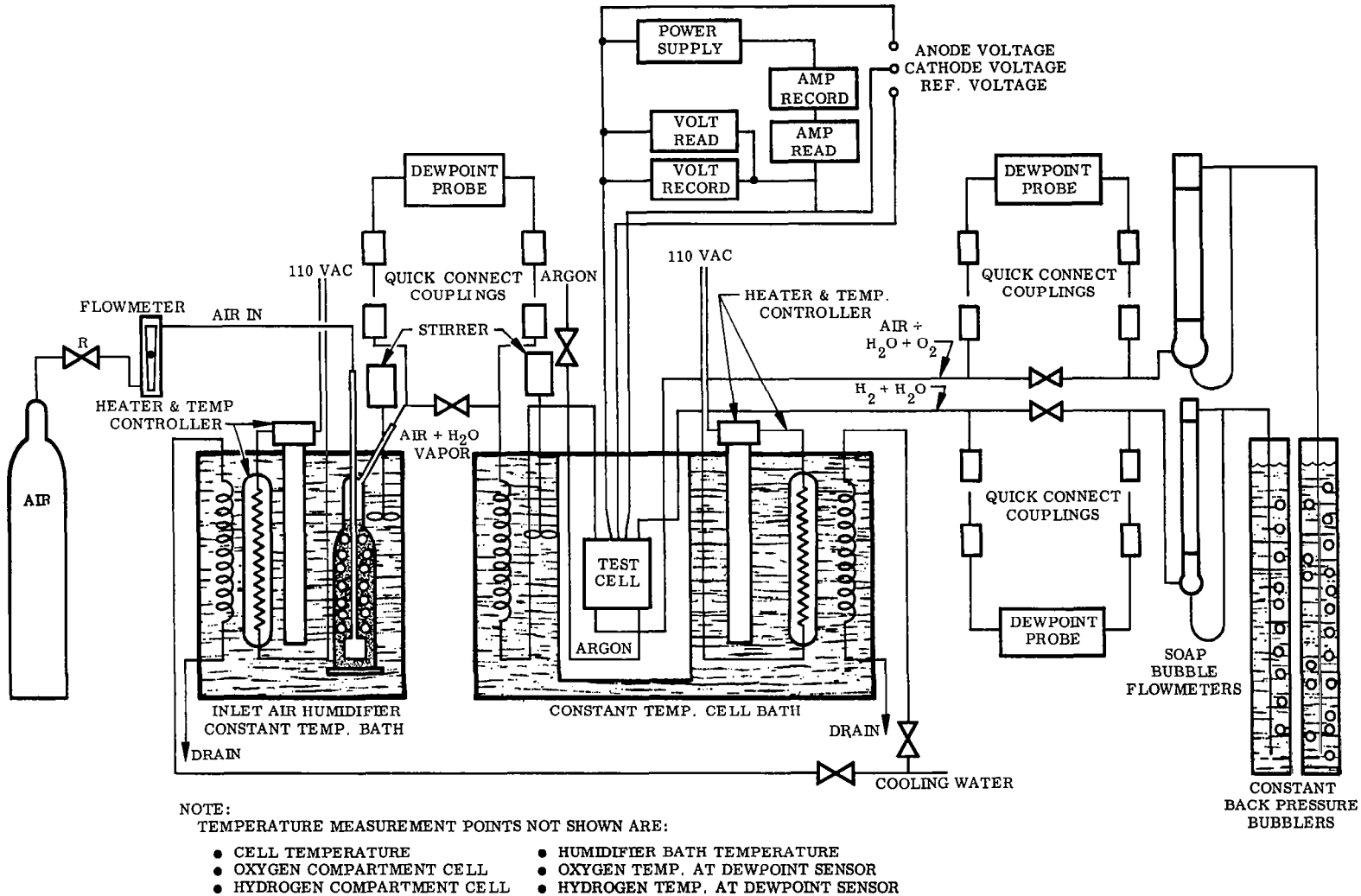

NOTE:
TEMPERATURE MEASUREMENT POINTS NOT SHOWN ARE:

- CELL TEMPERATURE
- OXYGEN COMPARTMENT CELL
- HYDROGEN COMPARTMENT CELL
- HUMIDIFIER BATH TEMPERATURE
- OXYGEN TEMP. AT DEWPOINT SENSOR
- HYDROGEN TEMP. AT DEWPOINT SENSOR

Fig. 2-15 Immobilized-Matrix Water Vapor Electrolysis Cell Test System

Three thermocouples are provided for each test cell compartment to measure the compartment, the oxygen, and the hydrogen temperatures. The cell electrical leads are connected to an electrical control panel where the voltages and current of each cell can be measured. The cell voltage and current can be recorded for long term tests. The cell resistance is also measured at this panel.

Air from a compressed air bottle is supplied to the test cell after passing through a flowmeter and a humidifier. The humidifier is controlled at a constant temperature to maintain the dewpoint of the inlet air at a set point. A plug-in bypass line to the dewpoint measurement circuit* is available at the outlet from the humidifier to permit periodic or continuous dewpoint monitoring as required. The humidified air is heated to the cell test compartment temperature as it passes through a coil immersed in the constant temperature bath. The inlet air relative humidity can be determined from this temperature and the dewpoint temperature. The three test cells can be operated at the same or at a different inlet air relative humidity, but the compartment temperature is the same for all three cells.

The air then enters the test cell and passes over the oxygen electrode where water vapor is absorbed into the electrolyte. The electrolysis reaction produces oxygen which is fed into the air stream passing through the oxygen chamber. Another dewpoint measurement circuit is available for determining the dewpoint of the effluent air from the cell. After the humidity measurement, the gas flows through a soap-bubble flowmeter and into a static water head bubbler which controls the back-pressure in the oxygen chamber of the cell. Hydrogen produced in the cell flows through a similar circuit for the measurement of humidity and gas flow rate and then through a back-pressure bubbler. Argon is available to the hydrogen side of the cell to remove air from the hydrogen circuit.

*Dew Probe, Minneapolis Honeywell.

The stability of the controlled parameters in the test facility was determined. The degree of control achieved is shown below:

Cell compartment temperature (without operating cell)	±1.2°F
Absolute humidity	$\pm 0.28 \times 10^{-6}$ gms H_2O/cm^3 dry air
Air flow rate	±0.2 cm^3/sec
Current density	±0.5 mA/cm^2

The measuring devices used in the system were calibrated to the accuracy given below:

Temperature	±0.2°F
Dewpoint	±0.5°F
Gas flow rate	±1.5%
Current	±0.005 amp
Voltage	±0.0005 V

An automatic readout system connected to the test facility provides a means of recording hourly readings of all of the above parameters except gas flow rate.

2.3.3 Test Cell Design

The requirements for a cell suitable for the testing of an immobilized-electrolyte electrolysis system were evaluated, and a design for such a cell was formulated. A view of the parts of a typical cell and the schematic of this cell are shown in Figs. 2-16 and 2-17 respectively. The cell end plates were machined from clear acrylic so that the electrodes could be viewed during the operation of the cell. O-rings were used to provide the necessary gas seal. Provision was made for inserting a thermocouple probe in the gas space of each end plate. Tantalum sheet stock was used for the electrode support rims, and the active electrode material was spotwelded to the rims to provide electrical contact. The active area of the electrodes was 18 cm^2. The inactive area of the rim was covered with vinyl-backed tape to prevent electrolysis

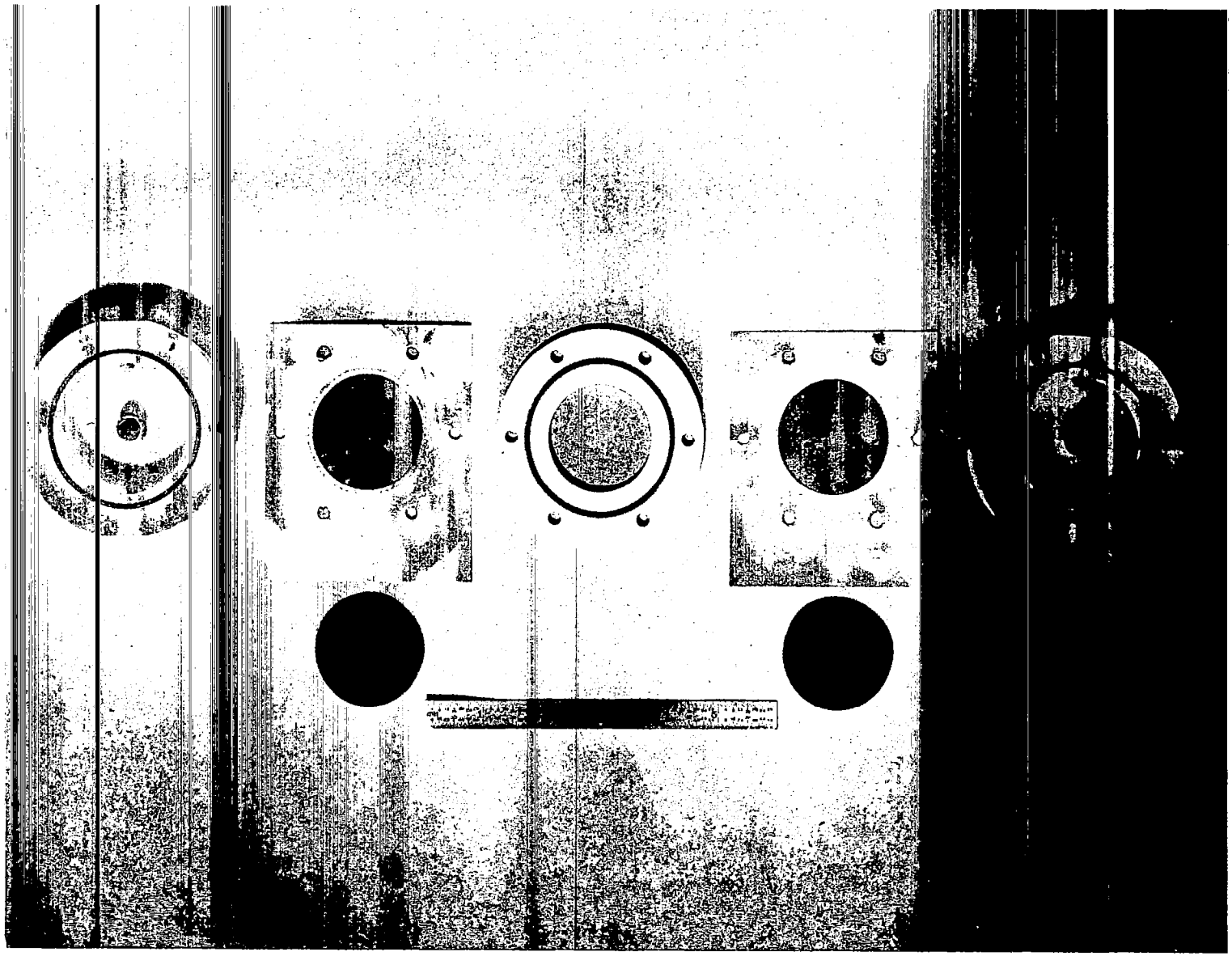

Fig. 2-16 Immobilized-Matrix Test Cell Parts

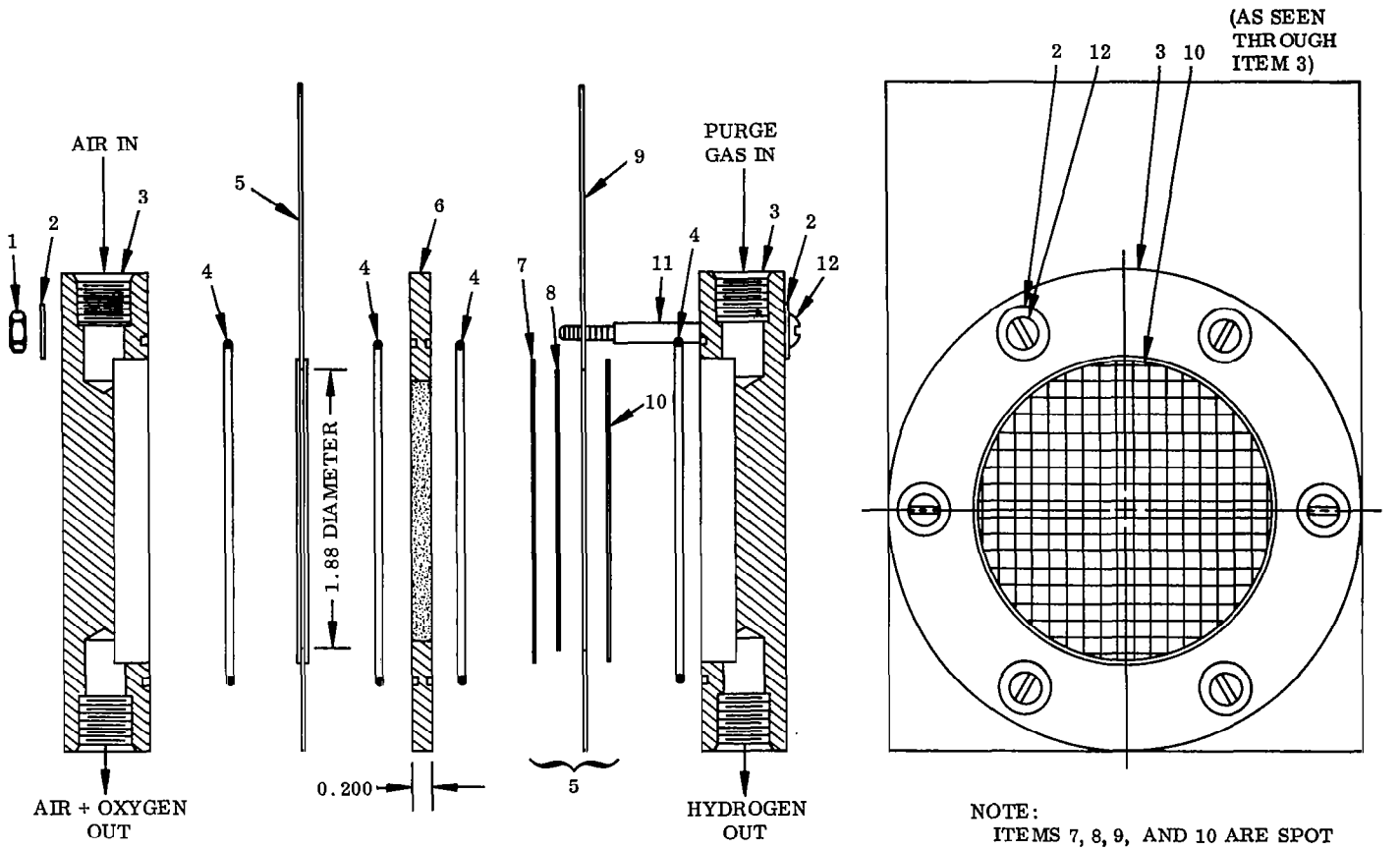

1. NUT
2. WASHER
3. TRANSPARENT END PLATE
4. O-RING
5. ELECTRODE ASSEMBLY
6. MATRIX RING
7. ELECTRODE MATERIAL
8. TANTALUM SPACER SCREEN
9. TANTALUM ELECTRODE RIM
10. TANTALUM SUPPORT SCREEN
11. INSULATED SCREW SECTION
12. ASSEMBLY SCREW

Fig. 2-17 Immobilized-Matrix Test Cell Schematic

from taking place there. The spacer plate in the cell was made of cast epoxy. It was gasketed with O-rings and was used to contain the electrolyte matrix.

During operation of the cell, air was passed into the oxygen end plate, over the electrode, and out through the exit port. One port is provided in the hydrogen end plate for an inert purge. The other port is used as the exit line for the produced hydrogen.

The test cell configurations used in the study of the immobilized electrolyte or gel-type cells are shown schematically in Fig. 2-18. Cell types 1 and 2 were used to investigate the effect of matrix thickness on cell performance. Because the electrolyte matrix can lose rigidity when extremely wet or when subjected to vibration, cross leakage of gases in a cell with an unsupported matrix is a potential problem. Cell types 3, 4, and 5 contain a dual purpose asbestos sheet. The asbestos sheet prevents gas cross leakage and serves as mechanical support for the matrix.

2.3.4 Test Results

The study of the properties of sulfuric acid and the immobilizing matrix materials provided data which were used to guide the test cell work. The areas of investigation encompassed in cell testing are:

- Determination of an optimum matrix material
- Improvement in cell design
- Study of cell performance as a function of time and operating parameters

Within this framework, specific problem areas, such as efficiency of water absorption, cross-leakage of gases, and electrolyte leakage, were considered. The cell tests, in general, were conducted under adverse inlet air conditions; as a result time to failure was reduced. Optimization of cell operating parameters, therefore, includes a definition of operating limits and the life expectancy of the system under adverse conditions.

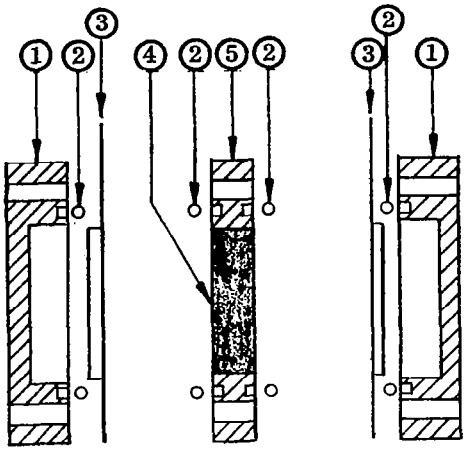

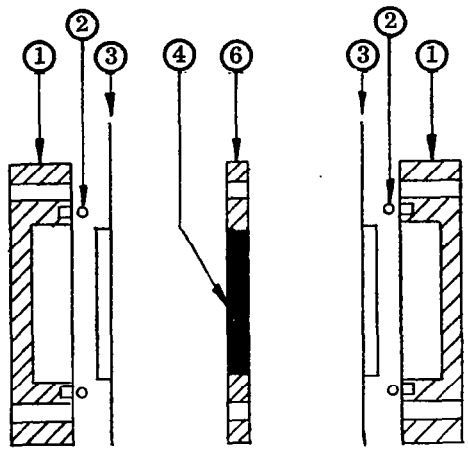

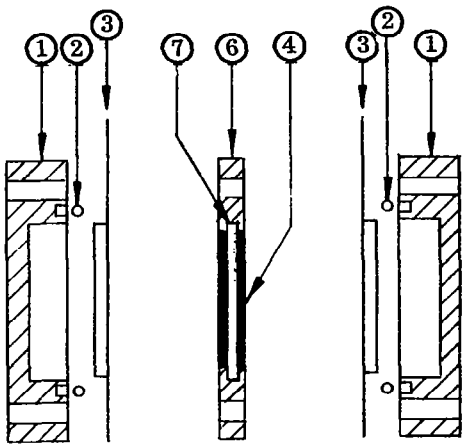

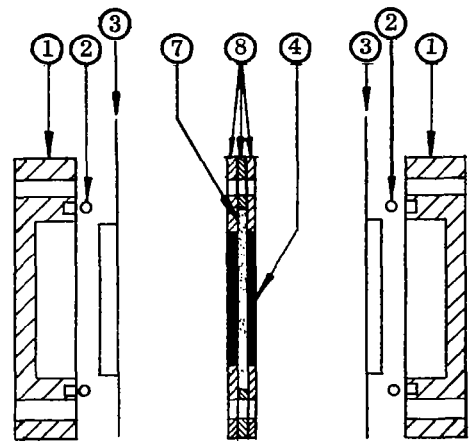

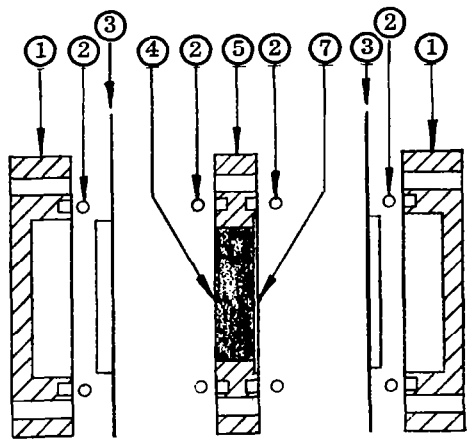

KEY
1. END PLATE
2. O-RING
3. ELECTRODE RIM AND ELECTRODE (SPOTWELDED ASSEMBLY) ACTIVE AREA 18 cm^2 (2.72 $in.^2$)
4. GEL TYPE MATRIX
5. CAST EPOXY SPACER RING, 0.15 INCHES THICK
6. NEOPRENE SPACER, 0.075 INCHES THICK
7. ASBESTOS GAS BARRIER
8. NEOPRENE SPACER, 0.019 INCHES THICK

Fig. 2-18 Immobilized-Matrix Test Cell Configurations

Fifteen single cells of the immobilized matrix type were tested. The description and results of these tests are summarized in Table 2-5.

Cell Number A-1. A cell of Type 1 as shown in Fig. 2-18 was assembled with a mixture of 8.1 M sulfuric acid and a synthetic zeolite* as the electrolyte matrix. The electrodes were fabricated from type AA-1** electrode material spotwelded to 0.018-cm-thick tantalum rims. The electrodes were spotwelded in a fixture designed to keep the rim and electrode material flat during the welding operation. After the electrode assembly was removed from the fixture, however, the assembly tended to bow slightly. Cell assembly was made difficult because the bowing tended to allow the matrix to flow into unwanted areas before the cell was closed. The center electrolyte ring was filled with electrolyte mixture with no attempt made to remove trapped air bubbles.

The initial specific resistance of the cell was 45.3 ohm-cm. The resistance decreased during the first 4 hr of operation to 16.3 ohm-cm. The cell had an initial voltage of 2.25 V at 25 mA/cm^2. Just before the cell failed due to a cross leak after 22 hr of operating time, the voltage had dropped to 2.09 V at 30 mA/cm^2. The voltage drop was attributed to cell resistance change, because the initial and final IR free voltages were not significantly different – 2.02 and 1.9 V, respectively. The final specific resistance was 15.3 ohm-cm.

The poor initial performance of this cell, as well as the cross leak which developed, were probably due to the problems encountered in assembling the cell. Large voids in the electrolyte matrix observed upon disassembly of the cell explain the high cell resistance and the cross leak. The electrodes appeared unharmed by the operation and were cleaned and dried for use in Cell A-2. Experience gained in assembling and operating this first cell was useful in the testing of subsequent cells. The experimental data were sufficient to indicate that the cell was performing as an electrolysis cell and that measurable amounts of water were being removed from the air stream as it passed over the oxygen electrode.

*Zeolon-H Norton Chemical Products, Worcester, Mass.
**American Cyanamid, Wayne, N. J.

Table 2-5

SUMMARY OF IMMOBILIZED MATRIX TEST CELL RESULTS

Cell No.	Matrix Material (Lot No.)	H_2SO_4 (Molarity)	Gas Barrier	Config-uration	Specific Resistance (ohm-cm)		Cell Voltage (V) at Current Density (mA/cm^2)		Life (hr)
					Initial	Final	Initial	Final	
A-1	Zeolon-H (BJ-2)	8.1	No	1	45.3	15.3	2.25 @ 25	2.09 @ 30	22
A-2	Zeolon-H (AD-20)	8.1	No	1	10.1	8.5	2.00 @ 30	2.04 @ 35	193
A-3	Silicic Acid	8.1	No	1	7.55	8.10	1.99 @ 35	2.03 @ 35	319
A-4	Cab-o-sil	8.1	No	2	10.4	14.8	1.96 @ 35	2.06 @ 35	6
A-5	Cab-o-sil	8.1	No	2	12.5	16.1	1.95 @ 35	2.05 @ 35	7
A-6	Zeolon-H (AD-20)	8.1	No	1	9.92	16.3	2.08 @ 35	2.14 @ 35	12
A-7	Zeolon-H (AD-20)	8.1	ACCO-1 Asbestos (20 mils)	3	23.4	–	2.08 @ 35	2.46 @ 35	505
A-8	Zeolon-H (AD-20)	8.1	Tilton Blue Asbestos (10 mils)	4	52.0	1129	2.07 @ 35	9.50 @ 35	144
A-9	Zeolon-H (AD-20)	8.1	Tilton Blue Asbestos (10 mils)	5	–	29.0	2.18 @ 35	2.46 @ 35	173
A-10	Zeolon-H (AD-20)	8.1	ACCO-1 Asbestos (20 mils)	4	43.8	–	2.27 @ 35	2.22 @ 35	7
A-11	Silicic Acid	8.1	ACCO-1 Asbestos (20 mils)	5	10.4	26.1	2.01 @ 35	2.15 @ 35	436
A-12	Zeolon-H (AD-20)	8.1	ACCO-1 Asbestos (20 mils)	5	14.0	141.0	2.15 @ 35	12.0 @ 35	123
A-13 14 15	ACCO-2 Asbestos (60 mils)	8.1	ACCO-2 Asbestos (60 mils)	4	cells not operated				

Cell Number A-2. Another cell was constructed using the same design as Cell A-1 but with a matrix of a different lot of synthetic zeolite. The electrolyte matrix was carefully packed into the center electrolyte ring and then pressed to 50 psi in a hydraulic press between two sheets of polyester film* to insure that no voids existed in the matrix.

The initial resistance of this cell was 10.1 ohm-cm which was considerably lower than the initial resistance of Cell A-1. The resistance decreased during the operation of the cell, mainly due to a temperature increase, to a value of 7.63 ohm-cm after 60 hr of elapsed time. The cell was run on constant current for the first 3.8 hr and on constant voltage for the next 22 hr. Because small changes in the voltage caused large changes in the current, the constant voltage power supply did not provide adequate control. At the 60-hr point, the operating mode was changed back to constant current at a level of 35 mA/cm^2. From this point, the cell voltage was stable at 2.00 V with no more than a ± 0.05 V variation for the remainder of the test. The lifetime performance of Cell A-2 is shown in Fig. 2-19. The results of a voltage-current run made at the 60-hr point are shown in Fig. 2-20. Without a reference junction in the cell, no conclusion can be made as to the nature of the polarization of either electrode.

The hydrogen flow rates measured with a bubble meter were in close agreement with the theoretical production rate. Measured values were within 1% of theoretical. The deviation may have been due to the difficulty involved in making accurate measurements of extremely small flow rates of the order of 0.068 cm^3/sec (at 30 mA/cm^2).

An analysis of the operating parameters at the 60-hr point indicated that approximately 16% of the available water was removed from the air in one pass through the cell. The operating conditions for the cell were 80° F inlet air at 59% relative humidity with an air flow rate of 25 cm^3/sec (2.83 ft^3/hr). The exit air stream was at 83° F and 46% relative humidity. Based on these parameters, the air stream was

*Mylar, E. I. DuPont, Wilmington, Delaware

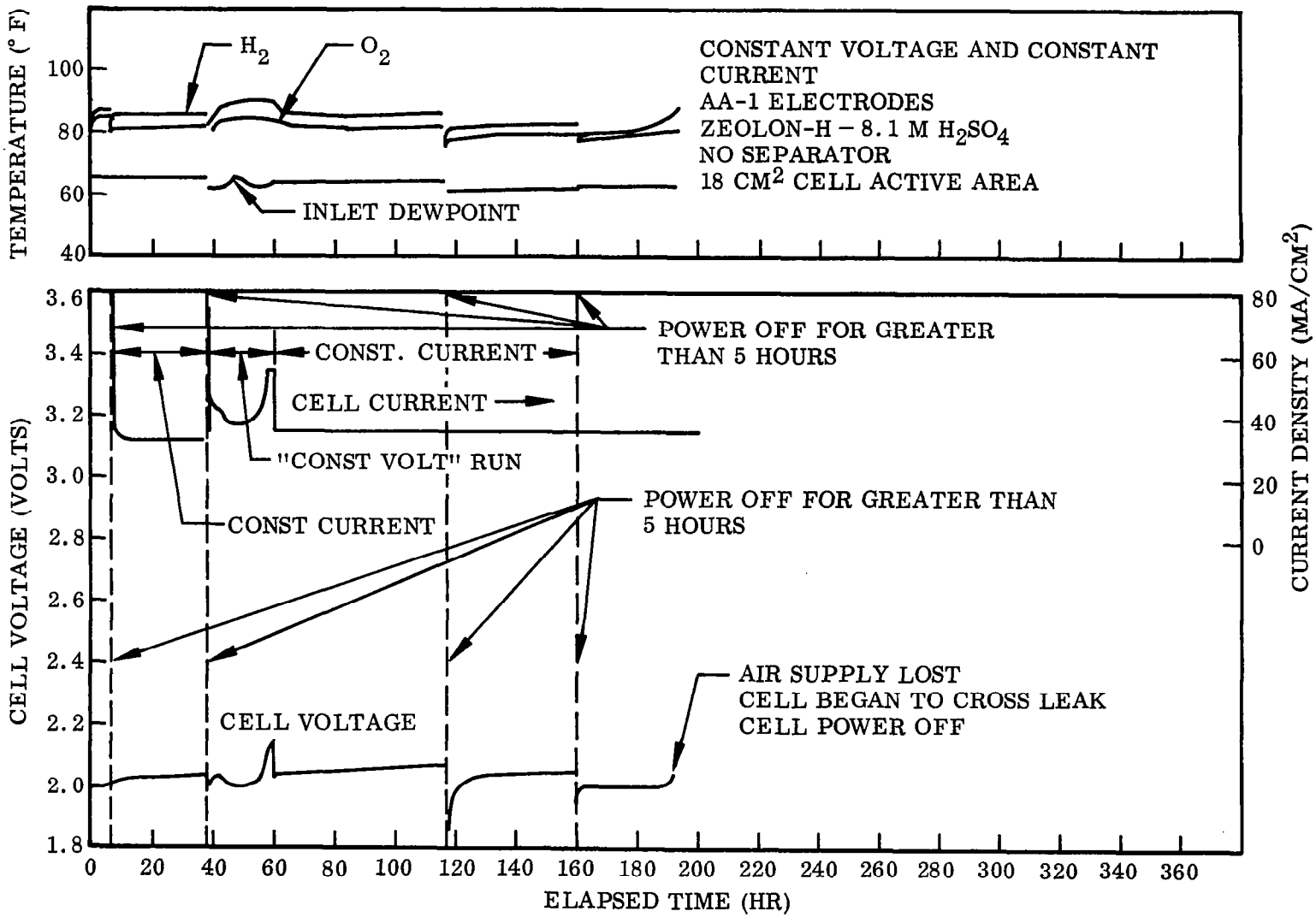

Fig. 2-19 Lifetime Performance Characteristics – Cell A-2

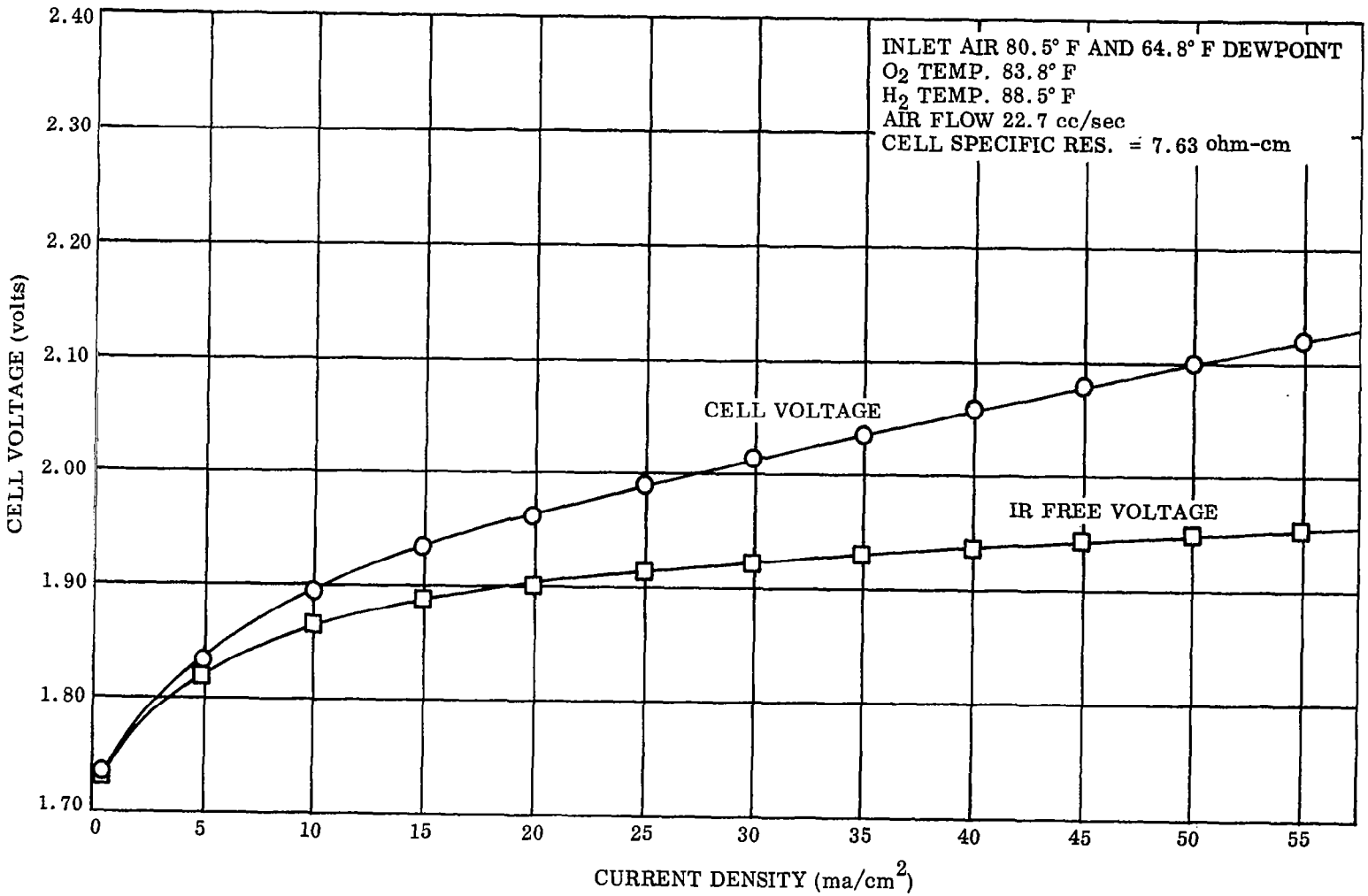

Fig. 2-20 Voltage-Current Characteristics for Cell No. A-2 at 60 Hours

supplying 86% of the water required for electrolysis. These data indicate that the electrolyte was being concentrated as more water was being electrolyzed than was being absorbed.

A major problem inherent in this type of cell became apparent when, as with Cell A-1,cross leakage of gas occurred during the latter part of the run.

Cell Number A-3. Silicic acid was used with 8.1 M sulfuric acid as the electrolyte in Cell A-3. The cell configuration was Type 1 as shown in Fig. 2-18 and was identical to the construction of Cell A-2 except for the use of a different matrix material.

The initial specific resistance was 7.5 ohm-cm. The cell was operated 35 mA/cm^2 for the duration of the experiment. Initial cell voltage was 1.86 V, and the final voltage after 319 hr was 2.03 V. Operation of the cell was intermittent with power shutdown for weekend periods. The highest voltage recorded for the cell during any continuous part of the run was 2.11 V. As can be seen from the fluctuations in inlet dewpoint (Fig. 2-21), poor control was achieved over the inlet air conditions. Inlet relative humidity varied from 38 to 69% at 75° F.

The test was terminated because of cross-leaking of gas through the matrix. When the cell was disassembled, the matrix was intact with no obvious holes or voids. However, cracks could be seen on the side of the matrix which had been in contact with the oxygen electrode. Depth of the cracks appeared to be approximately two-thirds of the total matrix thickness. The hydrogen side of the matrix was black. A cross section of the matrix perpendicular to the faces of the electrodes revealed that this black color penetrated approximately one-third of the matrix thickness as a front and then extended to the oxygen electrode through the cracks which originated at the oxygen side. It is believed that the discoloration was the result of black platinum migration.

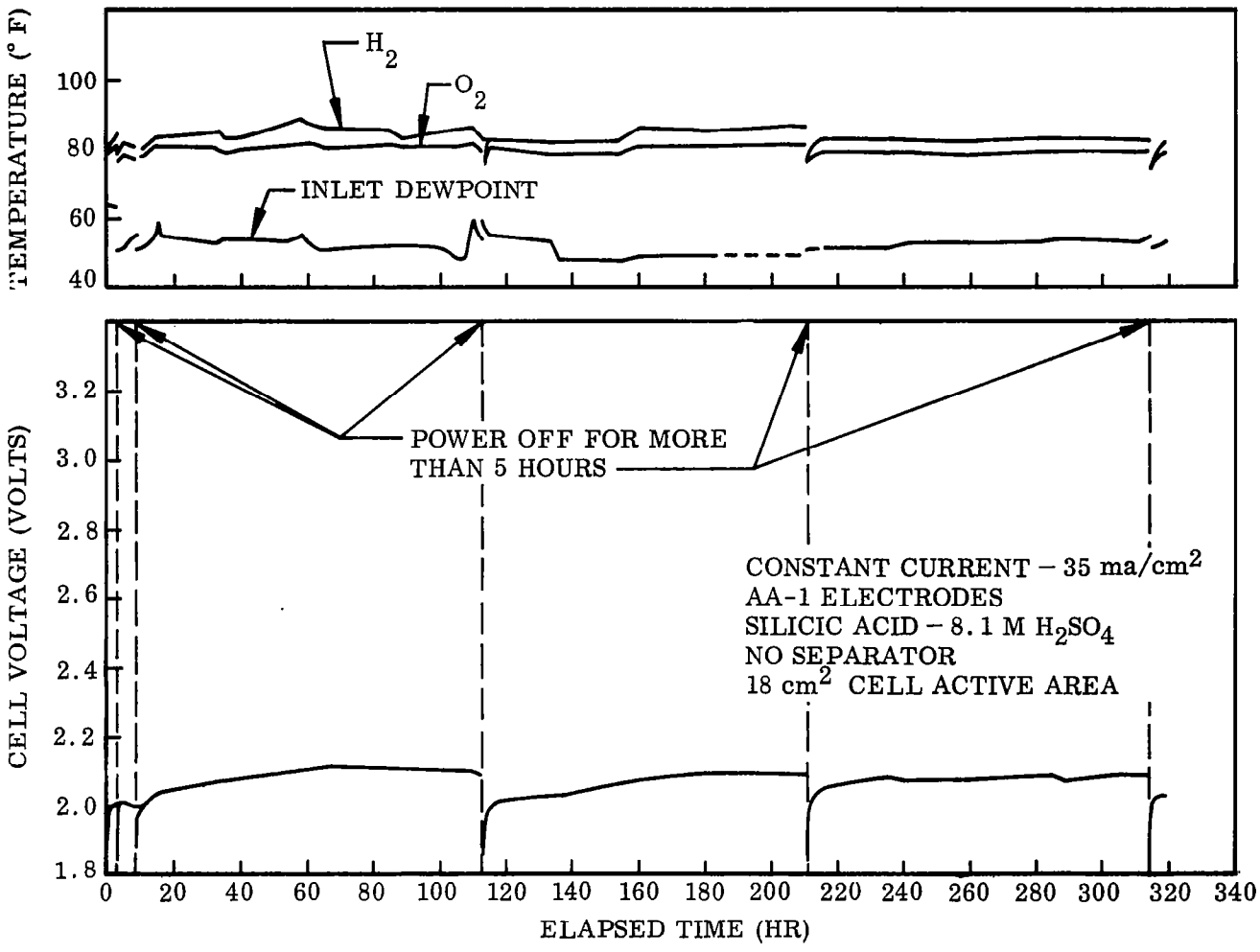

Fig. 2-21 Lifetime Performance Characteristics – Cell A-3

Previous studies (Section 2.1.3) showed that the presence of sulfur is an indication of the generation of SO_2. To learn whether the sulfuric acid in Cell A-3 had been reduced, the hydrogen electrode was examined for sulfur at the end of the test. The analytical method used was the benzoin reduction as presented by Feigl (Ref. 11). The practical minimum detection limit of this test was found to be about 5 micrograms of sulfur. The electrode was washed in deionized water after disassembly from the cell and was then tested according to the referenced procedure. No sulfur was detected. Thus, if sulfur were formed through this mechanism, it would take at least 10 years for the reduction of all the sulfuric acid in the cell matrix.

The failure of Cell A-3 was due to the drying and subsequent contraction of the matrix. The appearance of the cell components after disassembly indicated that the matrix had not been in uniform contact with the oxygen electrode. This condition resulted in non-uniform current distribution which in turn caused localized heating, drying, and cracking of the matrix.

Cells A-4 and A-5. A mixture of fine silica* and 8.1 M H_2SO_4 in a weight ratio of 1 to 9 was used as the matrix in these cells. Cell construction differed from that of previous cells in that a 0.188-cm-thick neoprene ring was used as the electrolyte spacer (Type 2 as shown in Fig. 2-18).

Each cell was assembled by placing an electrode on an end plate, followed by the neoprene spacer. A spatula was then used to smooth and compact the matrix in the spacer, and the procedure was completed by adding the other electrode and end plate.

The initial specific resistances were quite low, 10.4 and 12.5 ohm-cm for A-4 and A-5, respectively. Both cells were operated at inlet air conditions in the range of 44 to 50% relative humidity at a temperature of 75°F. Initial operating characteristics were quite good, but severe cross-leaking occurred in each case within a few hours of operation. Cell voltages at the termination of the tests were 2.06 V for A-4 and 2.05 V for A-5.

*Cab-o-sil, Cabot Corp., Boston, Mass.

When the cells were disassembled, it was discovered that a crack had developed which penetrated through the matrix and extended completely around its periphery at a distance of approximately 1/4 in. from the edge.

The cause of failure in these cells was analogous to the problem encountered with the silicic acid cell (A-3), i.e., localized drying and cracking of the matrix. Water contained in this matrix apparently had a limited mobility such that localized drying in areas of high current density could not be counteracted by sufficient mass transfer of water from lower current density areas in the matrix.

Cell Number A-6. Cell configuration Type 1 (Fig. 2-18) was used in assembling Cell A-6. The matrix consisted of 54% synthetic zeolite and 46% 8.1 M H_2SO_4.

In previous cell tests where the zeolite was used, difficulty was encountered in assembling the cells without trapping air in the matrix. Because of the thixotropic nature of the zeolite H_2SO_4 mixture, the material acts as a liquid when subjected to vibration. This property was used in assembling Cell A-6. The cast epoxy spacer ring was placed on a sheet of polyester and held on a vibrator platform. The matrix material was then packed into the ring. When the vibrator was turned on, the matrix flowed as a liquid to fill the voids which were present, and air bubbles could be seen rising to the surface. More material was added to completely fill the space, and the vibration was continued until it appeared that no more bubbles were rising to the surface. After the vibrator was turned off, the matrix-containing spacer ring could easily be handled, since the matrix was now rigid.

At 35 mA/cm^2, the cell voltage was initially 1.97 V and after 12 hr of intermittent operation had risen to 2.14 V. The specific resistance changed during this time from 9.92 to 16.3 ohm-cm. Inlet air conditions ranged from 42 to 60% relative humidity at 75°F. Twice during the run, cross-leaks developed, and each time the cell was disassembled and more matrix material was added in the manner described above. The test was stopped after cross-leaking occurred for the third time. It should be noted

that the entire cell assembly was subjected to vibration during its operation in the test environment. Stirrers and other equipment mounted on the test station were in operation throughout the test. Thus, it was very unlikely that the matrix maintained its original shape during testing. Although this experiment in improving cell assembly was not completely successful, the results indicated the need for greater mechanical support of the matrix than that provided by containing it within a spacer ring between two electrodes.

Cell Number A-7. After the results of previous experiments with the zeolite matrix (Cells A-1, A-2, and A-6) were reviewed, it was decided to evaluate asbestos materials for use as a gas barrier and matrix support in the cell assembly.

A piece of 0.020-in.-thick refined asbestos* of slightly larger diameter than the electrolyte space was inserted in a slit which had been made around the inside diameter of a 0.075-in.-thick neoprene spacer ring; the result was a ring with a sheet of asbestos located in its center. There was space on either side of the asbestos for the gel-type matrix. The cell configuration was Type 3 as shown in Fig. 2-18. The electrolyte spaces were filled with a mixture of 54% Zeolon-H and 46% 8.1 M H_2SO_4 by using the vibrator table as described in the discussion of the previous cell assembly (Cell A-6). A thin film of the matrix material was also applied to the surface of each electrode in the same manner.

Cell A-7 was operated for 505 hr at a current density of 35 mA/cm^2. The initial specific resistance was 18.0 ohm-cm and the cell voltage was 1.98 V. Performance of the cell during the first 500 hr of operation has been characterized graphically in Fig. 2-22. During the first 85 hr of operation, the cell voltage was fairly stable, ranging from the initial 1.98 V to a high of 2.11 V. Variation in cell voltage during this interval can be attributed to fluctuations in inlet air conditions. The inlet air dew point shown in Fig. 2-26 varied from 59° to 65°F, corresponding to a range of inlet relative humidity from 57 to 70% at 75°F.

At the 85-hr point, the air and water supply to the cell were depleted. Four hours later, the cell voltage had risen to 11.6 V. At this time the power was turned off,

*ACCO-1, American Cyanamid Co., Wayne, New Jersey.

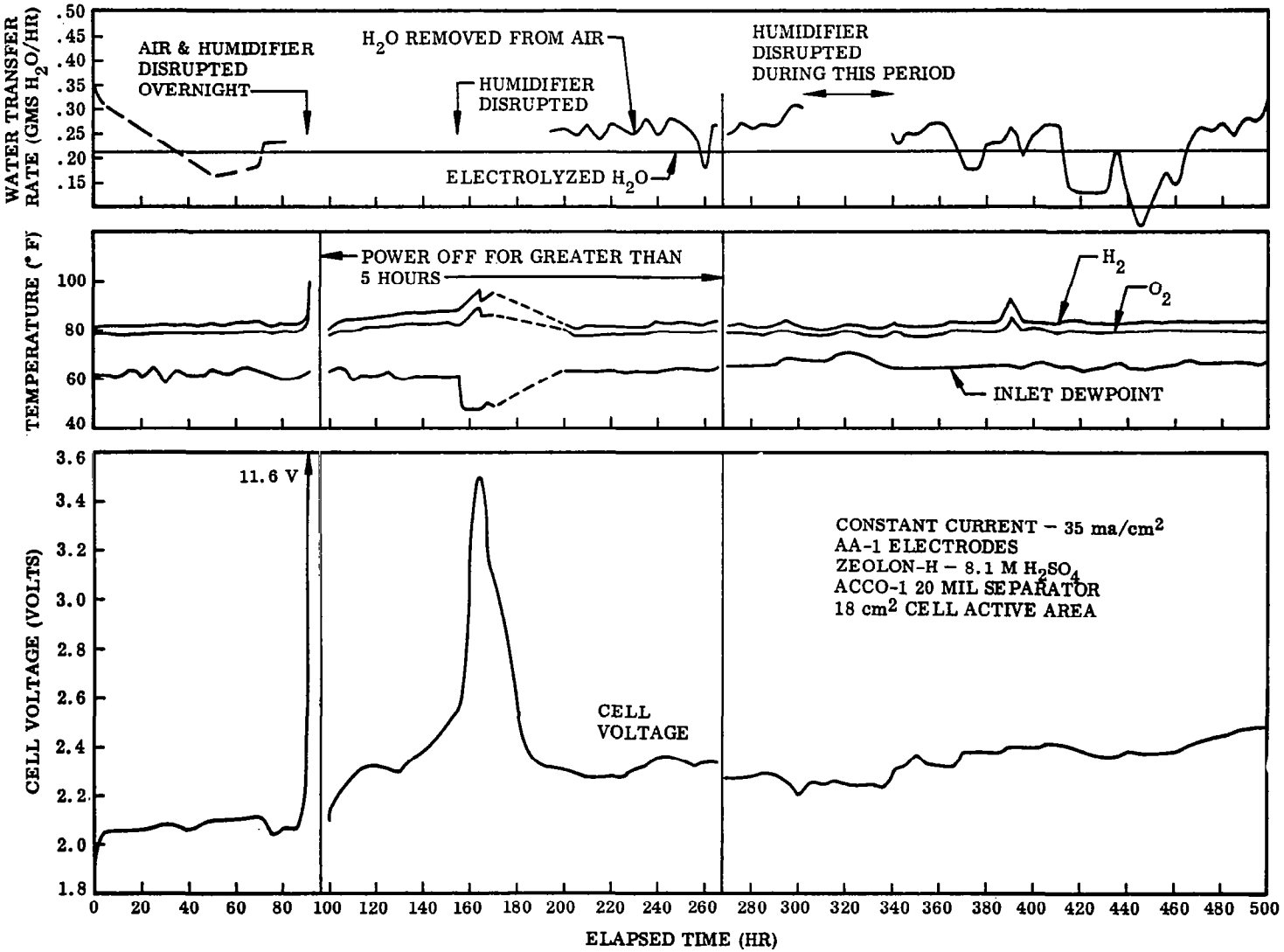

Fig. 2-22 Lifetime Performance Characteristics – Cell A-7

and the cell was allowed to stand for approximately 8 hours with humid air flow through the cell. During that time, the cell resistance was measured periodically. Power was applied to the cell after the specific resistance had dropped from a high at the time of shutdown of 334 ohm-cm to a value of 6.9 ohm-cm.

Subsequent performance of the cell was substantially poorer. The next irregularity occurred at approximately 165 hr of elapsed time. Here again water supply to the cell was depleted, but the problem was later rectified by increasing the relative humidity of the inlet air to 70%. The cell recovered from this treatment, but there followed a definite upward trend in the cell voltage. This trend can be attributed in part to leaching of the electrolyte from the matrix into the gas spaces in the end-plates. It is also probable that degradation of the matrix-acid mixture, described in Section 2.2.5, was taking place in the cell.

Hydrogen flow rate from the cell was measured periodically during the experiment, and at no time was a gas leak detected. Based on the measured hydrogen flow rate, Faradaic efficiency for water electrolysis was 100%. The asbestos center in the matrix spacer served adequately as a gas cross-leak barrier.

Cell Number A-8. A three-part spacer ring was constructed as shown in Fig. 2-18. A disc of 0.025-cm-thick blue asbestos* was placed in the center. The zeolite-H_2SO_4 gel was applied to either side of the spacer ring and to each electrode surface in the manner described for Cell A-7.

The cell was operated at 35 mA/cm^2 and inlet air conditions ranging from 55 to 75% relative humidity at 75° F. Initial specific resistance of the cell was 52.0 ohm-cm.

The first peak in cell voltage occurred at approximately 25 hr of elapsed time (Fig. 2-23). This was again the result of air and water supply depletion. The cell recovered very rapidly from these adverse operating conditions with a relatively

*Tilton Blue, Johns Mansville, New York, New York.

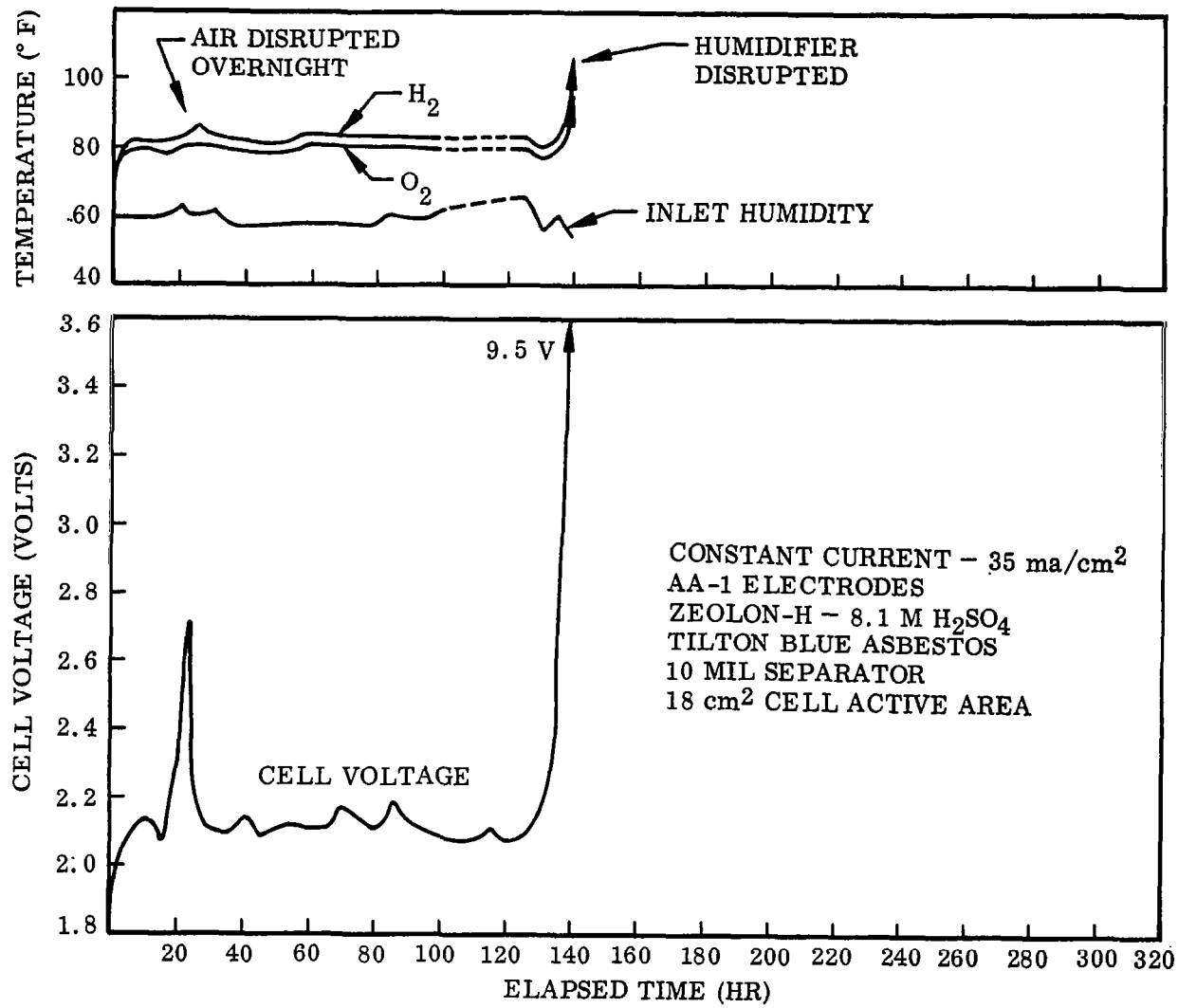

Fig. 2-23 Lifetime Performance Characteristics – Cell A-8

stable cell voltage recorded during the next 100 hr of operation. When another water supply depletion occurred and the cell voltage increased to 9.5 V, the test was stopped.

After the cell was taken apart, it was found that the matrix was completely dry and caked. On the oxygen side of the asbestos center barrier, the powder was a bright yellow color and had the odor of sulfur. On the hydrogen side, the matrix was white. The last recorded temperatures in thermocouple wells in the gas spaces were 147° F at the hydrogen electrode and 130° F at the oxygen electrode. The asbestos sheet was intact, and did not seem to have suffered from this treatment.

Despite failures in the auxiliary system during this experiment, the performance of the cell was satisfactory. During those periods of the experiment when the operating parameters allowed steady-state conditions to exist within the cell, the cell voltage was stable and at an acceptable level. No cross-leaking of gas through the asbestos barrier was indicated. Faradaic efficiency within experimental error was 100%, based on measured hydrogen evolution rate.

Cell Number A-9. In this experiment, a cast epoxy ring which had a 0.012-cm step on one side was filled to the level of the step with a zeolite acid mixture. The vibrator table was used during assembly to remove trapped air. Both electrodes were coated with a film of the matrix material in the same manner. A disc of 0.025-cm-thick blue asbestos was placed in the step, and the cell was assembled with the asbestos adjacent to the hydrogen electrode. The cell configuration is represented as Type 5 in Fig. 2-18.

The performance of the cell is shown in Fig. 2-24. Initial inlet-air conditions were 60% relative humidity at 75° F. The inlet air humidity was gradually increased to 80% as the run progressed. No flooding was observed in the cell operating at 80% relative humidity.

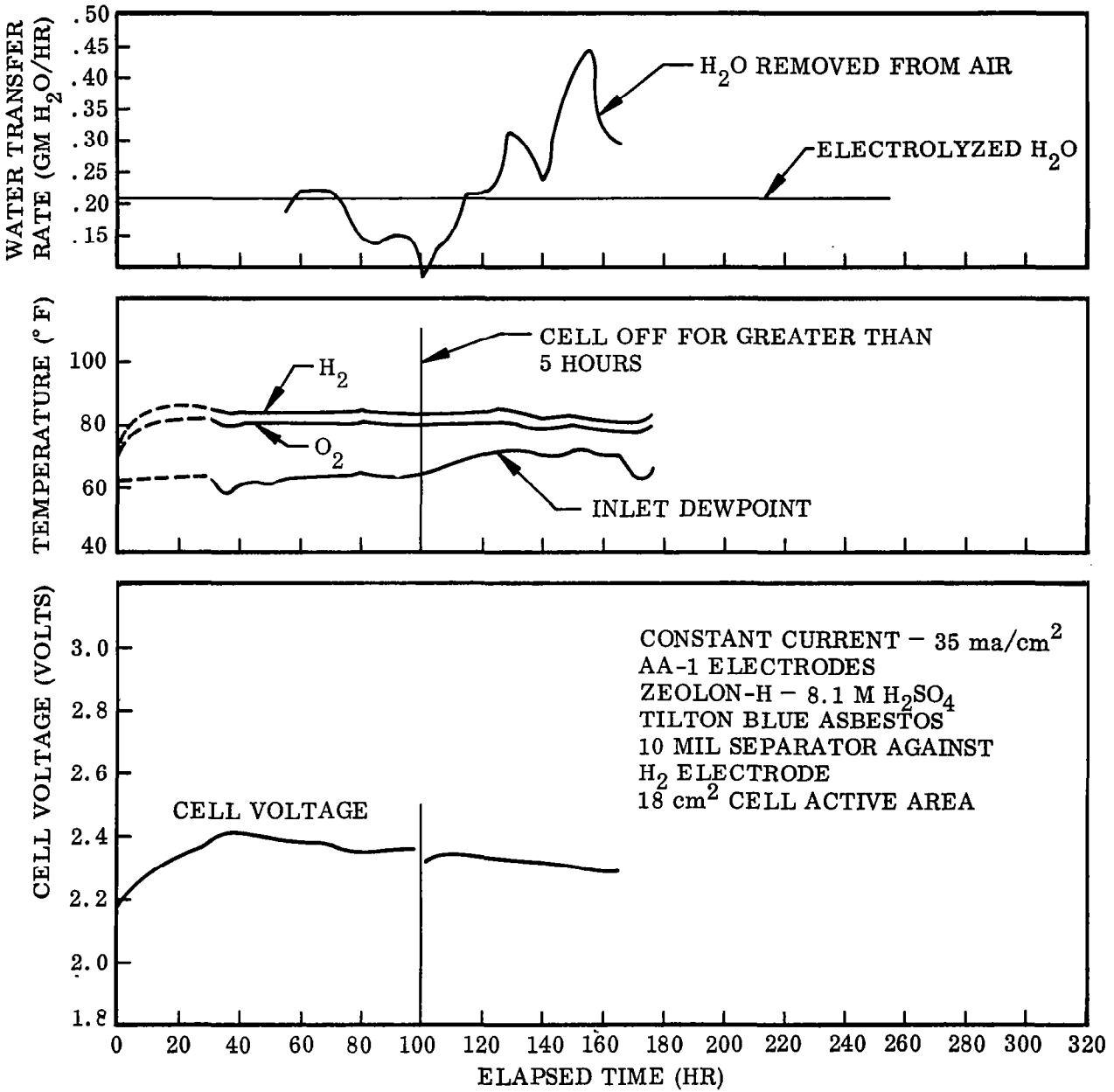

Fig. 2-24 Lifetime Performance Characteristics – Cell A-9

Although the cell was picking up excess water from the air stream during the last 50 hr of the test, the voltage, after steadily decreasing for a time, suddenly started to rise. When the test was stopped and the cell was disassembled, there appeared to be a gap between the asbestos and the bulk of the matrix, a condition which could explain the sudden rise in voltage. Except for the presence of the asbestos gas barrier in this cell, the construction was the same as that of Cell A-6. In both of these cells, the large bulk of relatively unsupported matrix material developed voids and gaps. This problem was not evident in Cell A-9 during the operation of the cell because the asbestos prevented any cross-leaking of gases. But the presence of a void between the asbestos and the matrix, a condition which was discovered when the cell was disassembled, further emphasized the need for matrix structural support.

Cell Number A-10. Cell A-10 consisted of a matrix spacer assembly of Type 4 as shown in Fig. 2-18. The asbestos* used in the center was 0.05-cm-thick. The zeolite acid mixture was prepared in a 1 to 1 weight ratio. Assembly of the cell was accomplished in the manner described for Cell A-8.

The initial specific resistance of this cell was 43.8 ohm-cm. Very poor initial performance of the cell was observed. The starting matrix was too wet, and this condition resulted in leaching of electrolyte from the matrix. The test was stopped within 7 hr because of buildup of liquid in the gas spaces of the end plates. The final cell voltage was 2.22 V.

This cell test verified the results of the matrix liquid capacity studies (Section 2.2.2) where a critical weight ratio range was shown to exist for Zeolon-H/acid mixtures.

Cells A-11 and A-12. Because of the variations in cell construction and operating conditions in previous cell tests, direct comparison of cells using silicic acid with cells using a zeolite cannot be derived from these data. To compare the performance of these matrix materials, Cells A-11 and A-12 were assembled with identical cell configurations (Type 5, Fig. 2-18). Silicic acid was used in A-11 and zeolite

*ACCO-1, American Cyanamid, Wayne, New Jersey.

in A-12. The operating conditions were nearly the same for the two cells for the first 75 hr of operation. A graphical comparison of their performance for this period is shown in Fig. 2-25. The superior electrical performance of the silicic acid cell is obvious from its voltage stability with time. The upward trend of voltage with time observed for the zeolite cell indicates a time-dependent degradation of the electrolyte matrix. The mechanism of this degradation was described in Section 2.2.5.

Comparison of the water absorption characteristics of the two cells was not possible because of malfunction of the dew probes. Lack of sufficient water for electrolysis apparently caused the eventual failure of both cells as indicated by the dry appearance of the matrices after disassembly of the cells. Operating life of Cell A-11 (silicic acid) was 436 hr as compared to 123 hr for Cell A-12 (zeolite). The lifetime comparison is not completely valid because of differences in operating conditions which existed after the first 75 hr of elapsed time. There was no indication from the results of these tests that steady state operation existed.

Cells A-13, A-14, and A-15. Three all-asbestos cells were constructed using a refined asbestos* with a binder as the matrix material. In each cell, chemical degradation of the matrix in contact with 8.1 M sulfuric acid occurred within a few hours after cell assembly. No operating performance data were obtained for these cells. The feasibility of using asbestos or some similar absorbent material as the immobilizing medium was not defined by the tests.

2.4 LIQUID ELECTROLYTE-ABSORBENT MATRIX CELLS

2.4.1 Introduction

The liquid-electrolyte cell differs from the matrix cells in that the electrolyte is not immobilized in an inert medium but flows as a liquid between the electrodes. Gas-liquid phase separation is achieved with a thin absorbent sheet of asbestos contiguous to each electrode. Differential gas-liquid pressure control is required to maintain

*ACCO-2, American Cyanamid, Wayne, New Jersey.

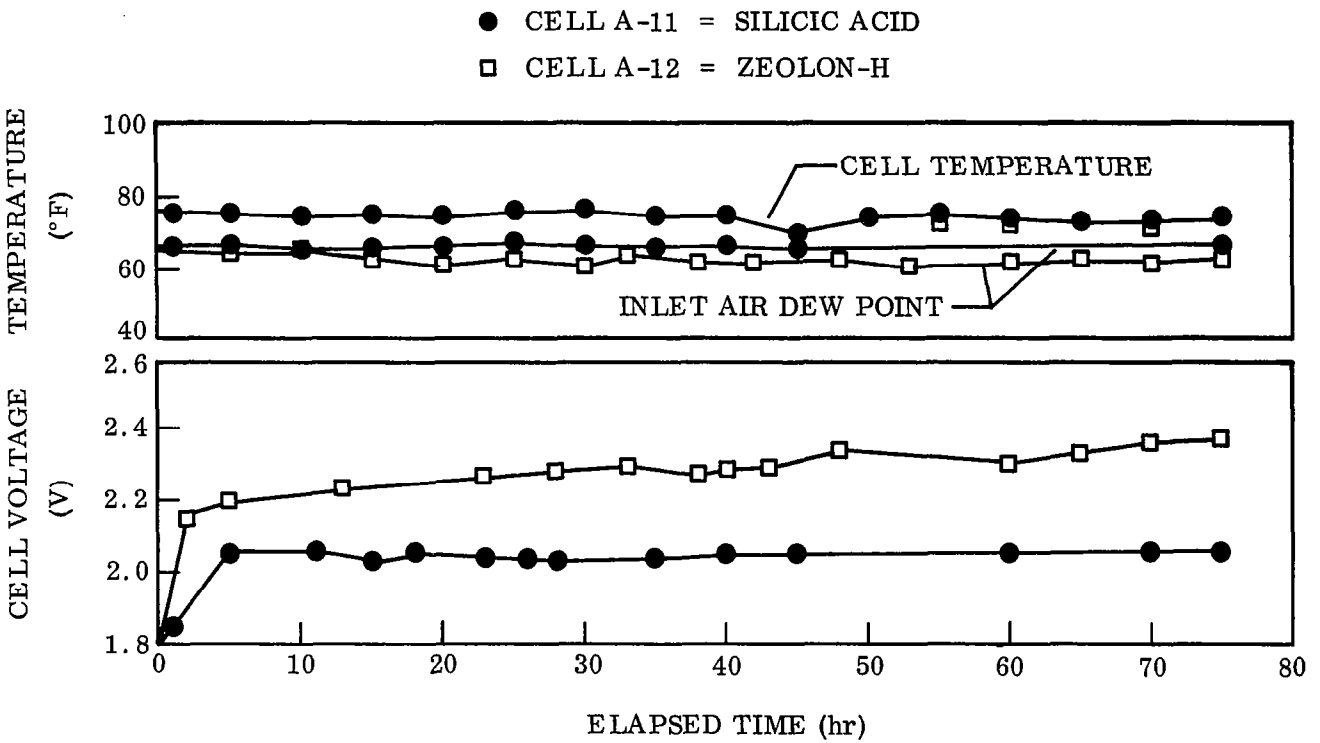

Fig. 2-25 Comparison of Performance of Two Matrix Types – Cells A-11 and A-12

the proper electrolyte interface position, i.e., in contact with the electrode. The liquid electrolyte is circulated through the cell and an external heat exchanger to remove heat generated in the cell. Electrolyte circulation, in addition, prevents the buildup of concentration gradients between the electrodes.

2.4.2 Test Facility

The matrix-cell test facility was modified for use in testing liquid-electrolyte cells. The air humidification system, measurement, and readout instruments, and controls were used in situ, as shown in Fig. 2-15. Test stations were installed on a laboratory bench to accommodate the cells and their auxiliary circulation and heat removal systems. The test compartment designed to hold the matrix cells was used to control the temperature of the inlet air to the cells. A schematic diagram of the modified test facility is shown in Fig. 2-26.

A polyethylene centrifugal pump was used to circulate electrolyte through the cell and the heat exchanger. By sensing the temperature from the exit electrolyte, a temperature controller regulated the flow of the coolant to the heat exchanger. Cell temperature was controlled to $\pm 1.0°$F over a set-point range from 70 to 80° F. Operation at temperatures as low as 65° F and as high as 95° F was possible.

The electrolyte circulation system, including the heat exchanger and flow-control values, was constructed of materials such as polyethylene, polycarbonate, and glass which had been tested and found to be resistant to concentrated sulfuric acid.

2.4.3 Test Cell Design

An electrolysis cell through which liquid electrolyte is circulated presents unique design requirements. In our work, entrance and exit ports, and a baffle system were necessary to provide a uniform liquid flow pattern through the cell. Steps were machined in the liquid spacer ring to accommodate center support screens and an

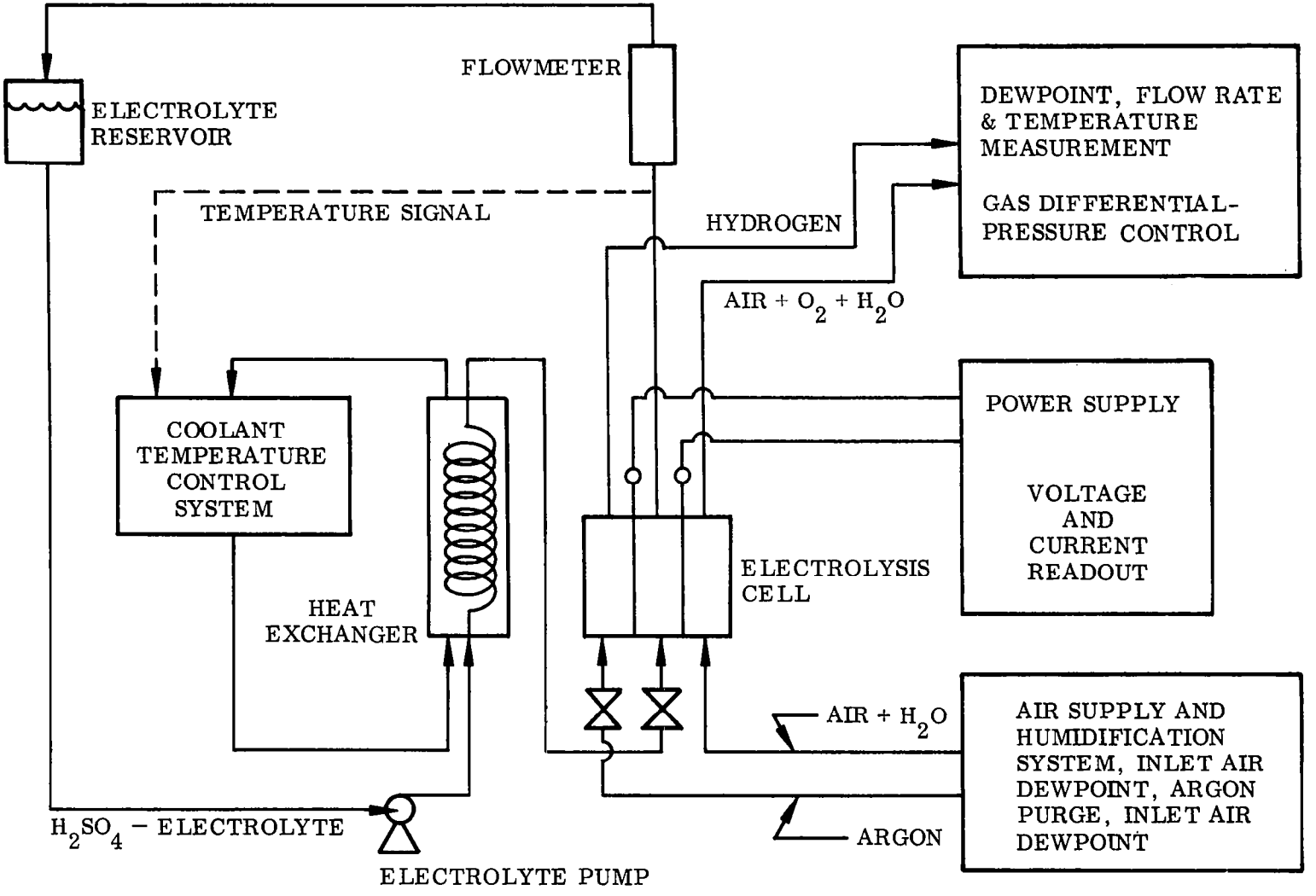

Fig. 2-26 Liquid Electrolyte-Absorbent Matrix Water Vapor Electrolysis Cell Test System

asbestos sheet contiguous to each electrode. The asbestos matrix served as a gas-liquid phase separator.

The liquid spacer ring, baffle, and end plates were made of transparent polycarbonate. Thermocouple wells made of polycarbonate were located in the liquid center ring and in the exit electrolyte line. Stainless steel thermocouple wells were used in the inlet and exit air lines.

The electrodes were made of AA-1 electrode material spot-welded to 0.025-cm-thick tantalum sheet stock rims. Tantalum screen was used to support the electrode material. Pressure strips cut from O-ring stock were used in the gas spaces of the cell to insure intimate contact between the electrodes and the asbestos sheets. These pressure strips also served as baffles in the air chamber of the cell to provide uniform air flow over the entire electrode surface. Cell construction and electrode configuration are shown in Fig. 2-27.

2.4.4 Test Results

Three liquid-electrolyte cells were assembled and operated. Cell performance characteristics, parameters for the electrolysis process, and factors affecting the water vapor absoprtion process were evaluated.

Cell A-16. The first liquid-center cell contained a 0.05-cm-thick sheet of asbestos* adjacent to each electrode. The electrodes consisted of active electrode material (18 cm^2) spot-welded to a tantalum support screen which in turn was spot-welded to sheet-stock tantalum rims.

Performance-time curves for this cell (Cell A-16) are shown in Fig. 2-28. The cell was operated at a current density of 75 mA/cm^2 using a constant-current power supply. A malfunction of the power supply caused a large increase in current density which persisted from 125 to 168 hr of elapsed time. Two sulfuric acid concentrations

*Tilton Blue.

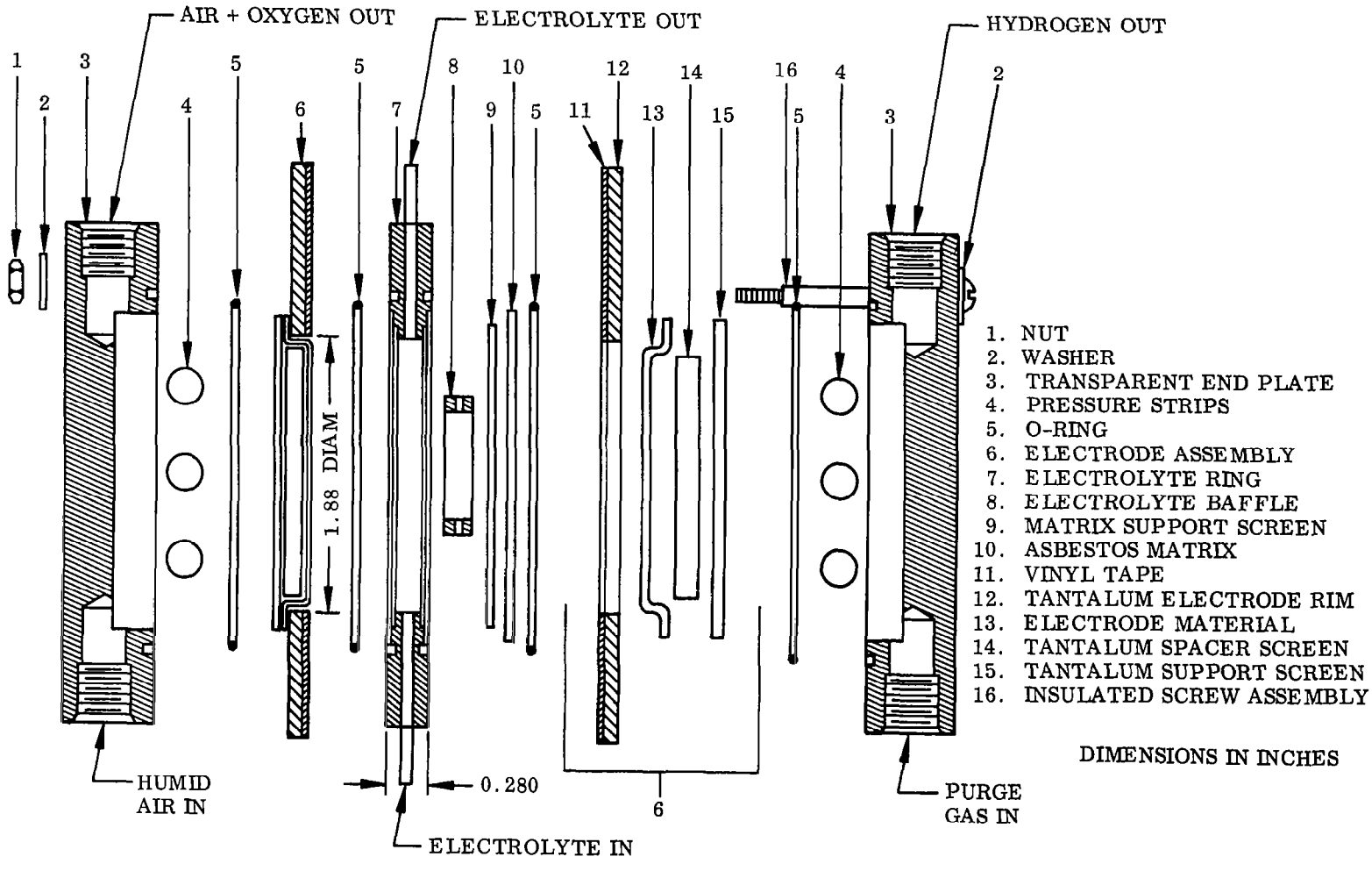

Fig. 2-27 Liquid Electrolyte-Absorbent Matrix Electrolysis Test Cell Schematic

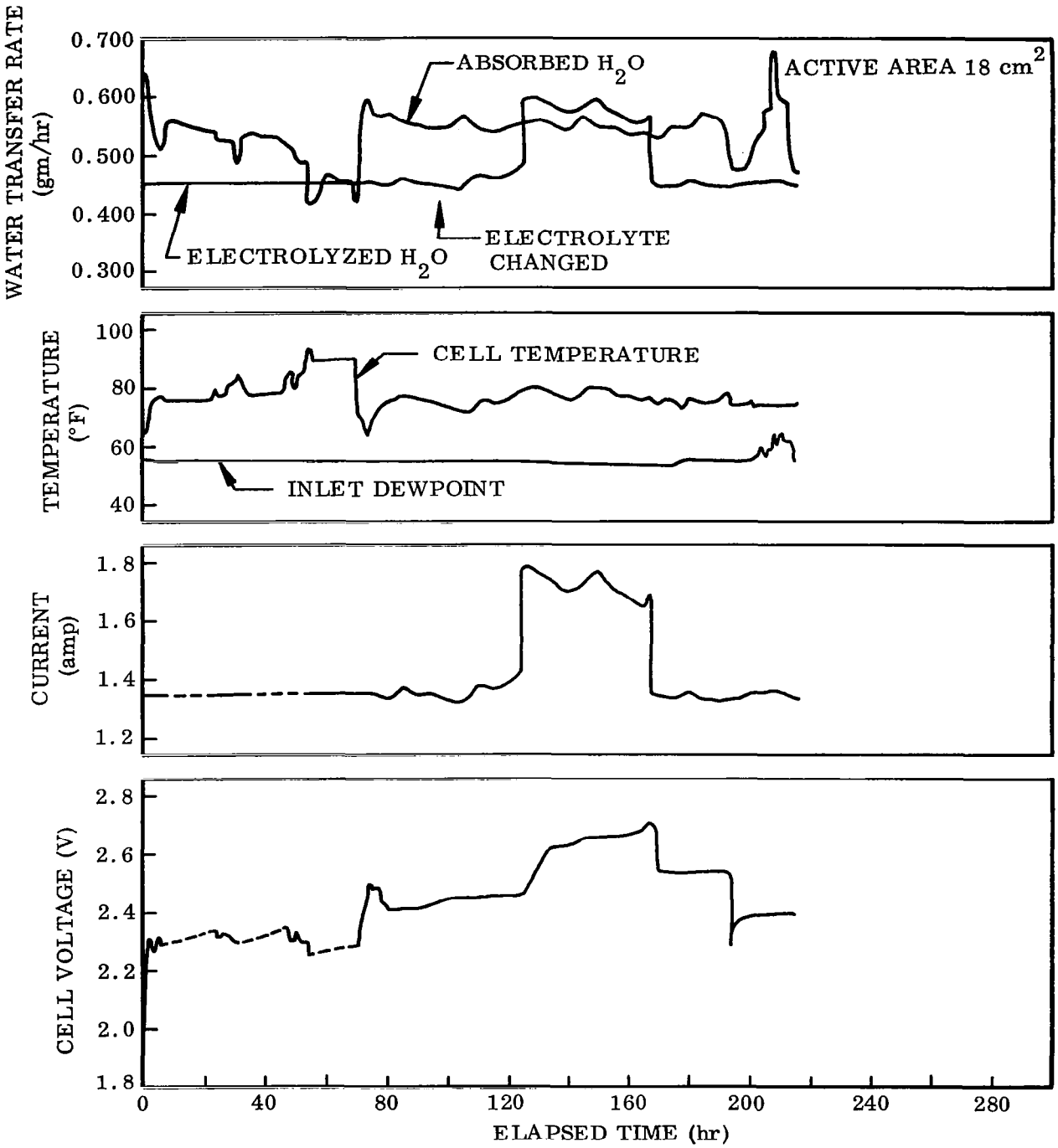

Fig. 2-28 Lifetime Performance Characteristics – Cell A-16

(9.1 and 9.6 M) were used during the test. Changes in acid concentration, noted in Fig. 2-28, were made to determine the effect of acid concentrations on cell performance. Initial and final cell specific resistance were 4.13 and 5.13 ohm-cm, respectively.

The cell voltage was measured as a function of current density at a cell temperature of 70°F to obtain the 70°F-polarization curve of Fig. 2-29. Below that curve in the figure is the IR free polarization obtained by subtracting the IR loss of the cell from the cell voltage. The polarization curves at 75°F were calculated from the experimentally determined relationship between cell voltage and cell temperature shown in Fig. 2-30.

When the cell was assembled, electrical contact was made to the asbestos-support screens inside the cell. With these contacts, the voltage drops within the cell were measured as indicated in the simplified cell cross-section shown in Fig. 2-31. A gradual increase in cell voltage (V_c) was noted in the performance-time data plotted in Fig. 2-28. Measurement of the internal voltages, V_{O_2}, V_E, and V_{H_2}, indicated that the rise in cell voltage was the result of an increase in V_{O_2}. The increase in V_{O_2}, and the resulting increase in V_c, has been attributed to an apparent time-dependent degradation at the oxygen electrode. When the cell was disassembled, however, after 215 hr of operation, there was no discernible change in the appearance of the oxygen electrode or the matrices.

Cell A-17. A cell with reduced asbestos thickness was assembled (0.025 cm) to study the effect on cell performance this cell characteristic might have. The cell exhibited very poor initial performance which was attributed to insufficient electrode-asbestos contact. This experiment was repeated using an improved electrode design (Cell Number A-19).

Cell Number A-18. Cell A-16 was reassembled with fresh sheets of asbestos and numbered A-18. The initial cell specific resistance was 4.01 ohm-cm. The cell

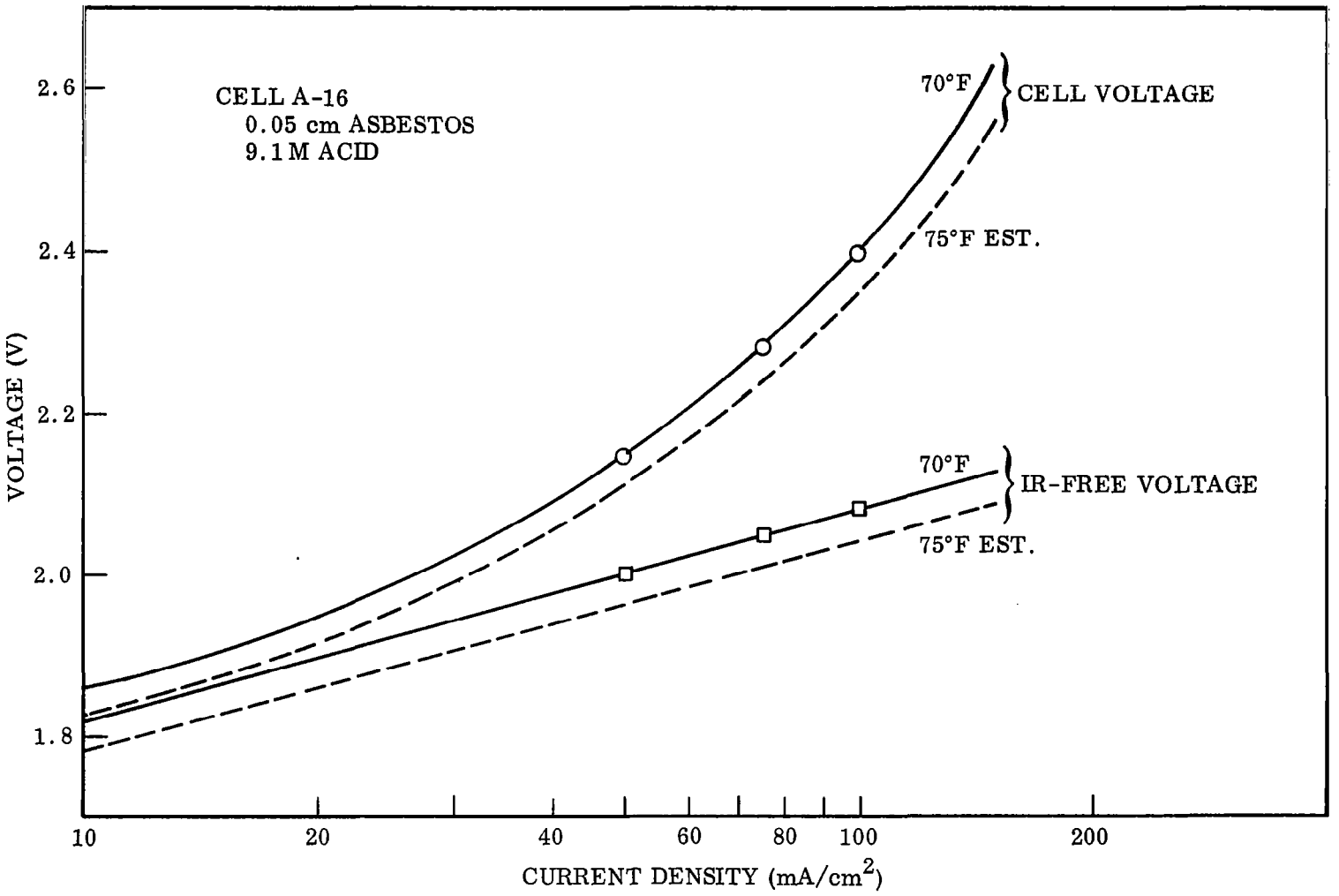

Fig. 2-29 Cell Voltage Variations With Current Density at Two Different Temperatures – Cell A-16

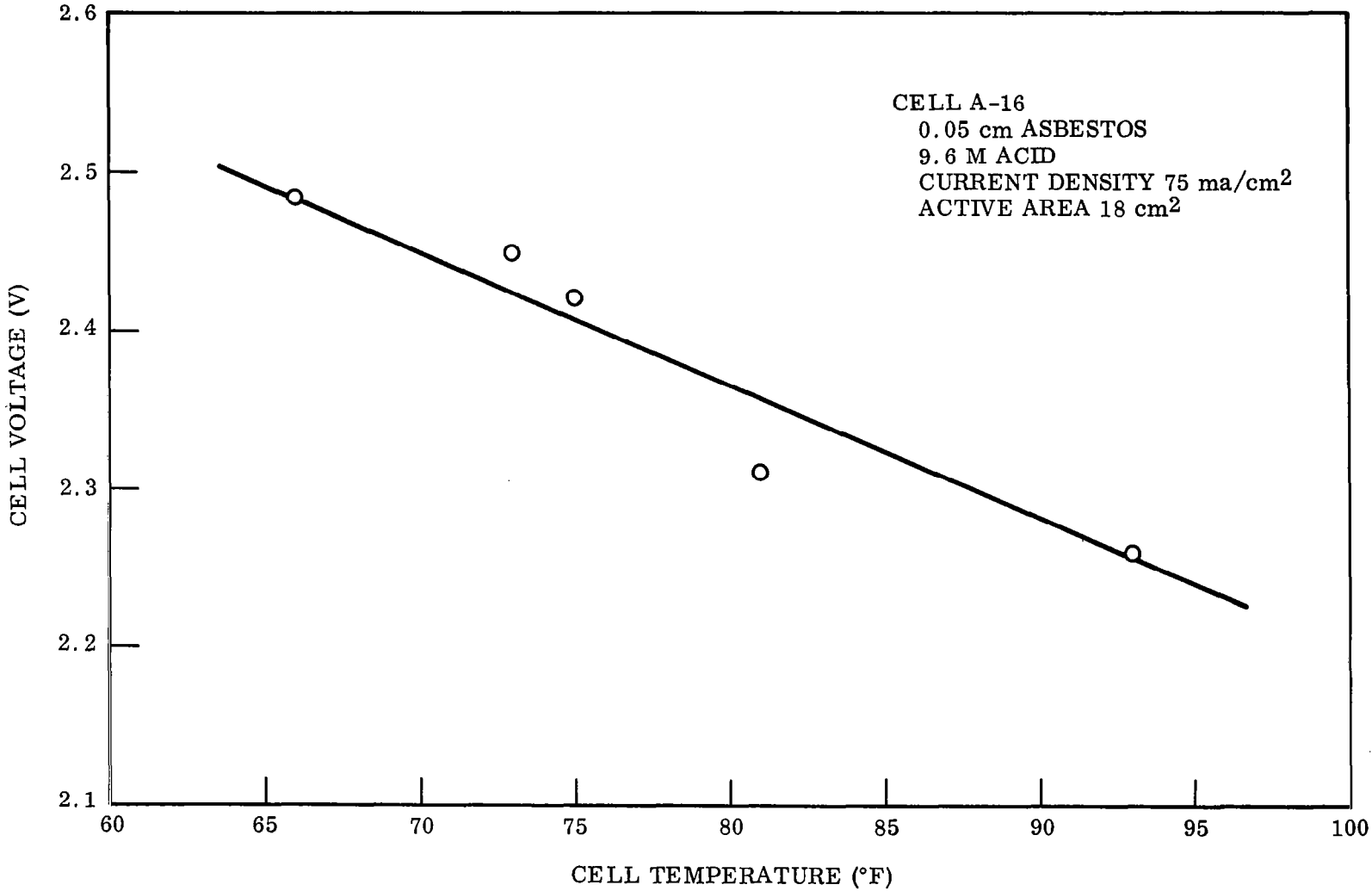

Fig. 2-30 Cell Voltage Variation With Cell Temperature – Cell A-16

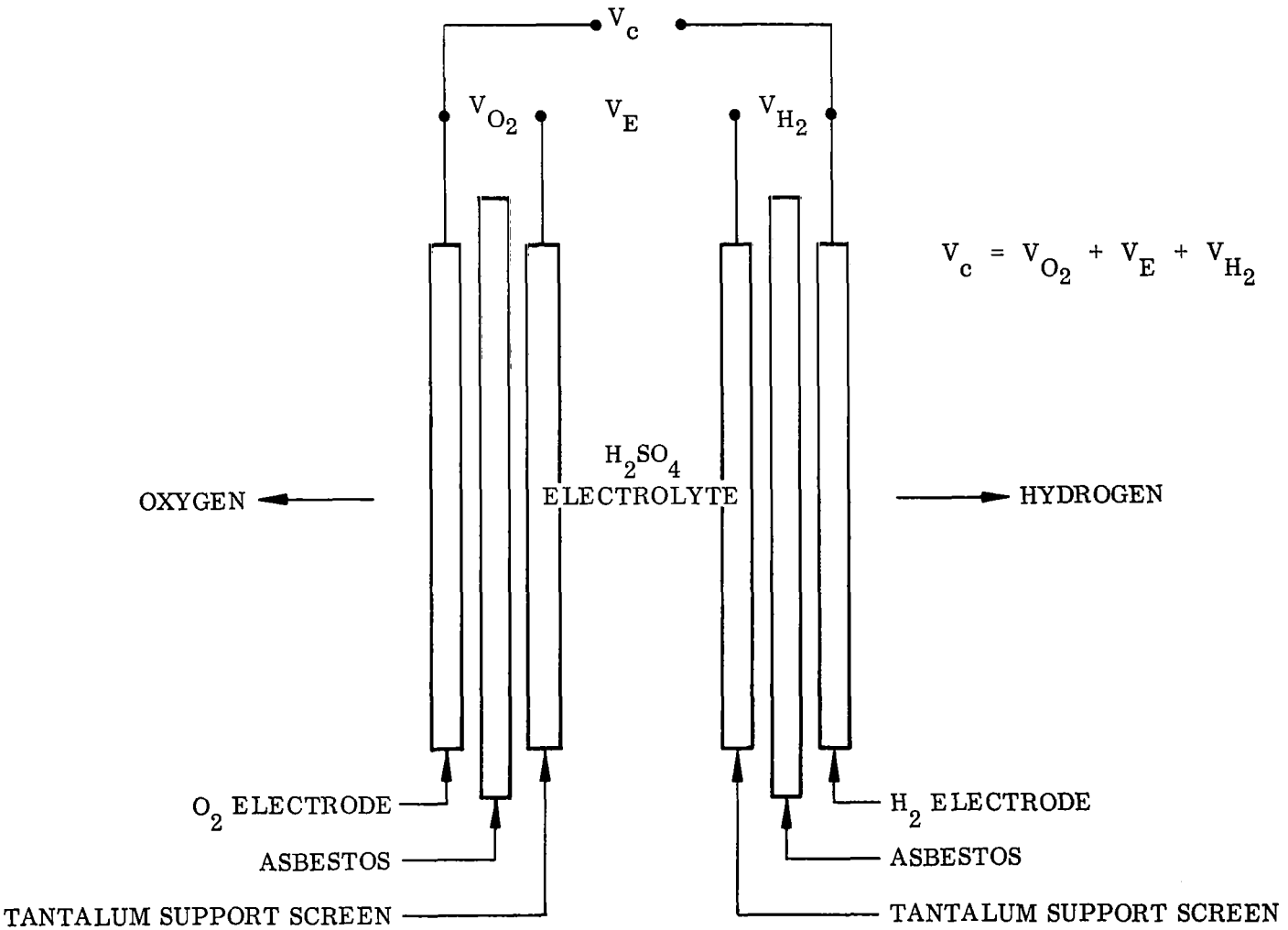

Fig. 2-31 Liquid-Electrolyte-Absorbent Matrix Test Cell Schematic Showing Internal Voltages

was operated for 287 hr at 75 mA/cm^2 with performance versus time behavior as shown in Fig. 2-32. Vertical lines in the figure represent cell shutdown for overnight and weekend periods. The numbers shown over the water transfer rate curves indicate air flow rate in cm^3/sec.

The electrolyte concentration was changed several times during the run. Decreasing the acid concentration resulted in a lower initial cell voltage because of the higher conductivity of the acid. The voltage rise with time, however, increased slightly when the acid concentration was decreased.

The ozone content of the evolved oxygen in Cell A-18 was measured at various cell voltages. The experimental results are plotted in Fig. 2-33. The threshold voltage for ozone production, obtained by extrapolating the data to zero ozone production, was found to be 2.33 V. The IR free cell voltage at this point was estimated from the initial cell resistance to be 2.09 V. The specific conditions which initiate ozone production could not be established from this experiment. The nature of the oxygen electrode polarization was not known, and the effects of acid concentration and cell temperature were not determined. This IR free voltage, however, is near the theoretical voltage for the generation of ozone, 2.07 V. Because the overvoltage of the hydrogen electrode is generally quite low, the IR free voltage is a reasonable approximation of the oxygen electrode overvoltage. It is believed that the production of ozone is harmful to the oxygen electrode, and therefore the cell should not be operated at a point where ozone is produced. An oxygen electrode voltage of 2.07 V is an upper limit on the operating current density of the cell for a given acid concentration.

Cell Number A-19. An improved electrode design and the effect of decreasing the asbestos thickness were evaluated in Cell A-19. The electrode configuration is shown in Fig. 2-27. Asbestos thickness was reduced by a factor of two, to 0.025 cm. The initial cell resistance with the thin asbestos was 0.124 ohms (3.15 ohm-cm) as compared to 0.163 ohms (4.13 ohm-cm) and 0.158 ohms (4.01 ohm-cm) for Cells A-16 and A-18 where 0.05-cm-thick asbestos was used. This reduction in cell resistance represents a decrease of approximately 53 mV in IR loss at 75 mA/cm^2.

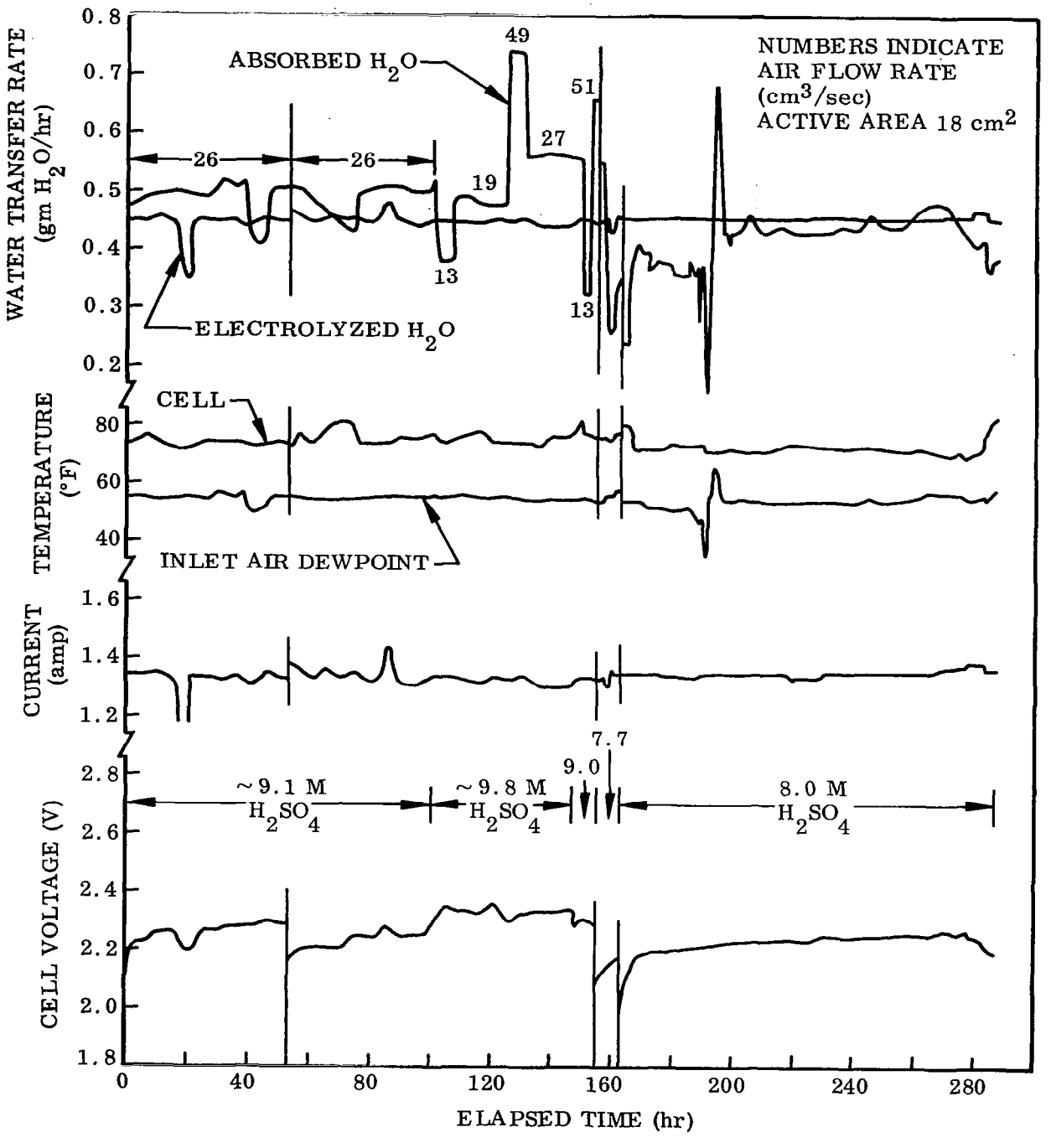

Fig. 2-32 Lifetime Performance Characteristics – Cell A-18

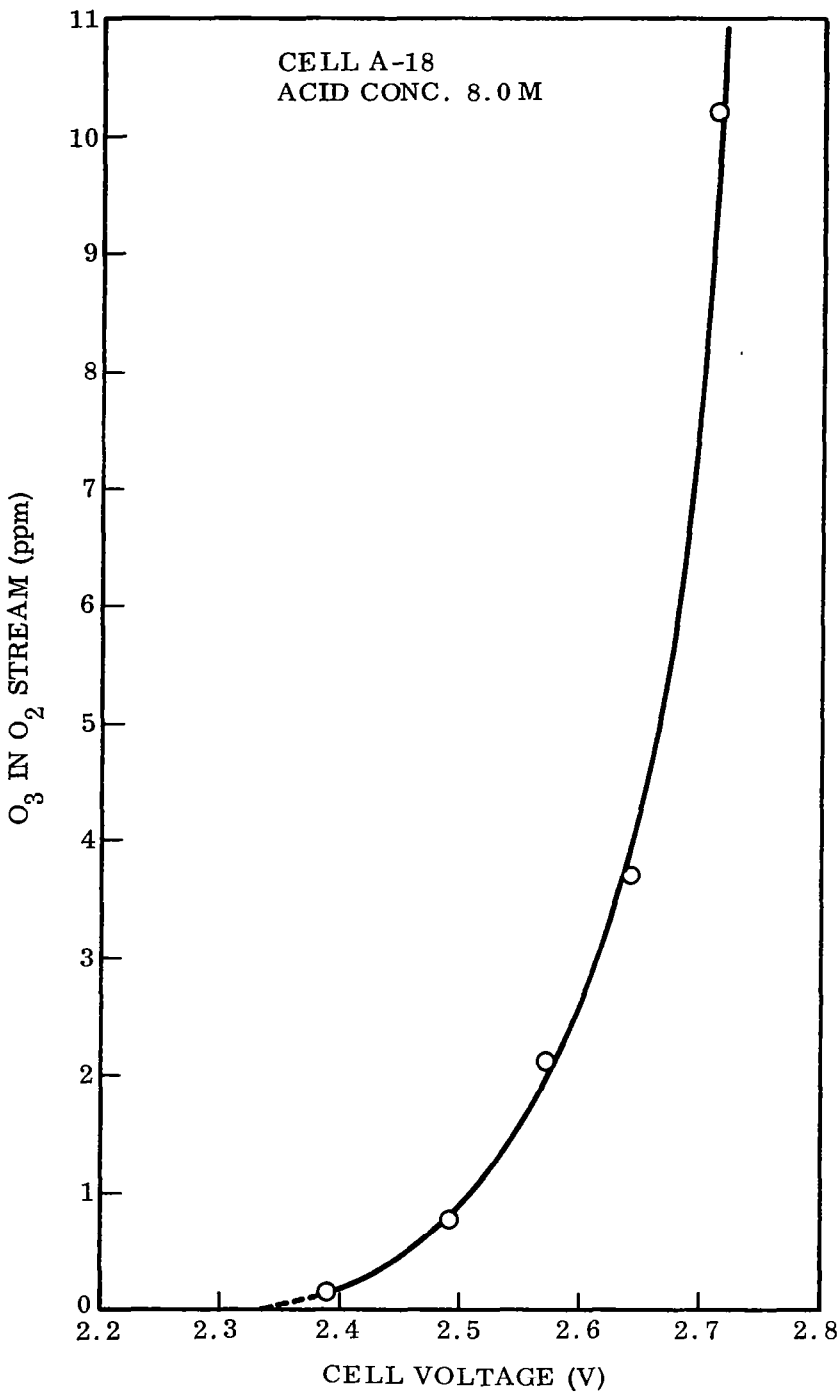

Fig. 2-33 Ozone Production Variation With Cell Voltage – Cell A-18

The performance of Cell A-19 as a function of elapsed time is shown in Fig. 2-34. Performance superior to that of the previous cells was observed. The cell operated at a lower cell voltage for the same current density, and exhibited a smaller change in cell voltage with time. The cell voltage was independent of relatively large changes in the water absorption rate.

The sudden increase in cell voltage shown in Fig. 2-34 at 298 hr of elapsed time was the result of a malfunction in the auxiliary system. The pump used to circulate the sulfuric acid electrolyte was a laboratory model not designed for use in acid systems. Seepage of acid in the polyethylene body of the pump contacted a stainless steel shaft which was chemically attacked by the acid causing a pump seal failure. The resulting loss of electrolyte caused the cell failure. Selection of the proper pump would have prevented this failure.

An estimated polarization curve for Cell A-19 (Fig. 2-35) was derived from the performance data at 75° F in 9.1 M acid (Fig. 2-34). The resulting IR free polarization compares closely with the 75° F IR free polarization estimated for Cell A-16 (Fig. 2-29). The cell voltage polarization curve is lower for Cell A-19 because of its smaller cell resistance.

The water absorption process. The water absorption studies were conducted at a constant electrolysis rate. It has been noted that cell voltage is not affected by changes in absorption rate over short periods of time (Cell A-19, Fig. 2-34). In absorption studies of Section 2.1.5, system parameters which were shown to affect the rate of absorption of water by sulfuric acid were investigated. The water absorption rate in the test cells was measured as a function of these parameters.

The cell temperature in Cell A-16 was varied at a constant air flow rate of 25 cm^3/sec (2.83 ft^3/hr) and an electrolyte concentration of 9.6 M. The absolute humidity of the inlet air was maintained at 13.2×10^{-6} gms of water/cm^3 of dry air (50% relative humidity at 75° F) during the test. Water absorption rate in gms/hr is shown in

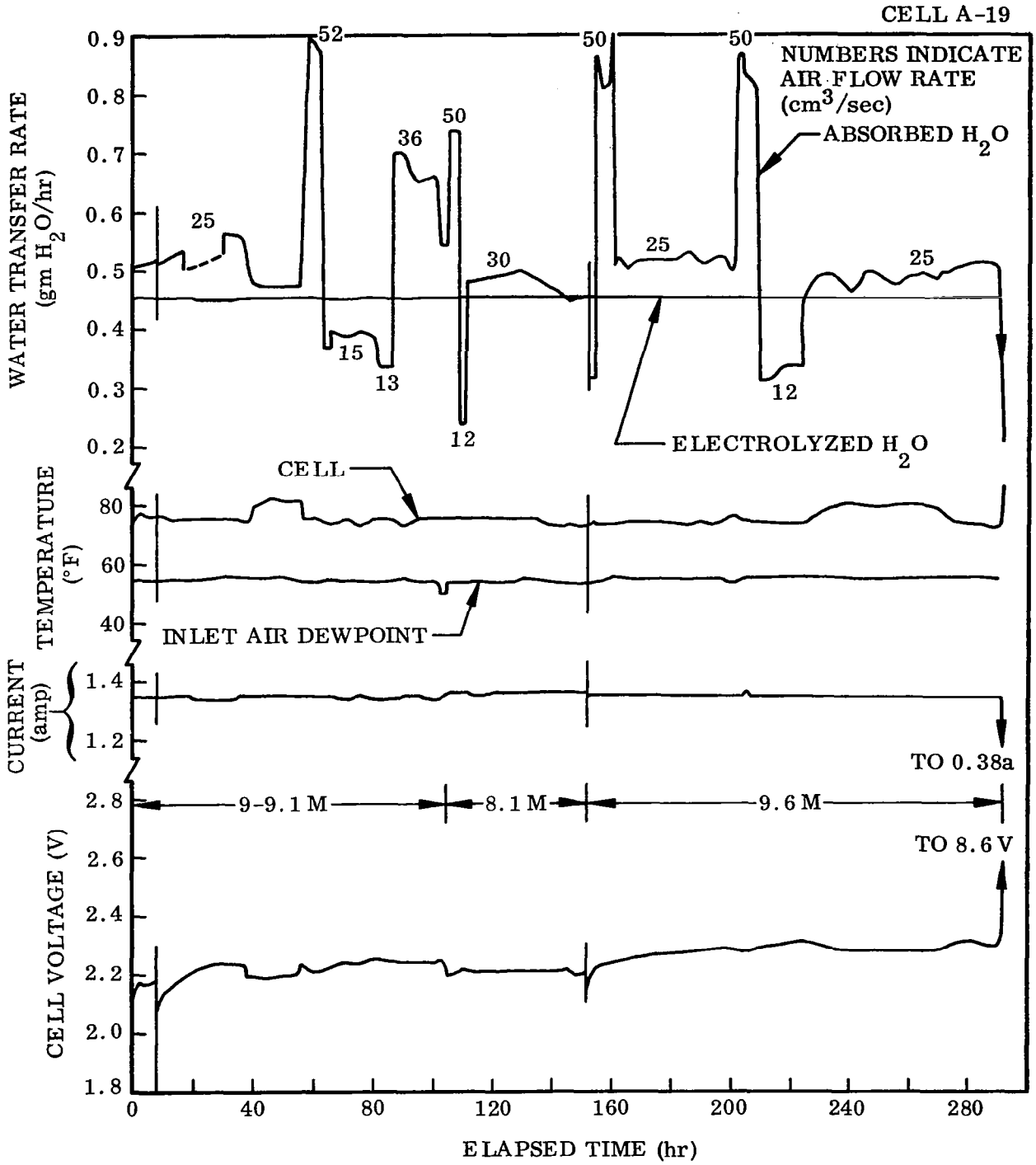

Fig. 2-34 Lifetime Performance Characteristics – Cell A-19

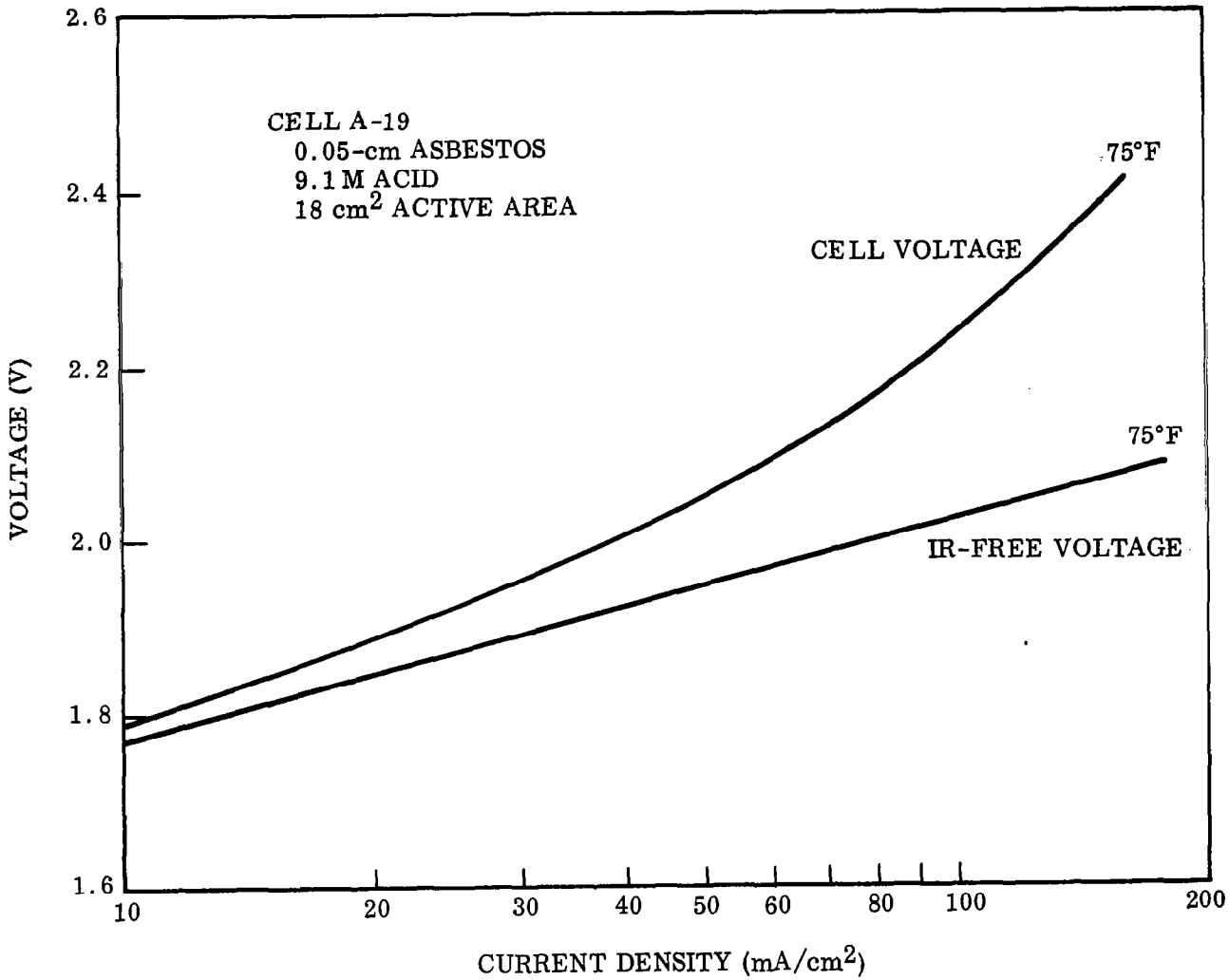

Fig. 2-35 Estimated Polarization Curve Cell A-19

Fig. 2-36 as a function of cell temperature. These data indicate that the cell temperature has little effect on the water absorption rate over the narrow range of temperatures which were studied. A 20°F change in cell temperature (from 70° to 90°F) resulted in a decrease in water absorption rate of approximately 9%.

Water absorption rate was measured in Cell A-18 as a function of driving force, i.e., inlet air absolute humidity (or dewpoint), at constant bulk acid concentration. The experimental results are plotted in Fig. 2-37 as water transfer rate (gm/hr) versus inlet air dewpoint (°F). Relative humidity of the air at 75°F corresponding to dewpoint is indicated in the figure. The bulk acid concentration in the cell during the test was 8.0 M, and the air flow rate was 27 cm^3/sec (3.05 ft^3/hr). The water absorption rate is directly proportional to the absolute humidity of the inlet air when the absorption rate is not greatly different from the electrolysis rate. For a constant electrolysis rate, a very low absorption rate causes concentration of the acid at the surface in contact with the air. Similarly, an absorption rate in large excess of the electrolysis rate causes dilution of the acid at the gas-liquid interface. The resulting change in acid concentration temporarily changes the effective driving force for absorption. This is shown by the deviation from a straight line at the ends of the curve in Fig. 2-37 where the dewpoint probably was not maintained a sufficient length of time for steady state condition to exist.

The effect of the volumetric air flow rate on water absorption rate was investigated. Water absorption rate as a function of air flow rate was measured in Cells A-18 and A-19 at three bulk acid concentrations. The experimental results are shown in Figs. 2-38 and 2-39. The inlet air dewpoint in both cells was maintained at 54°F (approximately 48% relative humidity at 75°F). Cell temperature was 75°F. In each experiment, the relationship between absorption rate and air flow rate was

$$dw/dt \propto q^m \qquad (19)$$

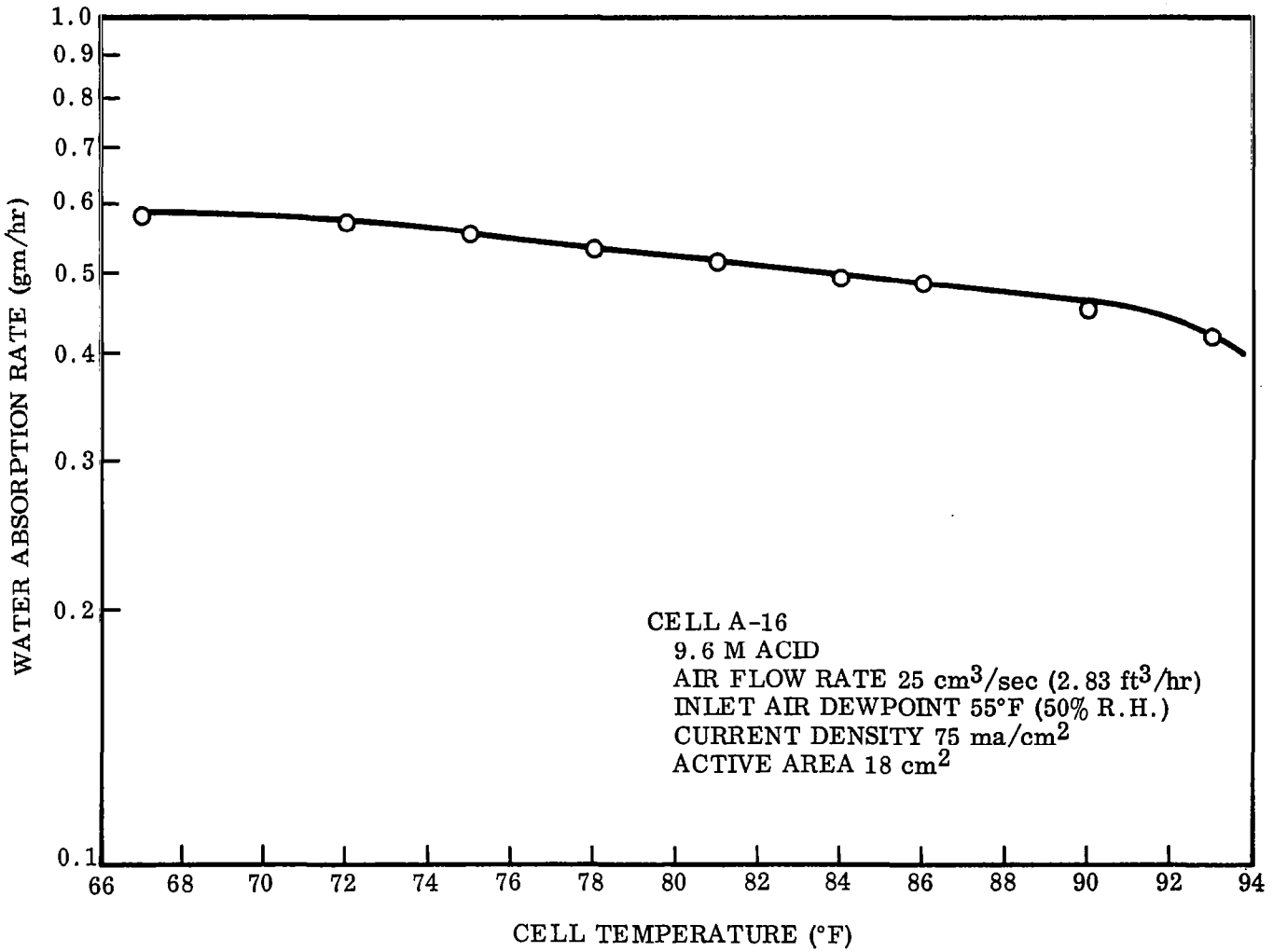

Fig. 2-36 Water Absorption Rate Variation With Cell Temperature – Cell A-16

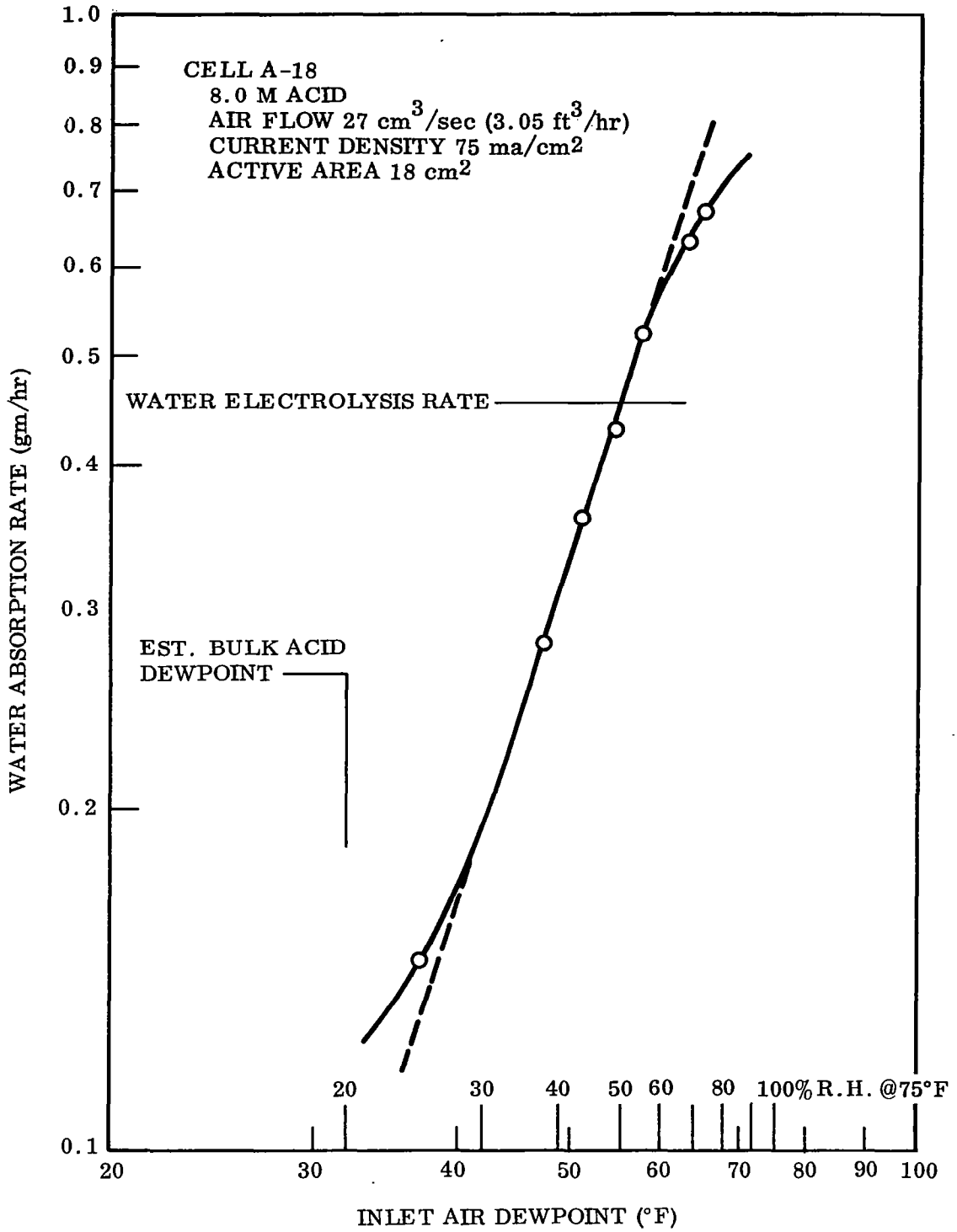

Fig. 2-37 Water Absorption Rate Variation With Inlet Air Dewpoint – Cell A-18

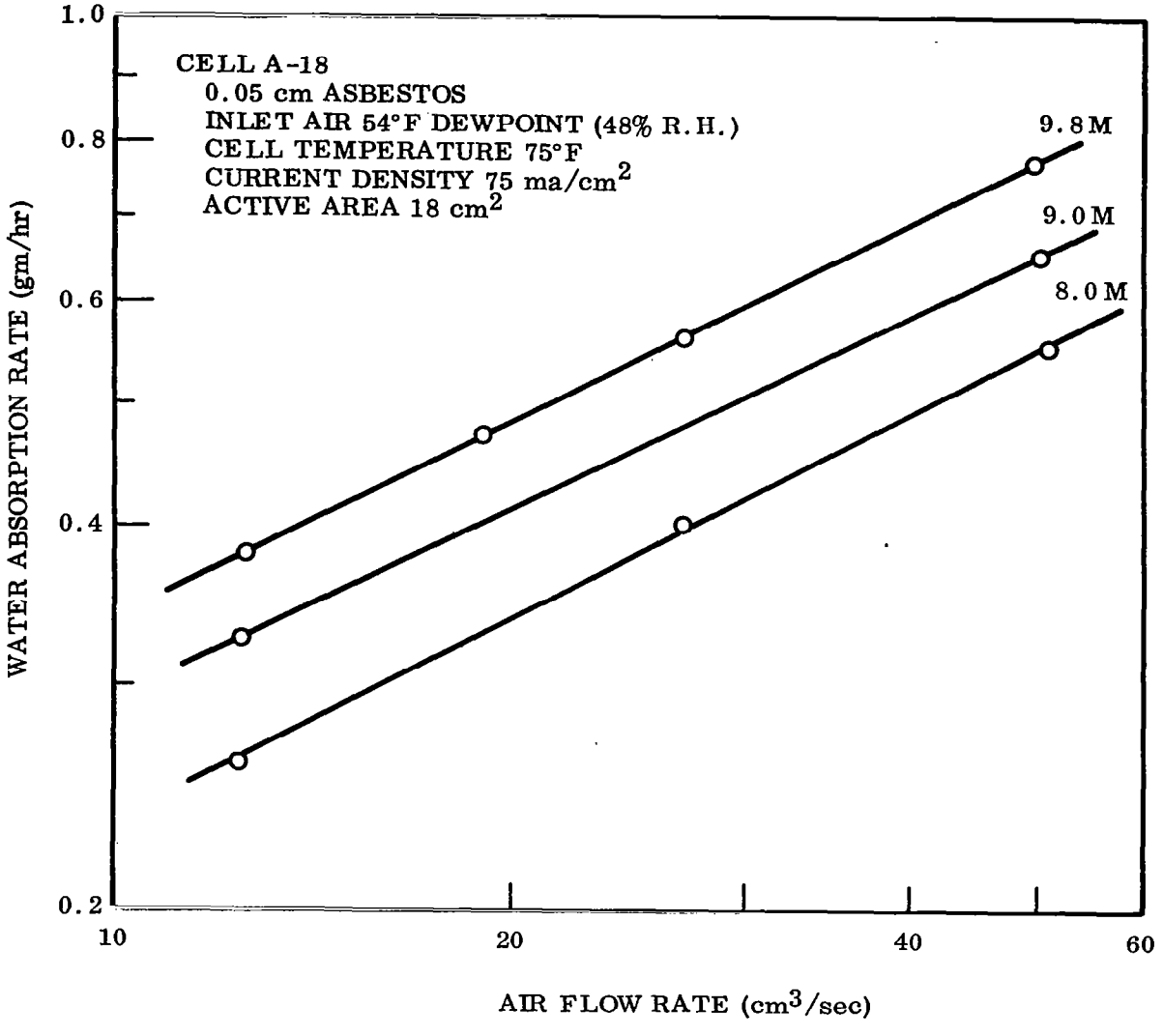

Fig. 2-38 Water Absorption Rate Variation With Air Flow Rate at Different H_2SO_4 Concentrations – Cell A-18

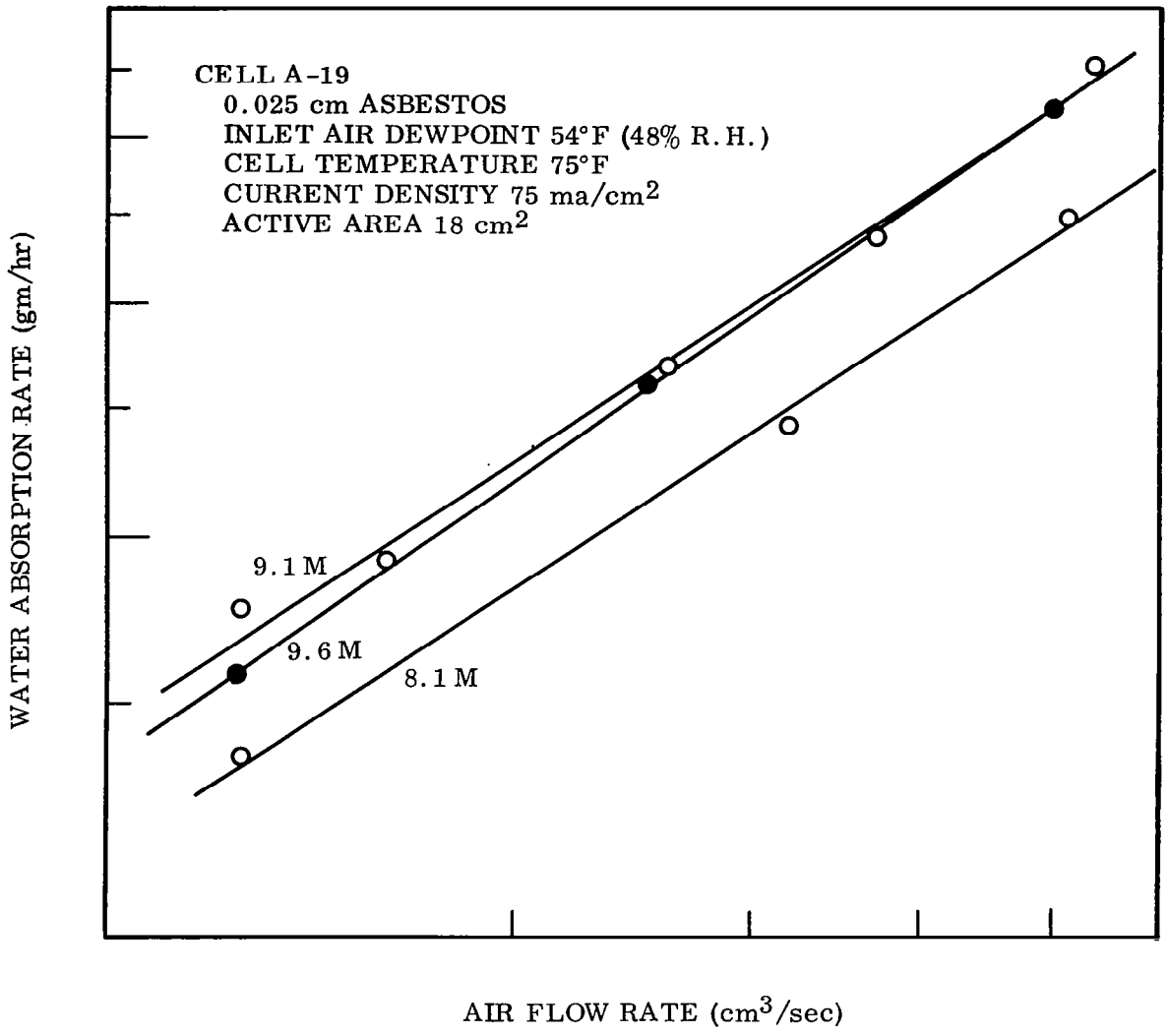

Fig. 2-39 Water Absorption Rate Variation With Air Flow Rate at Different H_2SO_4 Concentrations – Cell A-19

where

dw/dt = water absorption rate, (gm/hr)

q = air flow rate, (cm^3/sec)

m = slope of the curve ln(dw/dt) versus ln q

The average value of m was 0.52 for Cell A-18 and 0.66 for Cell A-19. These values compare well with the value of 0.5 determined in the bulk acid studies of Section 2.1.5.

No explanation for the coincidence of the 9.1 M and 9.6 M air flow versus water transfer curves for Cell A-19 (Fig. 2-39) was apparent from the experimental data.

A dehumidification efficiency was defined for the test cells according to the equation

$$\%\text{eff} = (H_i - H_o/H_i - H_a) \times 100 = (\Delta H_{actual}/\Delta H_{ideal}) \times 100 \qquad (20)$$

where

H_i = inlet air absolute humidity

H_o = outlet air absolute humidity

H_a = absolute humidity over the acid

This dehumidification efficiency was calculated from experimental data at various air flow rates for Cells A-16, A-18, and A-19. The resulting curves are shown in Fig. 2-40. With the exception of anomalous results for Cell A-19 at 9.6 M acid (Fig. 2-39), the dehumidification efficiency is shown to be independent of acid concentration within a cell of fixed geometry and to depend only on the air flow rate. The three cells had comparable efficiencies at the lower air flow rates, but the efficiency in Cell A-19 was 10% higher than in Cell A-18 at the higher flow rates. Care was taken in assembling the two cells to make the air chamber geometries as nearly identical as possible. Small differences may have existed, however, sufficient to

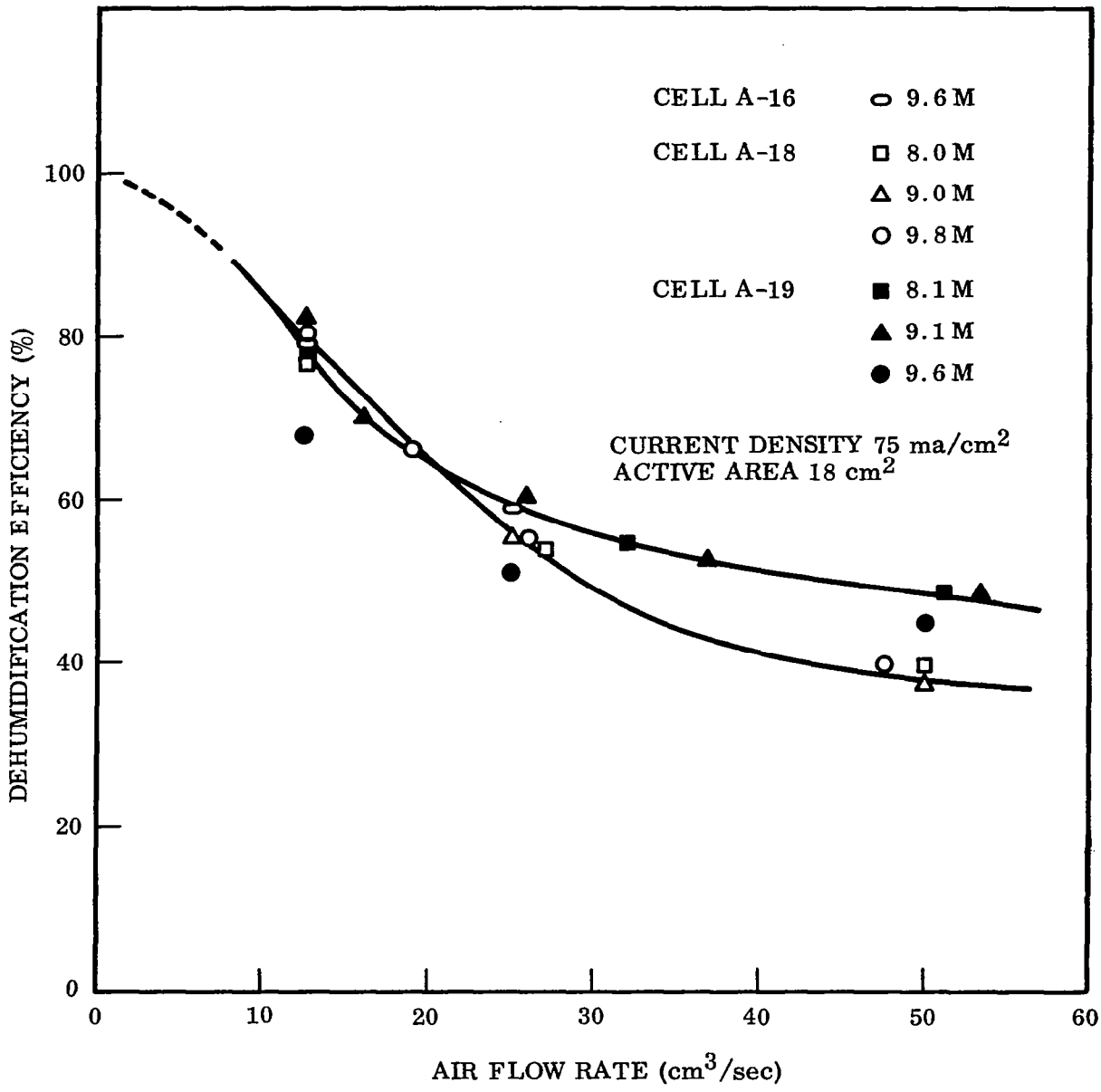

Fig. 2-40 Dehumidification Efficiency Variation With Air Flow Rate at Different H_2SO_4 Concentrations – Cells A-16, A-18, and A-19

contribute to the observed difference in dehumidification efficiency. Two other, perhaps more significant, differences in cell construction offer a better explanation of the efficiency difference. Cell A-19 contained electrodes of an "improved" design which may have provided better contact with the acid contained in the asbestos matrix. The thinner asbestos used in the Cell A-19 may have reduced diffusion resistance between the acid-air interface and the bulk liquid. Insufficient experimental data are available to completely define the nature and the magnitude of the factors affecting the dehumidification efficiency.

2.5 COMPARISON OF THE IMMOBILIZED MATRIX CELLS AND THE LIQUID ELECTROLYTE-ABSORBENT MATRIX CELLS

2.5.1 Electrolysis Power Requirements

Although both systems, the immobilized matrix "gel cell" and the liquid electrolyte-absorbent matrix cell "liquid center cell," were not operated under identical conditions, the voltage performance at different current densities may be compared. Some of these comparisons are extrapolated from the previously presented data, but the error in doing so is small. Table 2-6 presents a comparison for the voltages and cell resistances.

Table 2-6

VOLTAGE-CURRENT COMPARISON OF GEL TYPE AND LIQUID CENTER TYPE CELLS

Cell Type	Cell No.	Acid Concentration (mole)	Initial Sp. Res. 75° F (ohm-cm)	Voltage After 10 hr of Operation (80° F)	
				35 mA/cm^2	75 mA/cm^2
Zeolon-H	A-2	8.1	10.1	2.04	2.19(a)
Zeolon-H with gas barrier	A-12	8.1	14.0	2.15	–
Silicic Acid	A-3	8.1	7.6	1.99	–
Silicic Acid with gas barrier	A-11	8.1	10.4	2.01	–
Liquid center cell	A-19	9.1	3.2	1.94(a)	2.11(a)

(a) Extrapolated from existing data.

There is little performance difference between the gel cells without gas barrier and the liquid center cells. However, voltage of the zeolon gel cell with a gas barrier is markedly higher, mainly due to the higher specific resistance. The silicic acid gel cell with gas barrier retains a good specific resistance which accounts for the small change in voltage with and without the gas barrier. It should be pointed out that sustained operation of the gel cells (with or without the gas barrier at 75 mA/cm^2) would be markedly poorer than the liquid center cell; the gel cells would undoubtedly fail due to drying. Although the high current densities were not tried with the gel cells, the mode of failure experienced (drying out) at 35 mA/cm^2 indicate that this current density may be near the maximum operating level. The sustained operation of the liquid center cell on 8.1 M acid at 75° F was 2.20 V. Had the cell been operating at 80° F, the voltage would probably have been 2.16 V.

2.5.2 Long Term Performance

The work on the liquid center cells was performed late in the program and long term performance data (greater than 280 hours) not available. However, LMSC experience with a KOH cell of the same design has shown operational lifetimes of at least 2000 hours without failure (other than what may be caused by auxiliary, non-optimized equipment). The gel cells, on the other hand, failed due to drying in periods of 500 hours or less; many of the cells operated for periods less than 300 hours. In nearly all the cases, the voltage required to sustain the current at the end of the test was unreasonably high. Degradation of the Zeolon-H during all operations probably rules it out as a candidate for a gel type cell. The Silicic acid and Cabosil, however, show promise and could be built into reliable cells with the use of a gas cross-leakage barrier. The maximum operating current density for these cells will be lower than the liquid center cells to prevent cell failure by excessive drying; this will increase the number of cells required for the generation of a fixed amount of oxygen.

2.5.3 Water Vapor Absorption

Water vapor absorption characteristics in operating cells of the gel and liquid center type are compared in Table 2-7. The dehumidification efficiency used in the table

Table 2-7

WATER TRANSFER COMPARISON OF GEL TYPE AND LIQUID CENTER TYPE CELLS

Cell Type	Cell No.	Current Density (mA/cm^2)	Dewpoint (°F)	Air Flow Rate (cm^3/sec)	Acid Conc. (mole)	Cell Temp. (°F)	Water Transfer Rate (gm/hr)	Dehumidification Efficiency (%)
Silicic Acid	A-3	35	54	25	8.1	80	0.255	44
Silicic Acid with gas barrier	A-11	35	67	25	8.1	80	0.315	32
Zeolon-H with gas barrier	A-12	35	58	25	8.1	80	0.194	26
Liquid Center Cell	A-18	75	54	25	8.0	75	0.380	57
			58	27	8.1	72	0.482	57
			65	27	8.1	72	0.676	52
Liquid Center Cell	A-19	75	54	25	8.1	75	0.430	60

is defined in Eq. (2), Section 2.4.4. These experimental data show that the liquid center type cells are considerably more efficient in removing water from the air then the gel type cells under comparable conditions. The silicic acid cells appear to be more efficient than the Zeolon-H cells, but insufficient data were taken to prove this point conclusively. Effects of operating current density on the water transfer process were not evaluated in either type of cell, although water transfer rates capable of sustaining a current density of 150 mA/cm^2 were obtained in the liquid center cells operating at 75 mA/cm^2.

2.5.4 Reliability

The problem of reliability is important as the water vapor electrolysis cells became more highly developed. Intrinsic to reliability is the ease and efficiency of cell assembly. The importance of cell sealing cannot be overemphasized. The very nature of the gel cell increases the complexity of cell assembly and sealing. Stacking the cells into a module is difficult since the electrolyte has to be carefully placed to insure good electrode-electrolyte contact. On the other hand, the liquid center cell has been built into modules and the assembly is efficient and the sealing is good; no gas or liquid leaks have been detected.

The overwetting or overdrying of the gel cells was noted in some tests and this problem constitutes a cell failure. A liquid center cell, with the proper differential pressure control, has no flooding of the electrode. Differential pressure control on the gel cells cannot and did not prevent electrode flooding; only close control of water absorption can do this through control of cell temperature, electrolysis rate, and inlet humidity.

Section 3
CONCLUSIONS

1. Sulfuric acid is an effective electrolyte for use in a water vapor electrolysis system.

2. Water absorption rates capable of sustaining an operating current density of 150 mA/cm^2 are easily achieved using sulfuric acid in an absorbent matrix-liquid electrolyte cell. Parameters controlling the absorption rate are air flow rate, inlet air humidity, acid concentration, cell temperature, and cell geometry.

3. The performance of electrodes in a sulfuric acid electrolyte is primarily dependent upon acid concentration, the electrode catalyst, and the electrode structure. Anode overvoltage is the parameter which most completely describes electrode performance.

4. The principal secondary cell reaction which occurs in a sulfuric acid electrolysis cell is the production of ozone at the anode. The threshold for the reaction is an anode voltage of 2.07 V versus a hydrogen reference.

5. The first requirement of a matrix material used in an immobilized-electrolyte electrolysis cell is chemical stability. Silicic acid is inert as a matrix in combination with sulfuric acid. A synthetic zeolite degrades with time in contact with sulfuric acid and, therefore, is not a satisfactory matrix material. Immobilized-matrix electrolysis cells have the feature of gas-liquid phase separation compatible with a zero-gravity environment. Disadvantages are sensitivity to vibration, susceptibility to gas cross leakage, and limited operational capability under adverse operating conditions. A typical performance level for a cell using silicic acid (asbestos gas barrier) with 8 M sulfuric acid is 2.10 V at 35 mA/cm^2. Replenishment of electrolyzed water at this operating level is accomplished under thest typical conditions: 25 cm^3/sec (2.81 ft^3/hr) air flow; 60% inlet air relative humidity at 80°F and 80°F cell temperature. The relative humidity of the effluent air is 50% at 80°F.

6. The liquid electrolyte-absorbent matrix electrolysis cell has the advantages of high water absorption efficiency, low voltage at high current density, and efficient external cooling which reduces the cooling load. The disadvantage is the auxiliary system requirement, including the need for differential pressure control. A typical long-term performance level for a small single cell of this type (18 cm^2) using 8 M sulfuric acid as the electrolyte is 2.20 V at 75 mA/cm^2. Replenishment of electrolyzed water at this operating level is accomplished under these typical conditions: 27 cm^3/sec (3.05 ft^3/hr) air flow rate; 48% inlet air relative humidity at 75°F, and 75°F cell temperature. The relative humidity of the effluent air is 32% at 75°F.

Section 4
SCALE-UP CONSIDERATIONS

4.1 SYSTEM SELECTION AND DESIGN CONSIDERATIONS

4.1.1 Introduction

Each water vapor electrolysis system has advantages and disadvantages which must be evaluated when the system is to be developed into a complete self-sustaining unit. The important parameters are the power requirement, reliability, weight, and volume of the finished unit. For reliability the cell design must have effective sealing for both the gas and the liquid. Performance should not degrade with time. The operational current density should be high to reduce the number of cells required for a given oxygen generation rate. The overvoltage of the cell should be low to minimize power requirements. When these factors were taken into consideration, the gelled matrix cells tested appeared to be poor candidates for scale-up. On the other hand, the liquid electrolyte-absorbent matrix cell readily meets most of these requirements.

4.1.2 Advantages of the Liquid Electrolyte-Absorbent Matrix Cell

As previously described, the liquid electrolyte-absorbent matrix cell, to be called the liquid center cell in this section, utilizes circulating H_2SO_4 between two absorbent matrices that are contiguous to the electrodes. The phase separation takes place at the interface of the electrode and the absorbent matrix. The circulating electrolyte serves many functions, the most important of which is its use as the heat exchange medium for the cell. Because the waste heat from the cell is removed by the electrolyte, the cell temperature may be controlled for effective cell operation. Liquid-liquid heat exchange is more efficient than gas-gas heat transfer which is required in an immobilized matrix cell. Keeping the cell temperature low allows

the cell to absorb a greater amount of water from the air in a single pass; good dehumidification is accomplished with the cell. With an inlet humidity of 50% at 75°F, exit humidities range from 20 to 32% (depending upon the air flow rate) at 75°F. This high absorption rate reduces the blower power requirements. Little or no temperature change occurs in the flowing air stream as nearly all of the cell heat is removed by the electrolyte in an external heat exchanger. The penalty* applied to gas-gas heat transfer in a spacecraft is larger than that applied to liquid-liquid heat transfer effecting additional weight savings and improving operational efficiency of the unit as a dehumidifier.

Because the electrolyte supply is large relative to that absorbed in an immobilized matrix cell, there is little chance for the cell to dry or flood with unfavroable operating conditions. If the electrolysis rate is greater than the rate of water pick up from the air (due to changes in the inlet humidity or air flow rate) water may be supplied to the cell by injecting liquid water directly into the circulating electrolyte. If on the other hand, the water absorption rate is too high, the electrolyte will tend to dilute and the excess electrolyte may be stored in an external reservoir. The concentration changes due to the high or low absorption rates take place slowly because of the large capacity of the electrolyte in the system. The resulting changes, however, have an effect on the absorption characteristics of the cell. The more concentrated electrolyte will tend to absorb more water from the air so that the lower inlet humidity which caused the electrolyte to concentrate can be better tolerated. The converse is true because the more dilute electrolyte, caused by too high of an inlet humidity, will absorb less water. These controlling features are also demonstrated by the immobilized matrix cell. However, because the electrolyte capacity of that type of cell is small, the cell may not operate under unfavorable humidity conditions very long before the cell either floods or dries out. Either of these responses results in a cell failure.

---

*The values generally used are 0.018 lb/Btu/hr for liquid-liquid heat transfer and 0.025 lb/Btu/hr for gas-gas heat transfer.

The water injection feature also provides for operation at levels higher than the design point. The addition of liquid water into the electrolyte, and the provision of additional power and cooling, allows the cell to operate at a higher gas evolution rate providing an emergency operating capability.

Because the matrix is readily equilibrated and wet by the bulk acid, the overvoltage of the cell is low. This provides a flat polarization curve and operational current densities as high as 125 mA/cm^2 are practical with this type of cell. Because of the high operational current density, the number of cells required for a given electrolysis rate is low compares to an immobilized matrix cell.

The liquid center cell can be efficiently sealed, allowing the generated gases to be directed to the desired locations without the hazard of intermixing the hydrogen with either the air or the produced oxygen. Many cells have been built during the development of this design concept for the Lockheed KOH electrolyte liquid water feed cell; in all cases the sealing of the generated gases and electrolyte was satisfactory.

4.1.3 Disadvantages of the Liquid Electrolyte-Absorbent Matrix Cell

Although the advantages of the liquid center cell are numerous, an evaluation must also be made of the disadvantages of the system. Because a circulating electrolyte is used, the equipment necessary to promote this circulation, along with the differential pressure control and the heat exchanger, add to the complexity of the complete system. The design of the cell is also complicated by the manifolding to direct the flow of electrolyte in the cell. The interelectrode and intercell spacing are large because of the o-ring seal requirements.

Because the electrode must make intimate contact with the matrix, additional cell weight is required for the support screens and the current takeoff rims, although these features are generally required in any cell design that operates efficiently.

The electrolyte-gas interface must be located at the electrode-matrix interface, and generally a differential pressure control is required between the gas and the liquid electrolyte. This control may complicate the operation of the system and may need to be quite sensitive, although progress has been made with the fabrication of an electrode that may eventually eliminate all but a gross control of the differential pressure.

4.1.4 Design Considerations

Once the system type has been selected, the design of the full-scale model may be made using theoretical guidelines, data from small test cells, and good design procedures. The data as described in Section 2.4.4 of this report were used for the scale-up calculations that follow in this section. Whenever a larger cell is scaled up from a small test cell, there are certain parameters that must be carefully evaluated to make sure that the large cell performs in a fashion similar to the small cell.

One design problem is the structure of the electrode and its support. A large cell operating at a high current density requires a good electrical contact to all portions of the electrode. It has been shown that if the electrical connection is made to one edge or corner of the electrode, a voltage drop occurs across the face of the electrode. The edge of the electrode near the connection point will operate at a higher current density and the electrolysis process will proceed at a faster rate than the average rate for the cell. At a point removed from the connection point, the voltage is lower because of the voltage drop, and the current density is less. The electrolysis rate is lower at this point than the average rate for the cell. There now occurs a mass transfer difference in the matrix between these two points and local heating and concentration of the electrolyte will tend to occur at the high-current density point. The overvoltage of the electrode at the high-current density point will be high and performance will deteriorate. To make all of the electrode work at a more uniform rate, a peripheral contact should be made to the electrode with a material capable of conducting a higher current with less voltage drop than the electrode. Additional contact may be made to the electrode with a metallic screen or porous plate in intimate contact with the entire face of the electrode. This latter device also serves to strengthen and stiffen the

electrode providing for a better contact between the electrode and the matrix. Woven or expanded metal screens provide a relatively lightweight support structure. Spot-welding the assembly provides a resistance free and structurally strong bond between the parts of the composite.

The effect of electrode stiffness and flatness is also important in the large cell. If portions of the electrode do not make intimate contact with the matrix, these portions will be inactive causing the portions that are in contact with the matrix to operate at higher current densities than the average rate for the cell. If the electrode is made of a material that is not stiff, this contact problem will be serious unless something is done to stiffen the structure. This may be accomplished, as mentioned above, by the use of backup plates or screens. If screens are to be used, they must be rigidly attached to the rim and care must be taken to assure that the rim and screen structure is flat.

The use of interelectrode spacing devices is an acceptable means for providing additional electrode support and assuring the maximum contact of the electrode with the matrix. Because the interelectrode spacer should be made from a nonconducting material, a good choice is an appropriate elastic material which is not only nonconducting, but which also provides a spring to provide good electrode-matrix contact.

In the liquid center cell, a matrix support is provided on the side of the matrix opposite the electrode. This pushes the matrix against the electrode and aids in the electrode-matrix contact. The matrix support screens are maintained a uniform distance apart by the electrolyte spacer plate and matrix support screen spacers.

In all cases, careful attention to the mechanical design is important to assure optimum assembly. By careful control of the tolerances of the cell parts and assembly procedures, a large cell will perform as well as, or better than, a small cell.

Intrinsic to the performance of a reliable cell is cell sealing. The use of elastic sealing materials coupled with a good design will result in a gas- and liquid-tight cell.

The selection of the elastomer and the correct use of it is important. Elastic o-rings provide a good solution. However, the use of this device unfortunately results in a relatively thick cell design since adequate material must be used to support the o-ring in its groove. The groove depth then becomes the limit on minimum cell thickness. Nevertheless, the extra cell thickness and weight that results over a cell design that does not use o-rings, is generally a good tradeoff for the superior sealing that is provided.

Hydrogen, an elusive gas to seal and manifold, must be collected and distributed away from the cell. In the liquid center cell, the electrolyte must also be manifolded into the cell, directed between the matrices in the cell, and out of the cell into the external loop. If the manifolding system for both the gas and the liquid is external to the cell, sealing procedures and cell assembly techniques become quite complicated. The obvious solution to this problem is in the use of manifolding that is integral with the cell parts. The design for the parts should make use of symmetry to reduce the number of parts that are required in the assembly of a large unit.

The selection of materials of construction for the cell is important for a good design. The concentrated acid and electrolytic reaction limit the materials that may be used for the water vapor electrolysis cell, especially at the electrode. Table 4-1 lists acceptable materials of construction with their unique properties and disadvantages for use in a water vapor electrolysis cell using concentrated sulfuric of phosphoric acid.

In general, only platinum and tantalum can be used for electrode materials, although columbium may be substituted for tantalum. None of these materials is inexpensive and all are heavy, requiring a design that uses them judiciously.

Because the electrodes must be electrically insulated from each other, the use of plastics for cell spacers is ideal. The selection of the correct plastic is a tradeoff of its physical and chemical properties. Polyethylene and polypropylene are quite

Table 4-1

MATERIALS OF CONSTRUCTION – WATER VAPOR ELECTROLYSIS CELL

Material	Specific Gravity	Machinability	Moldability	Corrosion Resistance	Unique Properties	Principal Disadvantages	Suggested Usage
Metals							
Columbium	10.8	Very poor	–	Excellent	Cheaper than Ta; forms a corrosion resistant oxide.	Relatively expensive; difficult to fabricate; not readily available in usable shapes.	Electrode rims, support screens
Tantalum	16.6	Poor	–	Excellent	Forms a corrosion resistant oxide; limited availability.	Difficult to fabricate; very expensive, very ductile.	Electrode rims, support screens
Platinum	21.5	–	–	Excellent	Active catalyst.	Extremely expensive, in short supply.	Electrode catalyst
Plastics							
Chlorinated Polyether	1.4	Excellent	Excellent	Attacked slowly	Low cold flow properties, tough, strong,	Low-temperature brittleness.	Cell spacer
Cast Epoxy (talc filled)	1.8	Excellent	Excellent	Excellent	Can be cast in simple molds.	Heavy, somewhat brittle	Cell spacer
Fluorocarbons	2.1	Poor	Poor	Excellent	Very corrosion-resistant.	Heavy, difficult to fabricate, poor cold flow properties, expensive.	Cell spacer
Polycarbonate	1.2	Good	Good	Attacked slowly	Transparent	Expensive, limited availability.	Cell spacer
Polyethylene	0.94	Good	Excellent	Attacked very slowly	Light, inexpensive, available.	Poor cold flow properties, low strength.	Cell spacer
Polycarbonate	0.90	Good	Good	Attacked very slowly	Light, inexpensive, available.	Poor cold flow properties (better than polyethylene)	Cell spacer
Elastomers							
Ethylene Propylene		–	–	Attacked very slowly	No cold flow, strong, good ozone resistance.	Relatively expensive.	Seals
Fluorocarbons		–	–	Excellent	Very corrosion resistant.	Poor cold flow properties, expensive, weak.	Seals

light in weight and are easy to mold, but their cold flow properties are poor. Chlorinated polyether is somewhat heavier, but is a good material because of its greater rigidity, lower cold flow properties, and good molding characteristics. Polycarbonates are useful since they are quite transparent providing a means for visual examination of the operating cell, useful especially in the development of a cell design. The epoxies, if chosen correctly, are good materials to use although they are generally quite heavy (at least twice the density of polyethylene and polypropylene). The advantage of the epoxy material is that it may be cast in simple openfaced molds in the laboratory, providing a means to develop a cell design without the expense of elaborate molds. The fluorocarbons, although they are the most corrosion-resistant, are heavy, expensive, and difficult to fabricate.

Considerations of mechanical design problems and cell operating conditions are important in the design of a large-scale electrolysis system. The first requirement for scale up is the design of a suitable cell. When the various details of the design have been worked out, the tradeoffs of current density, power, total equivalent weight, volume, and number of cells can be made.

4.2 SCALE-UP CALCULATIONS

For the calculations and conclusions reached in this section, a cell design similar to that developed by Lockheed Missiles & Space Company on internal funding was used. The cell was developed from a design concept to a working 4-man prototype using the considerations developed in the last section. The weights given in this section are from that design with the materials modified to be compatible with the H_2SO_4 system. Because the parts used for the weight analysis are made in the laboratory (the plastic cell spacer parts are cast from epoxy) the weight of the cell is not optimized.

The design utilizes an electrode area of 90 cm^2 (14-$in.^2$). The electrodes are placed in the cell bank in such a manner that each gas plate, either hydrogen or oxygen, services the same polarity electrode for two adjacent cells. The electrode stacking

arrangement is anode cell 1, cathode cell 1, cathode cell 2, anode cell 2, anode cell 3, cathode cell 3, cathode cell 4, etc. This arrangement reduces the number and complexity of the gas spacer parts. Air is fed into the cell through an open edge on each side of the oxygen electrode gas spacers. After air enters the cell it is split with a divider allowing half of the cell air stram to flow over one anode and the remainder over another anode.

Figure 4-1 shows the relationship of the cell parts. The assembly is stacked in the sequence shown and is held together with bolts inserted through the eight unsealed holes in the periphery. Complete modules are shown in Fig. 4-2. These units were designed for liquid water feed injected into the circulating KOH electrolyte. The only difference in the design for the water vapor electrolysis unit would be the use of oxygen gas spacer plates that are slotted and open to the air stream.

The estimated weight of a laboratory model of similar design capable of operating with concentrated H_2SO_4 is shown in Table 4-2. The electrode assembly represents a large proportion of the total weight, since the rim and supporting structure is fabricated from tantalum. It is conceivable that the electrode rim could be made from columbium, reducing the rim weight by 36%. Other weight saving features could and would be incorporated as the design became more sophisticated.

The data from the small cells and the weights from Table 4-2 were used to make design calculations that are presented graphically in Fig. 4-3. The value of 2 lb of oxygen per day per man was used for the calculation of the total operating current of 127 amp. The number of cells required is dependent upon the operating current density according to

$$N = \frac{I}{(CD)(A)} \tag{21}$$

where

I = operating current (127,000 mA)
N = number of cells
CD = current density (mA/cm^2)
A = area of each electrode (cm^2)

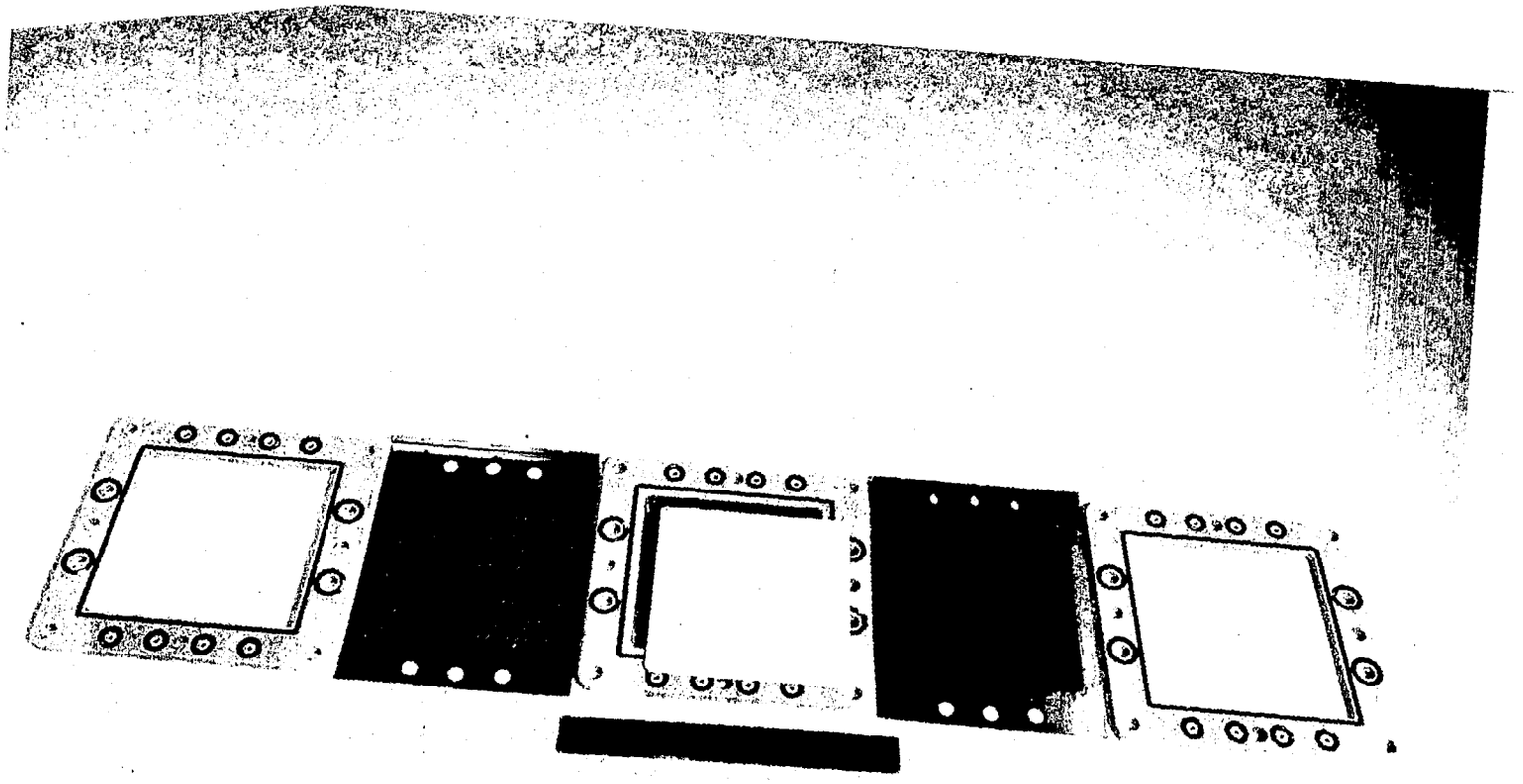

Fig. 4-1 Cell Parts of a KOH, Liquid Electrolyte-Absorbent Matrix, Liquid Water Feed Electrolysis Module

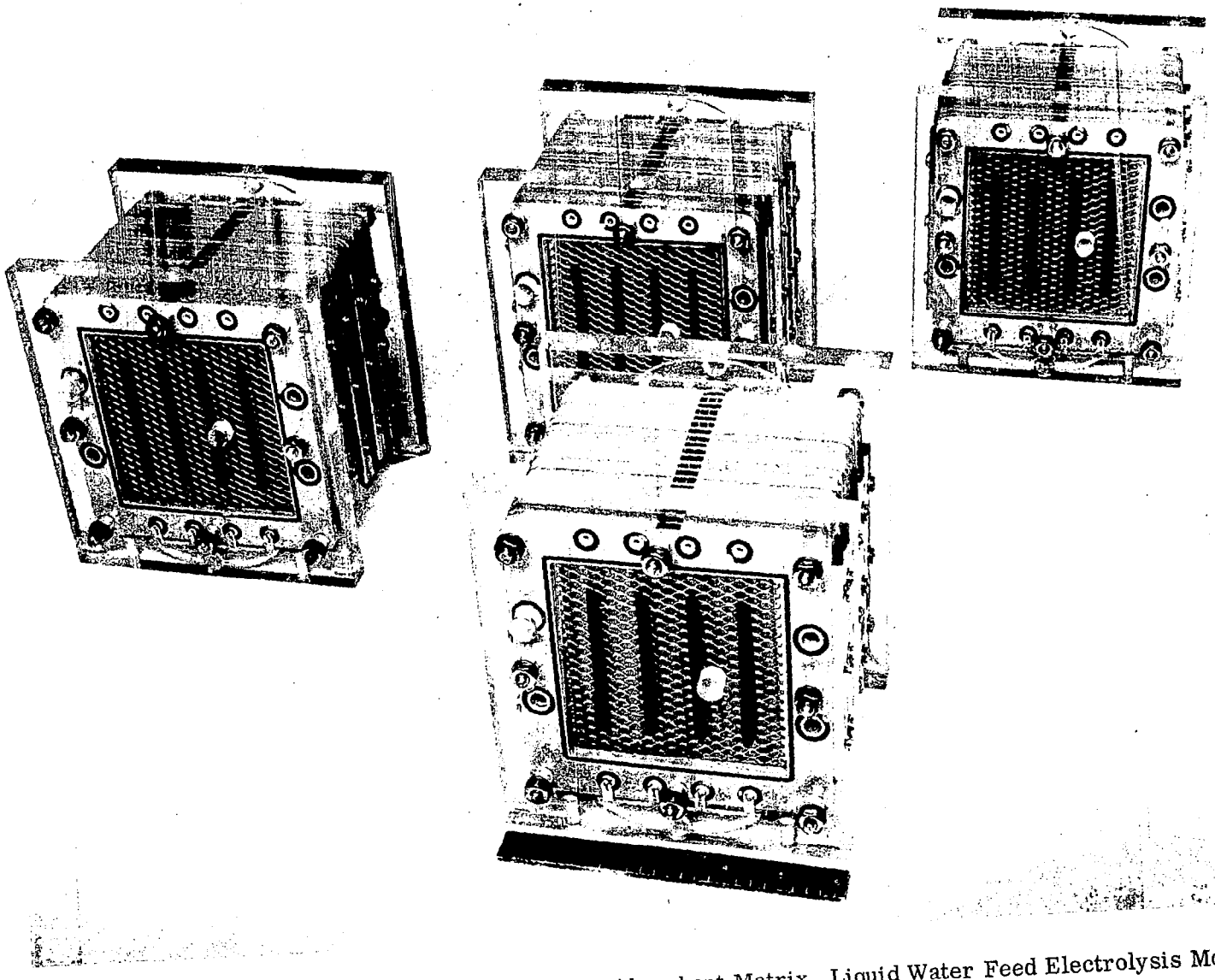

Fig. 4-2 Four, KOH, One-Man, Liquid Electrolyte-Absorbent Matrix, Liquid Water Feed Electrolysis Modules

Table 4-2

ESTIMATED COMPONENT WEIGHT OF A 1-MAN, LIQUID ELECTROLYTE-ABSORBENT MATRIX, H_2SO_4, WATER VAPOR ELECTROLYSIS UNIT[a]

Item	Component (gm)	Weight[b] (lb)
Anode	67	0.147
Cathode	67	0.147
Anode Matrix	4	0.009
Cathode Matrix	4	0.009
Electrolyte Plate With Support Screens	107	0.235
Hydrogen Gas Plate	81	0.178
Oxygen Gas Plate	65	0.143
Hydrogen Electrode Spacer	5	0.011
Oxygen Electrode Spacer	25	0.055
O-Rings	9	0.020
Assembly Hardware[c]	50	0.110
Electrolyte per Cell (60% H_2SO_4)	65	0.143
Total Cell Parts With Electrolyte	549	1.208
End Plates (2 required/bank)	545	1.199
Extra Plate (required/bank)	81	0.178
Total Extra Bank Parts	626	1.377

(a) Liquid electrolyte, absorbent matrix construction.
(b) Based on a LMSC design for a liquid water feed, potassium hydroxide, liquid electrolyte-absorbent matrix cell. Material weights listed in this table are for parts suitable for use in concentrated H_2SO_4.
(c) Prorated per cell. Includes assembly bolts, intercell connecting screws, etc.

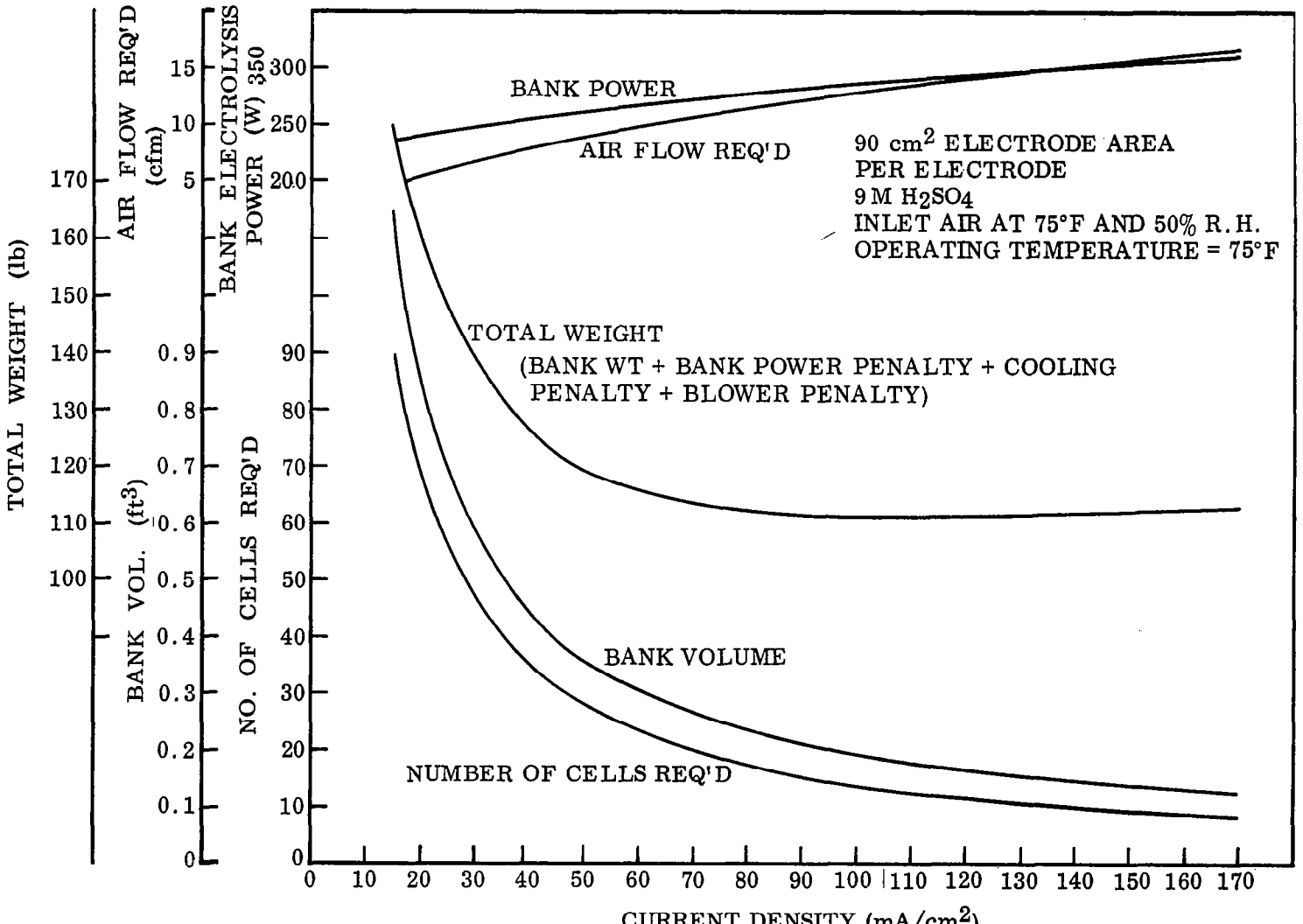

Fig. 4-3 Design Optimizing Curve for a One-Man, H_2SO_4, Liquid Electrolyte-Absorbent Matrix Water Vapor Electrolysis Unit

for the design used here (90 cm^2 active area);

$$N = \frac{141,000}{(CD)} \tag{22}$$

The cell voltage V_c may be obtained from the polarization curve of Cell A-19, Fig. 2-39. The total bank voltage is then

$$V_b = NV_c \tag{23}$$

where

V_b = bank voltage (volts)

V_c = cell voltage (volts)

Bank power is the product of the cell voltage and the total current

$$P_b = 127 V_c \tag{24}$$

where

P_b = bank power (watts)

Because any cell voltage over 1.48 V* results in heat that must be removed from the cell, the total heat that must be removed from the cell, in watts, is

$$P_h = 127(V_c - 1.48) \tag{25}$$

where

P_h = waste heat produced by the cell (watts)

*See Section 2.1.3.

From experimental data and the relationship of the air cavities for the large and the small cell, the air flow rate per cell for the large cell for any given water absorption rate should be

$$\frac{dw}{dt} = 0.0621\, q^{0.644} \tag{26}$$

where

dw/dt = water absorption rate (gm/hr)
q = air flow rate (cm^3 dry air/sec)

The water absorption rate should be equal to the electrolysis rate for no net gain or loss of water in the electrolyte. The water absorption rate per cell is dependent upon the current density as follows

$$\frac{dw}{dt} = 0.0304\ (CD) \tag{27}$$

Equating the required absorption rate to the actual absorption rate, the air flow rate required per cell can be expressed in terms of operating current density

$$q = 0.33(CD)^{1.55} \tag{28}$$

The Reynolds number for the air flow in the cell over one oxygen electrode is

$$Re = 1.178q \tag{29}$$

If the flow is laminar (Re less than 2100) the pressure drop between wide parallel plates, which approximates the cell design (Ref. 12), is equal to

$$h_T = 4.24 \times 10^{-4} q \tag{30}$$

where

h_T = air pressure drop through one cell for the cell design (inches of water)

The horsepower requirement for the fan for one cell is

$$HP_f = 6.68 \times 10^{-7} qh_T \tag{31}$$

where

HP_f = fan horsepower

An efficiency of 50% was used for the blower efficiency. The power requirement for the fan is another low number

$$P_f = 4.98 \times 10^{-4} qh_T \tag{32}$$

where

P_f = fan power requirement (watts)

To determine the total horsepower and power requirement for the bank, multiply Eqs. (31) and (32) by N. The pressure drop for the bank is the same as the drop for a single cell since the air flow through the bank is parallel. With these calculations made, the total equivalent weight of the system may be determined. This equivalent weight includes the weight of the cell bank and the penalties assessed to an operating system for the use of electrical power, both for electrolysis and cooling. The total equivalent weight is

$$W_T = W_p + W_c + W_b \tag{33}$$

where

W_T = total equivalent weight (lb)

W_P = weight penalty for use of electrical power (lb)

W_c = weight penalty for cooling (lb)

W_b = weight of the bank of cells (lb)

where

$$W_P = 0.3(P_b + P_f N) \tag{34}$$

and

$$W_c = 0.0615(P_h) \tag{35}$$

and

$$W_b = 1.208(N) + 1.377 \tag{36}$$

The volume of this design is again dependent upon the number of cells required. Accordingly

$$Y = 0.016(N) + 0.0325^{*} \quad (\text{For } N \geqq 30) \tag{37}$$

$$Y = 0.016(N) + 0.065 \quad (\text{For } 31 \leqq N \geqq 60) \tag{38}$$

$$Y = 0.016(N) + 0.0975 \quad (\text{For } 61 \leqq N \geqq 90) \tag{39}$$

*The end plate volume (0.0325) is not dependent on the number of cells up to a bank size of about 30 cells. Each cell bank requires an additional 0.0325 volume addition.

where

Y = bank volume, (ft^3)

When the data obtained by these calculations are plotted, as shown in Fig. 4-3, the lowest point on the current density versus total equivalent weight curve is approximately 100 mA/cm^2. Table 4-3 compares this cell with the H_3PO_4 cell. (Ref. 3).

Table 4-3

COMPARISON OF THE H_2SO_4 LIQUID CENTER CELL AND H_3PO_4 ELECTROLYSIS CELLS[a]

Item	H_2SO_4 System	H_3PO_4 System
Operating Current Density (mA/cm^2)	101.0	16.1
Cell Voltage (V)	2.24	2.25
Number of Cells	14.0	305.0
Bank Weight[b]	19.7	10.0
Bank Power (W)	284.0	286.0
Electrolysis Power Penality (lb)	85.2[c]	85.8
Cooling Penalty (lb)	6.0	8.6
Blower Power Penalty (lb)	0.2	1.1
Total Equivalent Weight (lb)	111.1	105.5
Bank Volume (ft^3)	0.19	0.12

(a) One-man oxygen generation system, 2 lb of oxygen/day (127-amp electrolysis rate).
(b) Does not include circulation system of approximately 4 lb/man. This weight will diminish as multi-man units are built.
(c) Based on a cooling penalty of 0.018 lb/Btu/hr for liquid-liquid heat exchange.
(d) Based on a cooling penalty of 0.025 lb/Btu/hr for gas-gas heat exchange.

The major difference in these two cells is the cell weight and the number of cells required for this electrolysis rate. The H_2SO_4 cell is quite heavy because the cell spacer parts were cast of a heavy epoxy. If weight reduction were paramount in future development, the weight of the cell could be cut by 25% making the total

equivalent weight nearly equal to the H_3PO_4 cell. The liquid center cell can be operated at a relatively high current density, reducing the number of cells required for the complete bank. These two features combine to provide a more reliable unit. Because the liquid center cell operates with a high water absorption efficiency and because the air flow is not required for cooling, the blower power for this cell is less than that required for the immobilized matrix cell.

Concentrated H_3PO_4 may also be used in the liquid center cell. The materials compatible with concentrated H_2SO_4 are also compatible with concentrated H_3PO_4. It must be shown that the long-term performance of one electrolyte is better than the other.

4.3 DESIGN AND DEVELOPMENT RECOMMENDATIONS

Future development of the liquid electrolyte-absorbent matrix system is warranted, and the development work should be directed in four areas. To further improve the competitive position of the water vapor electrolysis system using the liquid electrolyte-absorbent matrix cell, future design emphasis should be placed on a more compact design utilizing improved electrode fabrication techniques and lighter plastic cell parts. Sealing should be emphasized in all designs.

Cell performance and absorption studies should be the second area of study. Here the tradeoff of cell performance as governed by the cell temperature and the concentration of the electrolyte should be made against the water absorption rate. A specific determination must be made of the water absorption parameters. Optimization of these parameters may be done experimentally, although they lend themselves well to a computerized solution. Concurrent with performance and absorption studies is the evaluation of the trace contaminents that are evolved from the cell. Because future work will be done with large cells, the generation of contaminents such as ozone and sulfur dioxide may be in large enough quantities to allow reasonably accurate measurements.

Controls for a self-sustained unit must be developed. Because the inlet air conditions for the cell will vary when the unit is installed in a spacecraft, specific controls must be developed to allow the cell to operate at the design rate with variant inlet humidity conditions. An evaluation of constant voltage versus constant current electrolysis must be made.

When these areas have been studied, the integration of the unit with the rest of the life-support system should be contemplated. Here the requirements of ducting, manifolding and plumbing of the hydrogen, coolant interfaces, and power conditioning must be evaluated. Demonstration of self-sustained operation is important. Long-term performance should be evaluated. The system should be operated at electrolysis rates higher than the design point to demonstrate the emergency capabilities of the system.

The future work should be done with multiple cell models. Because the performance of the cells is dependent upon the inlet air conditions, a carefully controlled testing environment is necessary to be able to sort out the variables of the system during the water absorption and cell performance studies. A 1-man or larger system could be developed and bulk using the techniques of the liquid center cell within a year. After this period, with a moderate amount of bench testing, the unit would be ready for development into flight hardware incorporating solutions to the problems of heavy accelerations, vibrations, and sustained operation in the zero-g environment. The demonstration of feasibility of this system, along with its superior performance, makes the liquid electrolyte-absorbent matrix cell a prominent candidate for future development into flyable hardware.

Section 5
REFERENCES

1. J. Clifford, J. Gates, J. McCallum, and C. Faust, Research on the Electrolysis of Water Under Weightless Conditions, Report MRL-TDR-62-44, 6570, Aerospace Medical Research Laboratories, Wright-Patterson AFB, Ohio, May 1962

2. J. Clifford, J. Beach, J. Gurklis, et al., Study of Research and Development of a Water-Vapor Electrolysis Unit, Second Quarterly Report, Contract NAS 2-2156, Ames Research Center, National Aeronautics and Space Administration, Moffett Field, Calif., Jan 1965

3. J. Clifford, J. Gurklis, J. Beach, E. Kolie, et al., A Water Vapor Electrolysis Cell With Phosphoric Acid Electrolyte, Final Report Contract NAS 2-2156, Ames Research Center, National Aeronautics and Space Administration, Moffett Field, Calif., Apr 1965

4. National Research Council of USA, International Critical Tables, McGraw-Hill Book Company, New York, 1926

5. B. E. Conway, Electrochemical Data, Elsevier Pub., Inc., 1946

6. The Structure of Electrolytic Solutions, ed. W. J. Hamer, J. Wiley and Sons, Inc., New York, 1959

7. Handbook of Chemistry, ed. N. A. Lange, Handbook Publications, Inc., 1946

8. E. Condon and H. Odishaw, Handbook of Physics, McGraw-Hill Book Co., New York, 1958

9. W. Latimer, Oxidation Potentials, Prentice Hall, New York, 1953

10. W. Badger and J. Banchero, Introduction to Chemical Engineering, McGraw-Hill Book Co., New York, 1955 (p. 380)

11. J. Feigl, Spot Tests in Inorganic Analysis, Elsevier Publishing Company, New York, 1958

12. R. Perry, et al., Perry's Chemical Engineers' Handbook, Fourth Edition, McGraw-Hill Book Company, New York, 1963